FORMATION OF PV ABSORBER LAYER MATERIALS USING ELECTROCHEMICAL VERSIONS OF ATOMIC LAYER DEPOSITION: POTENTIAL PULSE ATOMIC LAYER DEPOSITION (PP-ALD), ELECTROCHEMICAL ATOMIC LAYER DEPOSITION (E-ALD)

by

JUSTIN MICHAEL CZERNIAWSKI

(Under the Direction of John L. Stickney)

ABSTRACT

This dissertation discusses the layer-by-layer deposition of Cu_2Se and In_2Se_3 using potential pulse atomic layer deposition (PP-ALD) and optimization studies of CdTe using electrochemical atomic layer deposition (E-ALD). PP-ALD is an electrodeposition methodology combining concepts from techniques such as sequential monolayer deposition (SMD) and E-ALD in order to create E-ALD quality films at increased deposition rates.

During PP-ALD cycles, potentials are alternated between cathodic and anodic potentials, foregoing cyclic voltammetry (CV) or solution alternation required in SMD and E-ALD. The cathodic potential is positioned at a co-electrodeposition potential for a time sufficient to form fractions of a monolayer (ML). The Anodic potential oxidatively strips elemental excess creating stoichiometric deposit surfaces. During pure co-dep,

potentiostatic or galvanostatic, localized excess of an element results in stoichiometry variations. Since the Cathodic pulse time limits the amount deposited, PP-ALD avoids burying elemental excess as it remains accessible to stripping during the Anodic pulse.

This is an ALD method since it is based on repeated application of surface limited reactions to grow deposits an atomic layer at a time. Electrochemical surface limited reactions are frequently referred to as underpotential deposition (UPD), which occurs at a potential that takes advantage of compound formation energetics to form a deposit of one element on another. In PP-ALD, the anodic potential produces UPD since only thermodynamically stable compound remains. The resulting Cu_2Se and In_2Se_3 film properties were characterized using coulometry, electron probe microanalysis (EPMA), CV, x-ray diffraction (XRD), and spectroscopic ellipsometry. In_2Se_3 deposits made from pH 1 solution were preferable to those made from pH 3 solution due to stoichiometry and homogeneity improvements. A PP-ALD solution made with Se^{+6} precursor was vetted as a replacement for the more reactive Se^{+4} ion. Selenic acid solution resulted in 0.1-0.3 ML of Se deposition when compared to selenous acid, which deposited 0.6 ML at the same potential. The lack of deposition limits the practicality of selenic acid as a replacement PP-ALD precursor. Finally, CdTe deposits were improved by excluding O_2 and H_2 gas formed during the deposition process through the use of CO_2 purging and less permeable gasket material.

INDEX WORDS: electrochemical atomic layer deposition, E-ALD, ALD, potential pulse atomic layer deposition PP-ALD, cadmium telluride, copper selenide, indium selenide, thin-film, electrodeposition, UPD, photovoltaics, spectroscopic ellipsometry, XRD, EPMA, cyclic voltammetry

FORMATION OF PV ABSORBER LAYER MATERIALS USING ELECTROCHEMICAL VERSIONS OF ATOMIC LAYER DEPOSITION: POTENTIAL PULSE ATOMIC LAYER DEPOSITION (PP-ALD), ELECTROCHEMICAL ATOMIC LAYER DEPOSITION (E-ALD)

by

JUSTIN MICHAEL CZERNIAWSKI

BS, The University of Georgia, 2011

A Dissertation Submitted to the Graduate Facility of The University of Georgia in Partial Fulfillment of the Requirements for the Degree

DOCTOR OF PHILOSOPHY

ATHENS, GA

2015

FORMATION OF PV ABSORBER LAYER MATERIALS USING ELECTROCHEMICAL VERSIONS OF ATOMIC LAYER DEPOSITION: POTENTIAL PULSE ATOMIC LAYER DEPOSITION (PP-ALD), ELECTROCHEMICAL ATOMIC LAYER DEPOSITION (E-ALD)

by

JUSTIN MICHAEL CZERNIAWSKI

Major Professor: John L.Stickney
Committee: Jason Locklin
Jeffrey Urbauer

Electronic Version Approved:

Suzanne Barbour
Dean of the Graduate School
The University of Georgia
December 2015

DEDICATION

I would like to dedicate this dissertation to my family and friends. Oh hi. It's been a while. Thank you all for keeping me grounded and sane throughout this whole adventure. Just having all of you present drove me to finish this part of my life. I hope I can make all of you proud. I will never forget about you and hopefully this new chapter of my life will be just as exciting for you as it is for me! I love all of you.

ACKNOWLEDGEMENTS

No words can describe how thankful I am to John Stickney. I have grown much more than I ever though was imaginable and feel completely prepared for whatever life throws at me. He knew when to advise, knew when to challenge, and knew exactly how to get the most productivity out of me. Thank you for being passionate and caring. I never once felt like you had anything but my best interest in mind. I hope we stay in contact and that you continue to grow students the way you have me. I would also like to thank the former and present members of the Stickney group who were always around for advice, information, great discussions, and friendship. I wish all of you the absolute best! No matter what challenges all of you face or will face, know you are some of the best people I have ever had the privilege of calling friends.

TABLE OF CONTENTS

CHAPTER 1

INTRODUCTION AND LITERATURE REVIEW

Affordable solar energy has long been desired as an alternative to fossil fuels.[1] Solar energy, however, will only be economically viable for large-scale production if the cost can be reduced to $0.33/Watts peak (Wp: watts produced at T = 25^0 C and incident radiation of 1000 Watts/m^2).[2] Current commercial 1st generation Si photovoltaic (PV) cells cost $0.85/Wp and only deliver a photon to electron conversion efficiency of 10-11%.[3] New materials and methods must be studied until ideal production costs can be obtained.

CdTe has long been considered one of the best choices for the absorber layer in a 2nd generation heterojunction configuration due to its ~1.5 eV band gap, the ideal value for photovoltaic conversion efficiency, and chemical stability.[4] Calculations indicate CdTe thin film solar cells have a maximum theoretical conversion efficiency of 28-30%, but to date the record observed for a CdTe cell has an actual efficiency of 17.3%.[5] CdTe is still a relevant PV absorber material but has largely been overshadowed by new, more earth-abundant multi-junction absorber materials.

One of the pioneering multi-junction absorber materials, $CuInSe_2$ (CIS), is a highly stable, p-type chalcopyrite semiconductor that has also been used in light-emitting diodes, optoelectronics, and nonlinear optical devices.[6-9] CIS has a direct bandgap around 1.08 eV[6, 9] and a high absorption coefficient (a ~ 10^5 cm^{-1}) leading to laboratory conversion efficiencies as high as 15%.[7-10] CIS has been formed using techniques such as

coevaporation,[11] flash evaporation,[12] chemical vapor deposition,[13] chemical spray pyrolysis,[14] chemical synthesis,[15] slenization of sputtered,[16] evaporated,[11] or electrodeposited[17] Cu and In stacked layers,[18] electrochemical codeposition,[19] and pulse electrodeposition.[6-8, 20] CIS though suffers from a non-ideal band gap and is also made from rare-earth materials.

CZTS represents a range of kesterite structured compounds, which are potential candidates for absorbers in p-type, earth-abundant, nontoxic photovoltaics.[21-23] Cu_2ZnSnS_4 is the primary composition, though CZTSe and alloys of the two with variable amounts of Se and S have been formed creating a tunable direct bandgap around 1.45 eV. Their solar absorption is high, with a single junction theoretical quantum efficiency of near 32%[24] and a demonstrated laboratory conversion efficiency near 9%.[23-26] CZTS, though, has been formed using a variety of techniques involving annealing and/or high pressures[25, 27] adding to the materials energetic cost.

It is possible these ternary or quaternary compounds could be synthesized by sequential deposition of binary sulfides and/or selenide compounds, such as copper selenide or indium selenide, given the identification of compatible precursors for the component elements.[7, 28-30]

Cu_2Se itself has potential applications as a photovoltaic window material, in optical fibers, solar cells, Li ion cells, thermoelectric converters, photo thermal conversion devices, and microwave shield coatings.[31] Cu_2Se has been formed using numerous techniques[23, 32]; a hydrazine solution based process has been used to create Cu_2Se, though at high temperatures and using toxic materials.[23] Paraffin liquids have been used, but contain contaminating organics and deposition control is limited.[33] In addition, melting,

annealing, and spark plasma sintering compaction require precise measurements and high temperatures.[22] Despite the effectiveness of these techniques, they do not meet the necessary demands for an inexpensive, clean and safe deposition process that would make solar a more competitive alternative to fossil fuels.

In_2Se_3 is another n-type, visible light-driven binary semiconductor material with a direct bandgap around 1.62 eV[34] that has potential applications as an absorber layer in photovoltaic devices.[35] In_2Se_3 has been formed using numerous techniques including chemical bath deposition,[36] sputtering,[37] MOCVD,[38] spray pyrolysis,[39] magnetron sputtering,[37] and electrochemical deposition.[35]

Electrodeposition has generally been considered a low cost, flexible, room temperature technique for the production of thin film materials. II-VI compound semiconductors, applicable for photovoltaic (PV) devices, have been successfully grown using electrodeposition since Kroger et al.'s single solution CdTe work in the 70's.[28, 40] Atomic layer deposition (ALD) in general refers to a group of deposition techniques where surface limited reactions are used to form deposits one atomic layer at a time. A cycle of these reactions is used to form a compound monolayer and the cycle is repeated to grow the deposit to a desired thickness. The author's group has conducted extensive studies on the development of E-ALD, the electrochemical version of ALD, to form CdTe and other compound semiconductors.[8, 41]

The vast majority of ALD work has been performed in vacuum concerning the formation of oxide nanofilms. E-ALD, however, is based on the use of precursor solutions made with ultrahigh purity water and electronic grade inorganic salts. These electrochemical surface limited reactions are referred to as underpotential deposition

(UPD), a phenomenon that occurs at a potential where one element can deposit onto a second element, but cannot deposit on itself due to the free energy associated with surface compound or alloy formation.[42]

In a typical E-ALD cycle, separate solutions containing precursors of different elements are introduced to the substrate at their UPD potentials resulting in an alternating deposition of atomic layers. After deposition of an atomic layer of the first element, the cell is rinsed with a blank solution and a precursor solution of the second element is introduced at its UPD potential, resulting in deposition of an atomic layer. The cycle is completed by rinsing again with blank. The advantages of using E-ALD are increased control of the thickness, homogeneity, crystallinity, and quality of the deposit. The drawback is the deposition rate, due to the need for multiple solution exchanges each cycle. The technique is thus best applied when nanofilms of a carefully controlled thickness and quality are required and the total number of cycles performed is minimized.[8, 43] E-ALD is generally impractical for μm thick film growth when compared to the co-electrodeposition used by BP to form μm thick CdTe PV absorber materials.[44]

Co-electrodeposition has been used to form a large number of compounds[45], such as CdSe.[46] Early CdSe co-electrodeposition studies indicated the presence of excess Se, for a Cd:Se ratio less than one.[47-49] Researchers were able to limit the deposition of Se by dropping the concentration or forming a complex with sulfite, thus shifting the deposition potential more negative. In a co-electrodeposition bath, however, this indirectly increased the overpotential used to deposit Cd resulting in deposits rich in Cd.[49, 50] A solution to the excess Cd and Se was proposed by Sailor et al., where instead of choosing a constant deposition potential, or current, they performed rapid and repeated cyclic voltammetry over

a small range of potentials, a technique referred to as sequential monolayer electrodeposition (SMD).[48] The idea was to cycle between a negative potential where co-electrodeposition takes place, and a positive potential where excess, bulk Cd oxidized, but the Cd bound as CdSe did not. By scanning rapidly, traces of bulk cadmium formed at the more negative potentials were oxidatively removed at the positive end of each cycle, before they were buried by depositing CdSe, avoiding a buildup of excess Cd. SMD has been used by Penner et al. to construct nanowire photo-sensors based on CdSe[30, 51] and Lee et al. to make 3-D macroporous structures of II-VI and III-V semiconductors.[52]

Another method proposed to control excess elemental deposition in $Bi_{2-x}Sb_xTe_3$ multilayers was described by Banga et al..[53] Pulsed potentiostatic electrodeposition (PPE) is a diffusion limited, single-bath, co-electrodeposition process where a duty cycle is established by pulsing for short periods of time (~2% duty cycle) down to a potential where a desired compound forms. The cell is then allowed to "rest" at the open-circuit potential to regenerate the diffusion layer. PPE creates highly crystalline deposits, but long resting times (2-10 s) are needed to carefully control precursor concentrations near the surface of the electrode.

This dissertation describes a compound electrodeposition methodology inspired by SMD, PPE, and E-ALD, where instead of cyclic voltammetry or changing solutions each cycle, the potential is alternated. As with E-ALD, sub-monolayer amounts are deposited each cycle, controlled by the surface-limited reactions between the depositing elements and selective stripping of any bulk elemental deposit formed. It is referred to here as potential pulse atomic layer deposition (PP-ALD). PP-ALD is based on optimized Cathodic and Anodic potentials, times, and solution composition. Given the differences in kinetics and

deposition potentials for the two elemental precursors, co-deposition can be performed (usually) at a Cathodic potential for a time sufficient to plate some fraction of a monolayer. The potential can then be stepped to an Anodic potential sufficiently positive to remove any elemental deposits of the more reactive element, leaving only a stable compound.

During co-deposition, given differences in over potentials and deposition kinetics for the individual elemental precursors, the deposit stoichiometry can vary with time. In PP-ALD, by limiting co-deposition to some fraction of a compound monolayer, excess deposition of an element should be left exposed to solution and can be selectively oxidized during the Anodic potential step. This process serves as a surface limited reaction, leaving only the stable compound. The major benefits of this methodology over E-ALD are the large increase in deposition rate, increased scalability, and the ease with which solutions can be recycled.

The deposits throughout this dissertation were made using the automated electrochemical flow cell deposition system seen in Figure 1.1 (Electrochemical ALD L.C., Athens, GA) which included a single variable speed pump (Cole Parmer Masterflex), 3 electrode cell controlled by a potentiostat, 5 solution reservoirs fed by 5 individually controlled valves housed in a Plexiglas box, and an electrochemical flow cell with Au wire inlayed into the face. The reference electrode was Ag/AgCl (BASi, West Lafayette, IN), the working electrode was a piece of Au on glass, and the bottles and valves were continuously purged with nitrogen to minimize O_2 in the system. The set potential and system was automated using an in house program called "SEQUENCER."[54]

Chapter 2 and 3 discuss the development of PP-ALD programs to create binary compound thin films of Cu_2Se and In_2Se_3. Cyclic voltammetry (CV) was used to determine

approximate deposition potentials for Cu, In, and Se. Anodic and Cathodic potentials were then systematically examined to develop separate pulse programs for Cu_2Se and In_2Se_3 formation, and the deposits were characterized. Cu_2Se film thickness, determined by spectroscopic ellipsometry, was shown to be proportional to the number of pulse cycles, and ranged from 50 to 160 nm, a growth rate of 0.02 nm/cycle. Electron probe microanalysis (EPMA) was used to follow the Cu:Se atomic ratios as a function of the deposition conditions, and X-ray diffraction (XRD) indicated polycrystalline orthorhombic Cu_2Se, with a suggestion of cubic. In_2Se_3 deposits were characterized and optimized deposits were annealed and re-characterized to examine quality improvement. Electron probe microanalysis (EPMA) was used to follow the In:Se atomic ratios as a function of the deposition conditions.

Chapter 4 describes an investigation into pH effects on precursor solution when depositing InSe thin films. The films were deposited at room temperature from a pH 3 and pH 1 aqueous solution containing both In^{+3} and Se^{+4} ions using potential pulse atomic layer deposition (PP-ALD) in order to determine optimum solution pH. Cyclic voltammetry (CV) was used to determine approximate deposition potentials for In and Se. Electron probe microanalysis (EPMA) was used to follow the In:Se atomic ratios as a function of Anodic and Cathodic potentials. Films made with a pH 3 precursor were thin and did not adhere to the substrate. In pH 1 conditions, thin films with an ideal stoichiometric composition of 2:3 In to Se could be grown. No crystallographic patterns could be obtained from the thin films.

In Chapter 5, Cyclic voltammetry (CV) was used to examine changes in the electrochemical profile for Au in Se^{+6} ions when compared to the profile of Au in Se^{+4}

ions. A CV of an Au substrate treated with underpotentially deposited Cu showed the amount of Se deposited from Se^{+6} solution was slightly higher, 0.3 ML, compared to the Se amount deposited on an untreated Au surface from the same solution, 0.1 ML. While Cu appeared to have a positive effect on Se^{+6} deposition, the increase is not practical enough to consider Se^{+6} precursor a viable replacement for Se^{+4} precursor.

Chapter 6 discusses optimization studies of CdTe deposits made with E-ALD. Minimization of O_2 and H_2 gas in the E-ALD system is paramount when creating reproducible crystalline deposits with minimal defects to prevent shorting in photovoltaic cells. Automated CO_2 cell purges were introduced in order to remove O_2 gas and H_2 gas formed inside the cell over time. Preliminary studies indicated that CO_2 cell purges followed by alkaline solution rinses are effective at removing O_2 and H_2. Understanding the deposition behavior of CdTe thin films made in acidic and basic media brought to light new strategies prohibiting the formation of harmful defects in deposits. Preliminary layer-by-layer deposition and stripping studies allow for quantification and tuning of E-ALD conditions in this effort to create defect-free deposits.

References

1. Birkmire, R. W.; Eser, E., Polycrystalline thin film solar cells: Present status and future potential. *Annual Review of Materials Science* **1997,** *27*, 625-653; Shah, A.; Torres, P.; Tscharner, R.; Wyrsch, N.; Keppner, H., Photovoltaic technology: The case for thin-film solar cells. *Science* **1999,** *285* (5428), 692-698.
2. US, D. o. E. Multi Year Program Plan 2008-2012. https://www1.eere.energy.gov/solar/pdfs/solar_program_mypp_2008-2012.pdf.
3. Wu, X., High-efficiency polycrystalline CdTe thin-film solar cells. *Solar Energy* **2004,** *77* (6), 803-814; Powalla, M.; Bonnet, D., Thin-Film Solar Cells Based on the Polycrystalline Compound Semiconductors CIS and CdTe. *Advances in OptoElectronics* **2007,** *2007*.
4. Zhou Fang, X. C. W., Hong Cai Wu, and Ce Zhou Zhao, Achievements and Challenges of CdS/CdTe Solar Cells. *International Journal of Photoenergy* **2011,** *2011*.
5. First Solar, I. First Solar Sets World Record for CdTe Solar PV Efficiency. http://investor.firstsolar.com/releasedetail.cfm?releaseID=593994 (accessed 11/1).
6. Hu, S.-Y.; Lee, W.-H.; Chang, S.-C.; Cheng, Y.-L.; Wang, Y.-L., Pulsed Electrodeposition of CuInSe2 Thin Films onto Mo-Glass Substrates. *Journal of The Electrochemical Society* **2011,** *158* (5), B557-B561.
7. Caballero-Briones, F.; Palacios-Padrós, A.; Sanz, F., CuInSe2 films prepared by three step pulsed electrodeposition. Deposition mechanisms, optical and photoelectrochemical studies. *Electrochimica Acta* **2011,** *56* (26), 9556-9567.

8. Banga, D.; Jarayaju, N.; Sheridan, L.; Kim, Y.-G.; Perdue, B.; Zhang, X.; Zhang, Q.; Stickney, J., Electrodeposition of CuInSe2 (CIS) via Electrochemical Atomic Layer Deposition (E-ALD). *Langmuir* **2012,** *28* (5), 3024-3031.

9. Hamrouni, S.; AlKhalifah, M. S.; Boujmil, M. F.; Saad, K. B., Preparation and characterization of CuInSe2 electrodeposited thin films annealed in vacuum. *Applied Surface Science* **2014,** *292* (0), 231-236.

10. Fangyang, L.; Ying, L.; Zhian, Z.; Yanqing, L.; Jie, L.; Yexiang, L., Preparation of Chalcopyrite Cuinse2 Thin Films by Pulse-Plating Electrodeposition and Annealing Treatment. In *Proceedings of ISES World Congress 2007 (Vol. I – Vol. V)*, Goswami, D. Y.; Zhao, Y., Eds. Springer Berlin Heidelberg: 2009; pp 1316-1320.

11. Guillén, C.; Herrero, J., Structure, morphology and photoelectrochemical activity of CuInSe2 thin films as determined by the characteristics of evaporated metallic precursors. *Solar Energy Materials and Solar Cells* **2002,** *73* (2), 141-149.

12. Ashida, A.; Hachiuma, Y.; Yamamoto, N.; Ito, T.; Cho, Y., CuInSe2 thin films prepared by quasi-flash evaporation of In2Se3 and Cu2Se. *Journal of Materials Science Letters* **1994,** *13* (16), 1181-1184.

13. Jones, P. A.; Jackson, A. D.; Lickiss, P. D.; Pilkington, R. D.; Tomlinson, R. D., The plasma enhanced chemical vapour deposition of CuInSe2. *Thin Solid Films* **1994,** *238* (1), 4-7.

14. Shirakata, S.; Murakami, T.; Kariya, T.; Isomura, S., Preparation of CuInSe2 Thin Films by Chemical Spray Pyrolysis. *Japanese Journal of Applied Physics* **1996,** *35* (1R), 191; Tomoaki Terasako; Sho Shirakata; Shigehiro Isomura, Photoacoustic

Spectra of CuInSe 2 Thin Films Prepared by Chemical Spray Pyrolysis. *Japanese Journal of Applied Physics* **1999,** *38* (8R), 4656.

15. de Kergommeaux, A.; Fiore, A.; Bruyant, N.; Chandezon, F.; Reiss, P.; Pron, A.; de Bettignies, R.; Faure-Vincent, J., Synthesis of colloidal CuInSe2 nanocrystals films for photovoltaic applications. *Solar Energy Materials and Solar Cells* **2011,** *95, Supplement 1* (0), S39-S43.
16. Guillén, C.; Martínez, M. A.; Herrero, J., CuInSe2 thin films obtained by a novel electrodeposition and sputtering combined method. *Vacuum* **2000,** *58* (4), 594-601.
17. Guillén, C.; Herrero, J., Improved Selenization Procedure to Obtain CulnSe2 Thin Films from Sequentially Electrodeposited Precursors. *Journal of The Electrochemical Society* **1996,** *143* (2), 493-498.
18. Liang, D.; Unveroglu, B.; Zangari, G., Electrodeposition of Cu-In Alloys as Precursors of Chalcopyrite Absorber Layers. *Journal of The Electrochemical Society* **2014,** *161* (12), D613-D619.
19. Bhattacharya, R. N., Solution Growth and Electrodeposited CuInSe2Thin Films. *Journal of The Electrochemical Society* **1983,** *130* (10), 2040-2042; Kaupmees, L.; Altosaar, M.; Volubujeva, O.; Mellikov, E., Study of composition reproducibility of electrochemically co-deposited CuInSe2 films onto ITO. *Thin Solid Films* **2007,** *515* (15), 5891-5894; Hernández-Pagán, E. A.; Wang, W.; Mallouk, T. E., Template Electrodeposition of Single-Phase p- and n-Type Copper Indium Diselenide (CuInSe2) Nanowire Arrays. *ACS Nano* **2011,** *5* (4), 3237-3241.

20. Palacios-Padrós, A.; Caballero-Briones, F.; Sanz, F., Enhancement in as-grown CuInSe2 film microstructure by a three potential pulsed electrodeposition method. *Electrochemistry Communications* **2010,** *12* (8), 1025-1029.

21. Wadia, C.; Alivisatos, A. P.; Kammen, D. M., Materials Availability Expands the Opportunity for Large-Scale Photovoltaics Deployment. *Environmental Science & Technology* **2009,** *43* (6), 2072-2077.

22. Ballikaya, S.; Chi, H.; Salvador, J. R.; Uher, C., Thermoelectric properties of Ag-doped Cu2Se and Cu2Te. *Journal of Materials Chemistry A* **2013,** *1* (40), 12478-12484.

23. Todorov, T. K.; Tang, J.; Bag, S.; Gunawan, O.; Gokmen, T.; Zhu, Y.; Mitzi, D. B., Beyond 11% Efficiency: Characteristics of State-of-the-Art Cu2ZnSn(S,Se)4 Solar Cells. *Advanced Energy Materials* **2013,** *3* (1), 34-38.

24. Suryawanshi, M. P.; Agawane, G. L.; Bhosale, S. M.; Shin, S. W.; Patil, P. S.; Kim, J. H.; Moholkar, A. V., CZTS based thin film solar cells: a status review. *Materials Technology* **2013,** *28* (1/2), 98-109.

25. Hongxia, W., Progress in Thin Film Solar Cells Based on Cu2ZnSnS4. *International Journal of Photoenergy* **2011**, 1-10; Wangperawong, A.; King, J. S.; Herron, S. M.; Tran, B. P.; Pangan-Okimoto, K.; Bent, S. F., Aqueous bath process for deposition of Cu2ZnSnS4 photovoltaic absorbers. *Thin Solid Films* **2011,** *519* (8), 2488-2492.

26. Kask, E.; Raadik, T.; Grossberg, M.; Josepson, R.; Krustok, J., Deep defects in Cu2ZnSnS4 monograin solar cells. *Energy Procedia* **2011,** *10* (0), 261-265; Minlin, J.; Dhakal, R.; Yong, L.; Thapaliya, P.; Xingzhong, Y. In *Cu2ZnSnS4 (CZTS)*

polycrystalline thin films prepared by sol-gel method, Photovoltaic Specialists Conference (PVSC), 2011 37th IEEE, 19-24 June 2011; 2011; pp 001283-001286; Bär, M.; Schubert, B.-A.; Marsen, B.; Wilks, R. G.; Blum, M.; Krause, S.; Pookpanratana, S.; Zhang, Y.; Unold, T.; Yang, W.; Weinhardt, L.; Heske, C.; Schock, H.-W., Cu2ZnSnS4 thin-film solar cell absorbers illuminated by soft x-rays. *Journal of Materials Research* **2012,** *27* (08), 1097-1104; Zhao, Y.; Burda, C., Development of plasmonic semiconductor nanomaterials with copper chalcogenides for a future with sustainable energy materials. *Energy & Environmental Science* **2012,** *5* (2), 5564-5576; Chen, S.; Walsh, A.; Gong, X.-G.; Wei, S.-H., Classification of Lattice Defects in the Kesterite Cu2ZnSnS4 and Cu2ZnSnSe4 Earth-Abundant Solar Cell Absorbers. *Advanced Materials* **2013,** *25* (11), 1522-1539.

27. Nitsche, R.; Sargent, D. F.; Wild, P., Crystal growth of quaternary 122464 chalcogenides by iodine vapor transport. *Journal of Crystal Growth* **1967,** *1* (1), 52-53; Steinhagen, C.; Panthani, M. G.; Akhavan, V.; Goodfellow, B.; Koo, B.; Korgel, B. A., Synthesis of Cu2ZnSnS4 Nanocrystals for Use in Low-Cost Photovoltaics. *Journal of the American Chemical Society* **2009,** *131* (35), 12554-12555; Prabhakar, T.; Nagaraju, J. In *Device parameters of Cu2ZnSnS4 thin film solar cell*, Photovoltaic Specialists Conference (PVSC), 2011 37th IEEE, 19-24 June 2011; 2011; pp 001346-001351; Ahmed, S.; Reuter, K. B.; Gunawan, O.; Guo, L.; Romankiw, L. T.; Deligianni, H., A High Efficiency Electrodeposited Cu2ZnSnS4 Solar Cell. *Advanced Energy Materials* **2012,** *2* (2), 253-259; Shin, B.; Gunawan, O.; Zhu, Y.; Bojarczuk, N. A.; Chey, S. J.; Guha, S., Thin film solar cell

with 8.4% power conversion efficiency using an earth-abundant Cu2ZnSnS4 absorber. *Progress in Photovoltaics: Research and Applications* **2013,** *21* (1), 72-76; Tatsuo, F.; Shin, T.; Tadayoshi, I., Enhancement of Conversion Efficiency of Cu 2 ZnSnS 4 Thin Film Solar Cells by Improvement of Sulfurization Conditions. *Applied Physics Express* **2013,** *6* (6), 062301.

28. Kröger, F. A., Cathodic Deposition and Characterization of Metallic or Semiconducting Binary Alloys or Compounds. *Journal of The Electrochemical Society* **1978,** *125* (12), 2028-2034.

29. Sato, N.; Ichimura, M.; Arai, E.; Yamazaki, Y., Characterization of electrical properties and photosensitivity of SnS thin films prepared by the electrochemical deposition method. *Solar Energy Materials and Solar Cells* **2005,** *85* (2), 153-165; Mathews, N. R.; Anaya, H. B. M.; Cortes-Jacome, M. A.; Angeles-Chavez, C.; Toledo-Antonio, J. A., Tin Sulfide Thin Films by Pulse Electrodeposition: Structural, Morphological, and Optical Properties. *Journal of The Electrochemical Society* **2010,** *157* (3), H337-H341.

30. Liu, F.; Huang, C.; Lai, Y.; Zhang, Z.; Li, J.; Liu, Y., Preparation of Cu(In,Ga)Se2 thin films by pulse electrodeposition. *Journal of Alloys and Compounds* **2011,** *509* (8), L129-L133.

31. Gosavi, S. R.; Deshpande, N. G.; Gudage, Y. G.; Sharma, R., Physical, optical and electrical properties of copper selenide (CuSe) thin films deposited by solution growth technique at room temperature. *Journal of Alloys and Compounds* **2008,** *448* (1–2), 344-348; Liu, K.; Liu, H.; Wang, J.; Shi, L., Synthesis and characterization of Cu2Se prepared by hydrothermal co-reduction. *Journal of*

Alloys and Compounds **2009,** *484* (1–2), 674-676; Yahia, I. S.; Fadel, M.; Sakr, G. B.; Shenouda, S. S., Memory switching of ZnGa2Se4 thin films as a new material for phase change memories (PCMs). *Journal of Alloys and Compounds* **2010,** *507* (2), 551-556; Ramesh, K.; Bharathi, B.; Thanikaikarasan, S.; Mahalingam, T.; Sebastian, P., Growth and Characterization of Electroplated Copper Selenide Thin Films. *Journal Of New Materials For Electrochemical Systems* **2013,** *16* (2), 127-132.

32. Bosio, A.; Romeo, N.; Mazzamuto, S.; Canevari, V., Polycrystalline CdTe thin films for photovoltaic applications. *Progress in Crystal Growth and Characterization of Materials* **2006,** *52* (4), 247-279; Jafarov, M. A.; Nasirov, E. F. In *Properties of the thin-film solar cells with heterojunctions Cu2S-Cd1-xZnxS and Cu2Se-Cd1-xZnxSe*, 2012; pp 84700I-84700I-5.

33. Deng, Z.; Mansuripur, M.; Muscat, A. J., Synthesis of two-dimensional single-crystal berzelianite nanosheets and nanoplates with near-infrared optical absorption. *Journal of Materials Chemistry* **2009,** *19* (34), 6201-6206.

34. Qasrawi, A. F., Temperature dependence of the band gap, refractive index and single-oscillator parameters of amorphous indium selenide thin films. *Optical Materials* **2007,** *29* (12), 1751-1755.

35. Yadav, A. A.; Salunke, S. D., Photoelectrochemical properties of In2Se3 thin films: Effect of substrate temperature. *Journal of Alloys and Compounds* **2015,** (0).

36. Asabe, M. R.; Chate, P. A.; Delekar, S. D.; Garadkar, K. M.; Mulla, I. S.; Hankare, P. P., Synthesis, characterization of chemically deposited indium selenide thin films at room temperature. *Journal of Physics and Chemistry of Solids* **2008,** *69* (1), 249-

254; Pathan, H. M.; Kulkarni, S. S.; Mane, R. S.; Lokhande, C. D., Preparation and characterization of indium selenide thin films from a chemical route. *Materials Chemistry and Physics* **2005,** *93* (1), 16-20.

37. Li, S.; Yan, Y.; Zhang, Y.; Ou, Y.; Ji, Y.; Liu, L.; Yan, C.; Zhao, Y.; Yu, Z., Monophase γ-In2Se3 thin film deposited by magnetron radio-frequency sputtering. *Vacuum* **2014,** *99* (0), 228-232; Yan, Y.; Li, S.; Yu, Z.; Liu, L.; Yan, C.; Zhang, Y.; Zhao, Y., Influence of indium concentration on the structural and optoelectronic properties of indium selenide thin films. *Optical Materials* **2014,** *38* (0), 217-222; Yan, Y.; Li, S.; Ou, Y.; Ji, Y.; Liu, L.; Yan, C.; Zhang, Y.; Yu, Z.; Zhao, Y., In-situ annealing of In–Se amorphous precursors sputtered at low temperature. *Journal of Alloys and Compounds* **2014,** *614* (0), 368-372.

38. Choi, H.; Nicolaescu, R.; Paek, S.; Ko, J.; Kamat, P. V., Supersensitization of CdS Quantum Dots with a Near-Infrared Organic Dye: Toward the Design of Panchromatic Hybrid-Sensitized Solar Cells. *ACS Nano* **2011,** *5* (11), 9238-9245.

39. Aydin, E.; Sankir, M.; Sankir, N. D., Influence of silver incorporation on the structural, optical and electrical properties of spray pyrolyzed indium sulfide thin films. *Journal of Alloys and Compounds* **2014,** *603* (0), 119-124; Reyes-Figueroa, P.; Painchaud, T.; Lepetit, T.; Harel, S.; Arzel, L.; Yi, J.; Barreau, N.; Velumani, S., Structural properties of In2Se3 precursor layers deposited by spray pyrolysis and physical vapor deposition for CuInSe2 thin-film solar cell applications. *Thin Solid Films* (0).

40. Panicker, M. P. R.; Knaster, M.; Kroger, F. A., Cathodic Deposition Of CdTe From Aqueous-Electrolytes. *Journal of the Electrochemical Society* **1978,** *125* (4), 566-

572; Gregory, B. W.; Stickney, J. L., Electrochemical atomic layer epitaxy (ECALE). *Journal of Electroanalytical Chemistry* **1991,** *300* (1-2), 543-561.

41. D. W. Suggs, I. V., B.W. Gregory, J.L. Stickney, Formation of CdTe and GaAs by electrochemical atoimc layer epitaxy (ECALE). *Mat. Res. Soc. Symp. Proc.* **1991,** *222*, 283; Colletti, L. P.; Stickney, J. L., II-VI compound semiconductor thin-film electrodeposition by ECALE. *Book of Abstracts, 210th ACS National Meeting, Chicago, IL, August 20-24* **1995,** (Pt. 1), INOR-297; Colletti, L. P.; Flowers, B. H.; Stickney, J. L., Formation of Thin-Films of CdTe, CdSe, and CdS by Electrochemical ALE. *JECS* **1997**; Colletti, L. P.; Slaughter, R.; Stickney, J. L., ZnS thin film formation by electrochemical ALE: preliminary doping studies. *Proceedings - Electrochemical Society* **1997,** *97-20* (Photoelectrochemistry), 1-10; Perdue, B.; Czerniawski, J.; Anthony, J.; Stickney, J., Optimization of Te Solution Chemistry in the Electrochemical Atomic Layer Deposition Growth of CdTe. *Journal of The Electrochemical Society* **2014,** *161* (7), D3087-D3092.

42. Kolb, D. M., Physical and Electrochemical Properties of Metal Monolayers on Metallic Substrates. In *Advances in Electrochemistry and Electrochemical Engineering*, Gerischer, H.; Tobias, C. W., Eds. John Wiley: New York, 1978; Vol. 11, p 125; Juttner; K.; Lorenz; W.J., *Z. Phys. Chem. N. F.* **1980,** *122*, 163; Adzic, R. R., Electrocatalytic Properties of the Surfaces Modified by Foreign Metal Ad Atoms. In *Advances in Electrochemistry and Electrochemical Engineering*, Gerishcher, H.; Tobias, C. W., Eds. Wiley-Interscience: New York, 1984; Vol. 13, p 159; Gewirth, A. A.; Niece, B. K., Electrochemical applications of in situ scanning probe microscopy. *Chem. Rev.* **1997,** *97*, 1129-1162.

43. Vaidyanathan, R.; Mathe, M. K.; Sprinkle, P.; Cox, S. M.; Happek, U.; Stickney, J. L., Electrodeposition of Cu2Se thin films by electrochemical atomic layer epitaxy (EC-ALE). *Materials Research Society Symposium Proceedings* **2003,** *744* (Progress in Semiconductors II--Electronic and Optoelectronic Applications), 289-294.

44. Turner, A. K.; Woodcock, J. M.; Ozsan, M. E.; Cunningham, D. W.; Johnson, D. R.; Marshall, R. J.; Mason, N. B.; Oktik, S.; Patterson, M. H.; Ransome, S. J.; Roberts, S.; Sadeghi, M.; Sherborne, J. M.; Sivapathasundaram, D.; Walls, I. A., BP Solar Thin-Film Cdte Photovoltaic Technology. *Solar Energy Materials and Solar Cells* **1994,** *35* (1-4), 263-270; Cunningham, D.; Rubcich, M.; Skinner, D., Cadmium telluride PV module manufacturing at BP Solar. *Progress in Photovoltaics* **2002,** *10* (2), 159-168.

45. Öznülüer, T.; Erdoğan, İ.; Şişman, İ.; Demir, Ü., Electrochemical Atom-by-Atom Growth of PbS by Modified ECALE Method. *Chemistry of Materials* **2005,** *17* (5), 935-937; Öznülüer, T.; Erdoğan, İ.; Demir, Ü., Electrochemically Induced Atom-by-Atom Growth of ZnS Thin Films: A New Approach for ZnS Co-deposition. *Langmuir* **2006,** *22* (9), 4415-4419.

46. Loizos, Z.; Mitsis, A.; Spyrellis, N.; Froment, M.; Maurin, G., Cadmium chalcogenide semiconducting thin films prepared by electrodeposition from boiling aqueous electrolytes. *Thin Solid Films* **1993,** *235* (1-2), 51-56.

47. Kazacos, M. S.; Miller, B., Studies in Selenious Acid Reduction and CdSe Film Deposition. *Journal of The Electrochemical Society* **1980,** *127* (4), 869-873; Skyllas Kazacos, M.; Miller, B., Electrodeposition of CdSe Films from

Selenosulfite Solution. *Journal of The Electrochemical Society* **1980,** *127* (11), 2378-2381; Houston, G. J.; McCann, J. F.; Haneman, D., Optimising the photoelectrochemical performance of electrodeposited CdSe semiconductor electrodes. *Journal of Electroanalytical Chemistry and Interfacial Electrochemistry* **1982,** *134* (1), 37-47; Tomkiewicz, M.; Ling, I.; Parsons, W. S., Morphology, Properties, and Performance of Electrodeposited n - CdSe in Liquid Junction Solar Cells. *Journal of The Electrochemical Society* **1982,** *129* (9), 2016-2022; Skyllas-Kazacos, M., Electrodeposition of CdSe and CdSe+CdTe thin films from cyanide solutions. *Journal of Electroanalytical Chemistry and Interfacial Electrochemistry* **1983,** *148* (2), 233-239; Wei, C.; Bose, C. S. C.; Rajeshwar, K., Compositional analysis of electrosynthesized semiconductor thin films by electrochemical quartz crystal microgravimetry: Application to the Cd + Se system. *Journal of Electroanalytical Chemistry* **1992,** *327* (1–2), 331-336.

48. Kressin, A. M.; Doan, V. V.; Klein, J. D.; Sailor, M. J., Synthesis of stoichiometric CdSe films via sequential monolayer electrodeposition. *Chem. Mater.* **1991,** *3*, 1015-1020.

49. Ham, D.; Mishra, K. K.; Rajeshwar, K., Anodic electrosynthesis of CdSe thin-films: Characterization and comparison with the passive/transpassive behavior of the CdX (X= S, Te) counterparts. *J. Electrochem. Soc.* **1991,** *138*, 100.

50. Cocivera, M.; Darkowski, A.; Love, B., Thin Film CdSe Electrodeposited from Selenosulfite Solution. *Journal of The Electrochemical Society* **1984,** *131* (11), 2514-2517; Loizos, Z.; Spyrellis, N.; Maurin, G.; Pottier, D., Semiconducting CdSex, Te1−x thin films prepared by electrodeposition. *Journal of*

Electroanalytical Chemistry and Interfacial Electrochemistry **1989,** *269* (2), 399-410; Krishnan, V.; Ham, D.; Mishra, K. K.; Rajeshwar, K., Electrosynthesis of thin films of CdZnSe: composition modulation and bandgap engineering in the ternary system. *J. Electrochem. Soc.* **1992,** *139*, 23; Krishnan, V.; Ham, D.; Mishra, K. K.; Rajeshwar, K., Electrosynthesis of Thin Films of CdZnSe : Composition Modulation and Bandgap Engineering in the Ternary System. *Journal of The Electrochemical Society* **1992,** *139* (1), 23-27.

51. Ayvazian, T.; van der Veer, W. E.; Xing, W.; Yan, W.; Penner, R. M., Electroluminescent, Polycrystalline Cadmium Selenide Nanowire Arrays. *ACS Nano* **2013,** *7* (10), 9469-9479.

52. Lee, Y.-C.; Kuo, T.-J.; Hsu, C.-J.; Su, Y.-W.; Chen, C.-C., Fabrication of 3D Macroporous Structures of II−VI and III−V Semiconductors Using Electrochemical Deposition. *Langmuir* **2002,** *18* (25), 9942-9946.

53. Banga, D.; Lensch-Falk, J. L.; Medlin, D. L.; Stavila, V.; Yang, N. Y. C.; Robinson, D. B.; Sharma, P. A., Periodic Modulation of Sb Stoichiometry in Bi2Te3/Bi2–xSbxTe3 Multilayers Using Pulsed Electrodeposition. *Crystal Growth & Design* **2012,** *12* (3), 1347-1353.

54. Colletti, L. P.; Flowers, B. H.; Stickney, J. L., Formation of thin films of CdTe, CdSe, and CdS by electrochemical atomic layer epitaxy. *Journal of the Electrochemical Society* **1998,** *145* (5), 1442-1449; Colletti, L. P.; Stickney, J. L., Optimization of the growth of CdTe thin films formed by electrochemical atomic layer epitaxy in an automated deposition system. *Journal of the Electrochemical Society* **1998,** *145* (10), 3594-3602; Wade, T. L.; Sorenson, T., A.; Stickney, J. L.,

Epitaxial Compound Electrodeposition. In *Interfacial Electrochemistry*, Wieckowski, A., Ed. Marcel Dekker: New York, 1999; pp 757-768; Stickney, J. L., Electrochemical atomic layer epitaxy. *Electroanalytical Chemistry* **1999,** *21*, 75-209; Stickney, J. L., Electrochemical atomic layer epitaxy (EC-ALE): nanoscale control in the electrodeposition of compound semiconductors. *Advances in Electrochemical Science and Engineering* **2001,** *7*, 1-105; Flowers, B. H.; Wade, T. L.; Garvey, J. W.; Lay, M.; Happek, U.; Stickney, J. L., Atomic layer epitaxy of CdTe using an automated electrochemical thin-layer flow deposition reactor. *Journal of Electroanalytical Chemistry* **2002,** *524-525*, 273-285; Lay, M. D.; Stickney, J. L., EC-STM studies of Te and CdTe atomic layer formation from a basic Te solution. *Journal of the Electrochemical Society* **2004,** *151* (6), C431-C435.

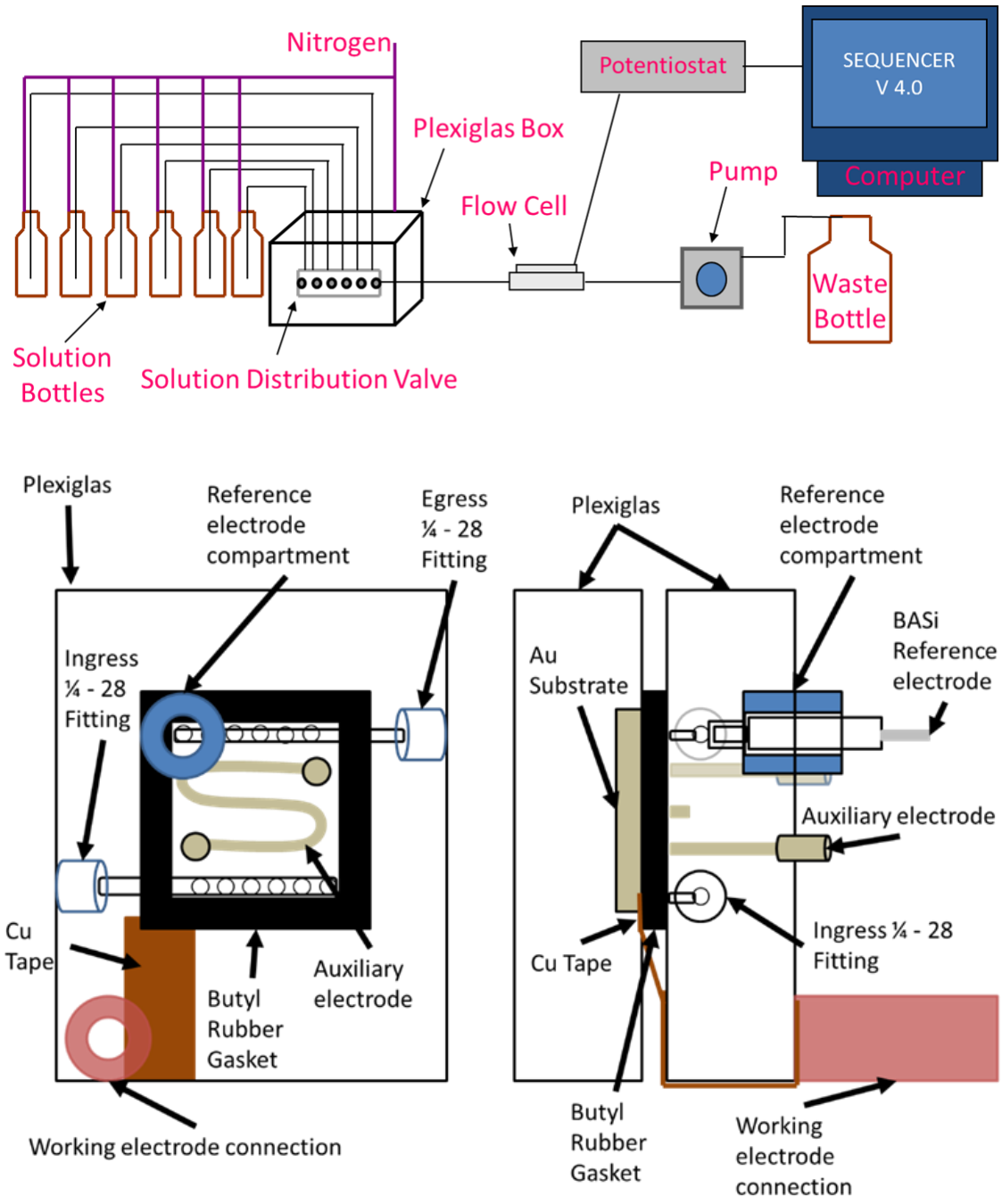

Figure 1.1 Schematics of the electrochemical flow cell deposition system and detailed view of the flow cell, Z cell. Solution is pulled from the solution bottles, through the distribution valve, into the cell (left to right, bottom to top).

CHAPTER 2

POTENTIAL PULSE ATOMIC LAYER DEPOSITION (PP-ALD) OF CU_2SE[1]

[1] J. M. Czerniawski, B. R. Perdue, J. L. Stickney, To be submitted to *Chemistry of Materials (2015)*

Abstract

Crystalline thin films of cuprous selenide (Cu_2Se) were electrodeposited at room temperature from an aqueous solution containing elemental precursors for Cu and Se, using a potential pulse version of atomic layer deposition (PP-ALD). Cyclic voltammetry (CV) was used to estimate Anodic and Cathodic cycle potentials for the formation of Cu_2Se, which were then examined to systematically optimize the cycle. Electron probe microanalysis (EPMA) was used to follow the Cu/Se atomic ratios as a function of the cycle parameters, and X-ray diffraction (XRD) was used to investigate deposit structure: polycrystalline orthorhombic Cu_2Se, with some cubic. Film thicknesses, from spectroscopic ellipsometry, were shown to be proportional to the number of cycles performed (0.02 nm/cycle), and SEM suggested the deposits were consistent with layer-by-layer growth as a function of the number of cycles.

Introduction

Electrodeposition is known as a low temperature, low-cost, and scalable thin film synthesis method. Compounds relevant to the formation of photovoltaics (PV) have been successfully grown using electrodeposition since the 70's.[1] The classic methodology is co-electrodeposition, described for CdTe deposition in work by Kroger et al..[2] The co-electrodeposition process is low-cost and simple, given the right solution chemistry. Many binary compounds have been formed using co-electrodeposition, at a controlled potential or current in a single solution containing precursors for both elements.[3] One of the drawbacks to co-electrodeposition is limited control over the process. The potential must be carefully controlled, within a few mV. In the case of CdTe deposition, it is

known that the type of semiconductor can change between n and p-type with a few mV change in potential.[4] In general post deposition annealing is required to form a crystalline material.[5]

CZTS denotes a range of kesterite-structured compounds, which are potential candidates as p-type absorbers in earth-abundant, nontoxic photovoltaics.[6-8] Cu_2ZnSnS_4 is the primary composition, though CZTSe and alloys of the two, with variable amounts of Se and S, have been created with direct bandgaps, tunable near 1.45 eV. Their solar absorption is high, with a single junction theoretical quantum efficiency of near 32%[9] and a demonstrated laboratory efficiency near 12.6%.[8-11] It has been formed using a variety of techniques, mostly involving high temperatures or pressures.[10, 12]

One synthetic methodology for the quaternary compound CZTS/Se involves sequential deposition of component binary compounds, such as copper selenide, zinc sulfide and tin sulfide followed by annealing. For example, sequential co-electrodeposition of binary sulfides and/or selenides, such as Cu_2Se, could be used to form a superlattice, which could then be annealed to form the desired kesterite structure. Compatible pairs of precursors would have to be identified to form the solutions used for co-electrodeposition of each binary.[1, 13, 14]

This report concerns investigations into the electrodeposition of Cu_2Se, a binary compound that could be used in the formation of CZTS. In addition, Cu_2Se itself has potential applications as a photovoltaic window material, in optical fibers, Li ion cells, thermoelectric converters, photo-thermal conversion devices, and microwave shield coatings.[15, 16] Cu_2Se has been formed using numerous techniques[8, 17], including a

hydrazine based process, though it required high temperatures and toxic materials.[8] Paraffin liquids have been used, but contain contaminating organics and control in deposition is limited.[18] In addition, melting, annealing, and spark plasma sintering compaction were investigated, but require precise measurements and high temperatures.[7] Despite the effectiveness of these techniques, they do not meet the necessary demands for an inexpensive, clean and safe deposition process that would help make solar a more competitive alternative to fossil fuels.

The author's group has been working on chemistries for the electrochemical growth of compound semiconductors for many years, and has developed an electrochemical version of atomic layer deposition (E-ALD).[19, 20] ALD refers to a group of deposition techniques where surface limited reactions are used to form deposits one atomic layer at a time. A cycle of these reactions is used to form a compound monolayer, and the cycle is repeated to grow thicker deposits. The vast majority of ALD studies have been performed in vacuum. E-ALD, however, is based on the use of precursor solutions made with ultrahigh purity water and electronic grade inorganic salts. Electrochemical surface limited reactions are referred to as underpotential deposition (UPD), a phenomenon where one element deposits on a second but not on itself, due to the free energy associated with surface compound or alloy formation.[21] In a typical E-ALD cycle, precursor solutions are sequentially introduced to the substrate at potentials that limit deposition to an atomic layer. After deposition of each atomic layer, the cell is rinsed with blank and the precursor solution for the second element is introduced. The advantages of using E-ALD rather than co-electrodeposition are increased control of the chemistry, thickness, homogeneity, and crystallinity of the deposit. The biggest drawback

is the slow deposition rate, as there are multiple solution exchanges each cycle. The technique is thus best applied when nanofilms of a carefully controlled thickness and quality are required and the total number of cycles performed is minimized.[20, 22] Given the time required to grow µm thick absorber layers, E-ALD is generally impractical compared with co-electrodeposition, which has been used by BP to commercially electrodeposit µm thick CdTe PV absorber layers.[5, 23]

Co-electrodeposition has been used to form a large number of other compounds[24], including CdSe.[25] Early CdSe co-electrodeposition studies indicated the presence of excess Se, for a Cd/Se ratio less than one.[26-28] Researchers were able to limit the deposition of Se by dropping the concentration or forming a complex with sulfite, thus shifting the Se deposition potential more negative. In a co-electrodeposition bath, however, a more negative Se deposition potential also increases the overpotential for Cd, resulting in deposits rich in Cd.[28, 29] A solution was proposed by Sailor et al., where instead of choosing a constant deposition potential, or current, rapid and repeated cyclic voltammetry, over a small range of potentials, was performed in a technique referred to as sequential monolayer electrodeposition (SMD).[27] The idea was to cycle between a negative potential where co-electrodeposition takes place, and a positive potential where any excess, bulk, Cd was oxidized away while Cd bound as CdSe was not. Traces of bulk cadmium formed at the more negative potentials were oxidatively removed at the positive end of each cycle. By scanning rapidly, the amounts deposited were kept in the monolayer range, and so any excess Cd was easily oxidized, not buried by the depositing CdSe. SMD has been used by Penner et al. to construct nanowire photo-sensors based on

CdSe.[14, 30] In addition, 3D macroporous structures of II-VI and III-V semiconductors were created using SMD by Lee and Chen et al..[31]

Pulse-reversal (PR) deposition is similar to SMD, but instead of a CV, the potential is pulsed cathodic, negative, to reduce the precursors and or surface oxide, and then anodic, positive, to equilibrate the depletion layer and remove unstable or dendritic material.[32] PR deposition was not designed for atomic layer control.

Another pulse method, proposed to control excess elemental deposition in $Bi_{2-x}Sb_xTe_3$ multilayers, was described by Banga et al..[33] Pulsed potentiostatic electrodeposition (PPE) is a diffusion limited, single-bath, co-electrodeposition process where a 2% duty cycle at the potential for compound formation was used, followed by open-circuit potential to regenerate the diffusion layer. PPE created highly crystalline deposits, though the "rest" times were significant.

This report describes a compound electrodeposition methodology inspired by SMD, PPE, E-ALD, co-electrodeposition, and PR deposition, and is referred to here as pulse potential atomic layer deposition (PP-ALD). Instead of changing solutions or using fast CV each cycle, the potential is alternated. As with E-ALD, sub-monolayer quantities are deposited each cycle, controlled by surface-limited reactions between the depositing elements. Selective stripping of any bulk elemental deposit formed is performed by controlling the Cathodic and Anodic pulse potentials and times.

During co-deposition, differences in diffusion coefficients, deposition kinetics and overpotentials between precursors can result in stoichiometry variations over time. To avoid such issues, deposits formed with PP-ALD limit the amounts deposited in a cycle

to some fraction of a compound monolayer, so that any excess deposition of an element during the Cathodic pulse would be left exposed to solution and selectively oxidized away during the Anodic pulse. This process thus serves as a surface limited reaction, leaving only the stable compound. Foreseeable benefits of this methodology are more control of stoichiometry during deposition, greatly increased deposition rates compared with E-ALD, increased scalability, more efficient use of reactants, and increased ease of solution recycling.

Experimental

The solution was pH 3, contained 1.5 mM $Cu(ClO_4)_2$ (98% purity from Sigma-Aldrich), 1.5 mM SeO_2 (Alfa Æsar 99.999% pure) and 0.5 M $NaClO_4$ in 18 MΩ Nanopure water (Millipore Advantage 10), fed by the house DI water source. Precursor concentrations were kept in the mM range to help limit deposited amounts to a fraction of a monolayer (ML) each cycle. A ML is defined for this report as one atom for each Au substrate surface atom, or about 1.2×10^{15} atoms per cm^2. Substrates were 100 nm thick Au films on 5 nm of Ti on glass, purchased from Evaporated Metal Films (Ithaca, NY), and were first cleaned by three 5 min sonication in fresh aliquots of acetone, then three in aliquots of Nanopure water. They were then dipped in concentrated nitric acid for 30 sec, rinsed with Nanopure water and dried with nitrogen before being placed in the electrochemical flow cell (Figure 2.1). The cell (Electrochemical ALD L.C.) was immediately flushed with 0.1 M H_2SO_4 (Fisher Scientific, certified ACS plus) and the potential was then alternated four times between +1400 mV and -200 mV, for 5 seconds at each potential, to complete cleaning of the Au surface.

Figure 2.1 is a diagram of the electrochemical flow cell used in these studies. The auxiliary electrode was an Au wire inlayed into the Plexiglas cell face. Cu tape was used to contact the working electrode to its post. The reference electrode was 3 M Ag/AgCl (BASi, West Lafayette, IN). Solutions were sucked from degassed solution reservoirs, though the ingress to the egress using a peristaltic pump.

Electron probe Microanalysis (EPMA) was performed on a JEOL 8600 Superprobe with a 10 KeV accelerating voltage, 15 nA beam current and 10 μm beam diameter. X-ray diffraction was performed on a PANalytical X'PERT Pro with an open Eulerian cradle utilizing a 1.54 Å Cu $K\alpha_1$ source and a parallel plate collimator. Scanning electron microscopy and energy dispersive X-ray spectroscopy (SEM-EDS) was performed on an FEI Inspect F FEG-SEM equipped with EDAX. Spectroscopic ellipsometry was performed on a J.A. Woolam M-200V.

Results and Discussion

Figure 2.2a is a window opening cyclic voltammetry (CV) study of Cu deposition on Au in 0.1 mM Cu^{2+} solution, pH 3. UPD began near 300 mV, and grew slowly into bulk Cu deposition, peaking near -150 mV. There are three oxidation features in the positive going scan, including bulk stripping at 50 mV, and two UPD stripping peaks near 200 mV. The formal potential, $E^{o'}$, was just negative of 0 mV in that Cu^{2+} ion solution, based on the zero current crossing potential in the positive going scan.

Figure 2.2b is a window opening study in a 0.1 mM $HSeO_3^-$ ion solution, pH 3. The $E^{o'}$ for $HSeO_3^-$ was near 550 mV, indicating that all Se deposition occurred at significant overpotentials, the result of slow deposition kinetics.[34] However, apparent

surface limited peaks, related to UPD, are evident at 275, 175 and 75 mV during the reduction scans. The oxidation peak positive of 600 mV corresponded to bulk stripping, while that at 775 mV was to surface limited stripping of Se. The oxidation peak at 925 mV demonstrates a fairly unique behavior. Normally, the most positive peak is associated with stripping the atoms most strongly bound to the surface, so the CVs negative to 200 (light blue) and 100 (orange) mV would be expected to display the most positive Se stripping peak seen at 925 mV, but they do not. The 925 mV oxidation peak only appeared when the potential was first scanned to 0 mV or below. The surface structure for electrodeposited Se on Au is known to change with increasing coverage.[35, 36] Previous work using in-situ EC-STM showed that a low coverage ($\sqrt{3}X\sqrt{3})R30°$ structure was formed on Au(111) with triangular defects at 1/3 ML, where the Se atoms were separated at distances near their van der Waals diameter, 0.50 nm.[35, 36, 37] At lower potentials a higher coverage structure, composed of eight member rings of Se, were formed with a coverage closer to 0.89 ML.[36] That is, at more negative potentials the adsorbed Se structure undergoes a phase change to a more densely packed, more stable structure. Such a phase change might explain the appearance of the peak at 925 mV and its apparent increased stability.

Figure 2.2c is a window opening study of an Au electrode, coated with a 0.6 ML Se adsorbed layer, in the Cu^{2+} ion solution. The voltammetry is very similar to that in Figure 2.2a, Cu deposition without Se, except that there is about twice as much Cu UPD, consistent with Cu UPD on the Se and the Au surface.

Figure 2.2d displays CVs for a pH 3 solution containing 1.5 mM Cu^{2+} and 1.5 mM $HSeO_3^-$. The first (red) scan starts negative from the open circuit potential (OCP),

550 mV. A reduction peak is evident at 350 mV, similar to the first reduction peak for Se deposition on Au (Figure 2.2b). No such peak was seen in Figure 2.2c since the Au had been precoated with Se. The reduction charge between 200 and 50 mV was similar to that in Figure 2.2c, where the electrode was precoated with Se. Below 50 mV, the reduction current increased rapidly, reaching 850 μA at -25 mV, after which the scan direction was reversed. The resulting oxidation peak at 50 mV was consistent with bulk Cu stripping (Figure 2.2a), followed by a feature between 100 and 350 mV resembling Cu UPD stripping from Au (Figure 2.2a) and Cu UPD striping from Se (Figure 2.2c). At 525 mV (Figure 2.2d) a small bulk Se oxidative stripping peak was evident, along with a similar peak, about 725 mV, consistent with oxidation of the low coverage, van der Waals packed, UPD like Se layer, noted in Figure 2.2b.

The second (black) cycle in Figure 2.2d was reversed at -100 mV. Note that the bulk Cu oxidation peak in the black cycle (75 mV) appears smaller than the peak in the red, though the subsequent peak for Cu stripping from Se in the black (300 mV) is twice that in the red. This suggests that at more negative potentials (black, -100 mV) a higher density of Se was available for Cu deposition. The first, presumably, bulk Se oxidation peak was present at 700 mV in the black, rather than the 625 mV in the first scan (red) suggesting a thicker Se layer with slower oxidation kinetics. This shift was consistent with the window opening shown in Figure 2.2b where a more negative scan deposited more Se and shifted the onset of bulk Se oxidation positively.

Based on the results shown in Figure 2.2, a potential cycle was developed, starting with a 0.13 s Cathodic pulse at -50 mV, where compound formation was expected (Figure 2.2d). The time was kept short in order to restrict deposition to a fraction of a

monolayer, so that excess Cu was not buried within the deposit. The Anodic potential pulse was 0.5 s at +50 mV, which was intended to oxidatively strip any excess Cu. The 0.5 s duration was also intended to helped the depletion layer equilibrate with the bulk solution. To assist in that process, fresh solution was continuously flowed through the cell at 4 mL/min. Figure 2.3 displays the potential cycle, as well as the resulting currents observed over five cycles. Figure 2.4 is a schematic of a PP-ALD cycle.

The thickness dependence of 3300 cycle deposits on the Anodic and Cathodic potentials is shown in Figure 2.5, from spectroscopic ellipsometry. In the black scan the Cathodic potential was held constant at -50 mV and the Anodic potential was varied. Decreasing the Anodic potential from 60 mV to -50 mV resulted in significant increases in the deposit thickness. 50 nm deposits resulted using an Anodic potential near 60 mV, while 160 nm deposits were formed when a -50 mV Anodic potential was used. The results suggest that more negative Anodic potentials lower the tendency for oxidative stripping of any bulk Cu formed at the Cathodic potential. In addition, at the more negative Anodic potentials, more deposition will occur during that pulse. In contrast, when the Anodic potential was held constant at 50 mV (Figure 2.5, red line) and the Cathodic potential was varied from -50 to 50 mV, the thickness varied little from 50 nm, showing much less sensitivity then observed with changes in the Anodic since any excess material not stabilized as a compound is removed.

The dependence of film stoichiometry on potential was investigated using EPMA. In Figure 2.6, the black line was obtained by holding the Cathodic potential at -50 mV and varying the Anodic potential between -50 and 60 mV, while the red line was obtained by holding the Anodic potential at 50 mV and varying the Cathodic between -50 and 50

mV. As with deposit thickness (Figure 2.5, red line), there was essentially no variation in stoichiometry as a function of the Cathodic potential, while the Anodic was held at 50 mV (Figure 2.6, red line), since any excess Cu is removed completely. EPMA indicated a stoichiometry of $Cu_{2.5}Se_1$ rather than the expected Cu_2Se_1 ratio, expected from the literature[15, 22] and by XRD. Subsequent analysis using the EDS system on a FEI Inspect SEM, however, indicated the expected Cu_2Se_1 ratio. Correction factor limitations and matrix effects, such as secondary Cu X-ray emission stimulated by Au substrate lines, appears to accounted for the discrepancy between EPMA and EDS.[38] EPMA results from thicker deposits support this conclusion, as they show stoichiometric ratios closer to 2, since the Au substrate is buried deeper and will contribute less to the stimulation of Cu signal (Figure 2.8, black).

Changes to the Anodic potential, while holding the Cathodic at -50 mV, produced a volcano curve in stoichiometry (Figure 2.6, black line) with a maximum Cu/Se ratio of 4.5 at 0 mV. That the ratio increased as the Anodic potential was decreased is consistent with removing less excess Cu at the Anodic potential. However, below 0 mV, the ratio starts to decrease, resulting in the lowest Cu/Se ratio when the Anodic potential was -50 mV. It is proposed that the slow kinetics for Se deposition increase at the more negative potentials, accounting for the increase in Se and a consequent drop in the Cu/Se ratio. At potentials below 0 mV, Cu deposition does not increase because it is already near the mass transfer limit.

To better understand how the deposits depended on the Anodic pulse time, a series of 3300 cycle deposits were formed using five different pulse times (Figure 2.7, Table 2.1). Based on the results described above, a Cathodic potential of -50 mV was

used, with an Anodic potential of +50 mV. The Cathodic pulse time was kept at 0.13 s, while the Anodic pulse was varied from 0.13 sec to 2 sec (Figure 2.7, Table 2.1). The deposits show macroscopic flow patterns, with the colors providing an indication of the deposit thickness, the film acting as interference filters. In the 0.13 s Anodic deposit (upper left, Figure 2.7), there are red, blue and yellow areas which are assumed to be thinner than the rest of the deposit. Over most of the deposit there are a series of 9 vertical stripes, dark at the bottom, become white in the middle, and light blue at the top. The brown smudges at the bottom of each vertical strip are an indication of excess growth at the ingress. That is, the fresh solution enters the cell at right angles, like a wall jet electrode, which leads to excessive growth and the formation of micron sized particles which scatter light, giving the appearance of smudges. The 9 vertical lines show that the flow was, for the most part, laminar between the 9 ingress and egress holes (see Figure 2.1). These observations were supported by EPMA measurements over the deposit.

Of the five deposits in Figure 2.7, the best was clearly the lower left, where the Anodic pulse was 0.5 s. The deposit showed no visible evidence of a flow pattern, which is consistent with deposition controlled by surface limited reactions, rather than convection. The deposits formed using Anodic pulse times of 1 and 2 s were thicker and rougher, as evidenced by their light scattering. In addition, the deposit formed using a 1 s Anodic pulse showed a brown “S” on an aqua background. The s-shape suggests the s-shaped auxiliary electrode (Figure 2.1) had some effect on the deposit. Previous studies of film growth of other materials using these “Z” cells resulted in similar figuring, usually connected with extensive bubble formation at the auxiliary electrode. A possible mechanism would be that as oxygen bubbles are formed on the auxiliary electrode, they

extend towards the deposit. The diffusion distance for the oxygen bubbles to the deposit decreases, and oxygen is known to interfere with the deposit.

Figure 2.8 shows the atomic ratios, from EPMA, at five positions across each deposit, from ingress to egress (Inlay). The green line was from the deposit where the Anodic pulse was 0.13 s/cycle, for a total deposition time of 14 min (Table 2.1), and shows a strong gradient in the Cu/Se ratio, from 4 at the ingress to 2 at the egress. On the other hand, the blue line is for the deposit where the Anodic pulse was 2 s, for a total deposition time of 117 min, and showed the expected Cu/Se ratio of 2 from ingress to egress. As noted above, the deposit where the Anodic pulse was 0.5 s, for a total deposition time of 35 min, was the most homogeneous.

One explanation of Figure 2.8 is that deposition was essentially diffusion limited while at the Cathodic potential (-50 mV), while at the Anodic potential (+50 mV) excess Cu was oxidatively stripped and some stoichiometric Cu_2Se growth occurred under more activation controlled conditions. The green line suggests that more deposition is occurring at the ingress, where the effect of convection is highest, and that deposition falls off as the solution flows towards the egress, and a depleted layer builds at the deposit surface. Some excess Cu is being stripped during the Anodic pulse, but there was not sufficient time to remove all the excess Cu near the ingress, where the amount was greater due to convection. As the Anodic pulse increased (0.5 s, orange line), complete removal of the excess Cu was achieved leaving a homogeneous deposit.

As previously stated, the orange line stoichiometry appears about 2.3 instead of 2 because of excessive Au substrate signal stimulating emission of more Cu signal, a

phenomenon not accounted for in the model used in the software. In the case of the blue line, all the excess Cu is removed during the 2 s Anodic pulse, and stoichiometric Cu_2Se growth during the Anodic pulse continued for 1.5 s/cycle longer than for the orange line. The blue line deposit was thus thicker, burying the Au and producing less of the extra Cu signal.

Glancing angle XRD measurements were performed (Figure 2.9) on the deposits shown in Figure 2.7, where the Anodic pulse was +50 mV and the time was varied, and the Cathodic pulse was -50 mV and was constant. The pattern in yellow was for the homogeneous deposit form with an Anodic pulse of 0.5 s. The patterns were consistent with a mixture of orthorhombic and cubic Cu_2Se polycrystalline deposits, predominately ortho- (orthorhombic card number 19-0401, cubic card number 01-071-0044).

Figure 2.10 is a graph of thickness vs. the number of cycles performed, measured using spectroscopic ellipsometry. Ideally, for smooth deposits, doubling the number of cycles should double the thickness for an ALD process, and the linear trend is consistent layer by layer growth, indicating a 0.02 nm/cycle growth rate.

Figure 2.11 shows the increase in particle size with the number of cycles. The grain growth appears consistent with layer-by-layer growth on the polycrystalline Au surface, if increasing numbers of cycles lead to grains subsuming their boundaries as they increase in size.

Conclusion

Deposits of Cu_2Se over a range of thicknesses were formed using PP-ALD, an electrochemical form of ALD, based on potential pulses. XRD showed the deposits to be

polycrystalline orthorhombic films, with possibly a trace of cubic, as deposited. The dependence of the deposit thickness and stoichiometry as a function of the Cathodic and Anodic pulse potentials were investigated as well as the dependence on the time used for the Anodic pulse. Deposit homogeneity was investigated visually, as well as by using EPMA to measure the stoichiometry across the deposits. The optimum deposition conditions from these studies were concluded to be 0.13 s pulse to -50 mV followed by a 0.5 s pulse to +50 mV repeated to achieve the desired thickness. The linear growth with the number of cycles was consistent with a layer by layer growth process, and the pulsing served to achieve the control expected from a surface limited process.

Acknowledgments

Support from the National Science Foundation, DMR #1410109, is gratefully acknowledged. Thanks to Chris Fleisher and the UGA Microprobe lab. Thanks to the Integrated Bioscience and Nanotechnology Cleanroom for the use of their facilities. Thanks to Dr. Rachelle Arnold, Jeremy Yatvin, Dr. Evan White, and Dr. Jason Locklin for helpful discussions regarding SE, SEM, and AFM. Thanks to Darrah Johnson-McDaniel, Dr. Tim Pope, Matt Davidson, and Dr. Tina Salguero for the use of their AFM, X-ray powder pattern database, and helpful discussion. Thanks to Yen-Jun and Dr. Zhengwei Pan for allowing the use of their SEM.

References

1. Kröger, F. A., Cathodic Deposition and Characterization of Metallic or Semiconducting Binary Alloys or Compounds. *Journal of The Electrochemical Society* **1978,** *125* (12), 2028-2034.
2. Panicker, M. P. R.; Knaster, M.; Kroger, F. A., Cathodic Deposition Of CdTe From Aqueous-Electrolytes. *Journal of the Electrochemical Society* **1978,** *125* (4), 566-572.
3. Hodes, G.; Engelhard, T.; Herrington, C. R.; Kazmerski, L. L.; Cahen, D., Electrodeposited layers of CuInS2, CuIn5S8, and CuInSe2. *Progr. Cryst. Growth Charact.* **1985,** *10*, 345; Hodes, G.; Cahen, D., Electrodeposition of CuInSe2 and CuInS2 films. *Solar Cells* **1986,** *16*, 245; Yuan, T.; Li, Y.; Jia, M.; Lai, Y.; Li, J.; Liu, F.; Liu, Y., Fabrication of Cu2ZnSnS4 thin film solar cells by sulfurization of electrodeposited stacked binary Cu–Zn and Cu–Sn alloy layers. *Materials Letters* **2015,** *155*, 44-47.
4. Turner, A. K.; Woodcock, J. M.; Ozsan, M. E.; Summers, J. G.; Barker, J.; Binns, S.; Buchanan, K.; Chai, C.; Dennison, S.; Hart, R.; Johnson, D.; Marshall, R.; Oktik, S.; Patterson, M.; Perks, R.; Roberts, S.; Sadeghi, M.; Sherborne, J.; Szubert, J.; Webster, S., Stable, high efficiency thin film solar cells produced by electrodeposition of cadmium telluride. *Solar Energy Materials* **1991,** *23* (2), 388-393.
5. Cunningham, D.; Rubcich, M.; Skinner, D., Cadmium telluride PV module manufacturing at BP Solar. *Prog. Photovoltaics* **2002,** *10* (2), 159-168.

6. Wadia, C.; Alivisatos, A. P.; Kammen, D. M., Materials Availability Expands the Opportunity for Large-Scale Photovoltaics Deployment. *Environmental Science & Technology* **2009,** *43* (6), 2072-2077.

7. Ballikaya, S.; Chi, H.; Salvador, J. R.; Uher, C., Thermoelectric properties of Ag-doped Cu2Se and Cu2Te. *Journal of Materials Chemistry A* **2013,** *1* (40), 12478-12484.

8. Todorov, T. K.; Tang, J.; Bag, S.; Gunawan, O.; Gokmen, T.; Zhu, Y.; Mitzi, D. B., Beyond 11% Efficiency: Characteristics of State-of-the-Art Cu2ZnSn(S,Se)4 Solar Cells. *Advanced Energy Materials* **2013,** *3* (1), 34-38.

9. Suryawanshi, M. P.; Agawane, G. L.; Bhosale, S. M.; Shin, S. W.; Patil, P. S.; Kim, J. H.; Moholkar, A. V., CZTS based thin film solar cells: a status review. *Materials Technology* **2013,** *28* (1/2), 98-109.

10. Hongxia, W., Progress in Thin Film Solar Cells Based on Cu2ZnSnS4. *International Journal of Photoenergy* **2011**, 1-10; Wangperawong, A.; King, J. S.; Herron, S. M.; Tran, B. P.; Pangan-Okimoto, K.; Bent, S. F., Aqueous bath process for deposition of Cu2ZnSnS4 photovoltaic absorbers. *Thin Solid Films* **2011,** *519* (8), 2488-2492.

11. Kask, E.; Raadik, T.; Grossberg, M.; Josepson, R.; Krustok, J., Deep defects in Cu2ZnSnS4 monograin solar cells. *Energy Procedia* **2011,** *10* (0), 261-265; Minlin, J.; Dhakal, R.; Yong, L.; Thapaliya, P.; Xingzhong, Y. In *Cu2ZnSnS4 (CZTS) polycrystalline thin films prepared by sol-gel method*, Photovoltaic Specialists Conference (PVSC), 2011 37th IEEE, 19-24 June 2011; 2011; pp 001283-001286; Bär, M.; Schubert, B.-A.; Marsen, B.; Wilks, R. G.; Blum, M.;

Krause, S.; Pookpanratana, S.; Zhang, Y.; Unold, T.; Yang, W.; Weinhardt, L.; Heske, C.; Schock, H.-W., Cu2ZnSnS4 thin-film solar cell absorbers illuminated by soft x-rays. *Journal of Materials Research* **2012,** *27* (08), 1097-1104; Zhao, Y.; Burda, C., Development of plasmonic semiconductor nanomaterials with copper chalcogenides for a future with sustainable energy materials. *Energy & Environmental Science* **2012,** *5* (2), 5564-5576; Qijie, G.; Yanyan, C.; Caspar, J. V.; Farneth, W. E.; Ionkin, A. S.; Johnson, L. K.; Meijun, L.; Malajovich, I.; Radu, D.; Choudhury, K. R.; Rosenfeld, H. D.; Wei, W. In *A simple solution-based route to high-efficiency CZTSSe thin-film solar cells*, Photovoltaic Specialists Conference (PVSC), 2012 38th IEEE, 3-8 June 2012; 2012; pp 002993-002996; Chen, S.; Walsh, A.; Gong, X.-G.; Wei, S.-H., Classification of Lattice Defects in the Kesterite Cu2ZnSnS4 and Cu2ZnSnSe4 Earth-Abundant Solar Cell Absorbers. *Advanced Materials* **2013,** *25* (11), 1522-1539; Wang, W.; Winkler, M. T.; Gunawan, O.; Gokmen, T.; Todorov, T. K.; Zhu, Y.; Mitzi, D. B., Device Characteristics of CZTSSe Thin-Film Solar Cells with 12.6% Efficiency. *Advanced Energy Materials* **2014,** *4* (7), n/a-n/a.

12. Nitsche, R.; Sargent, D. F.; Wild, P., Crystal growth of quaternary 122464 chalcogenides by iodine vapor transport. *Journal of Crystal Growth* **1967,** *1* (1), 52-53; Steinhagen, C.; Panthani, M. G.; Akhavan, V.; Goodfellow, B.; Koo, B.; Korgel, B. A., Synthesis of Cu2ZnSnS4 Nanocrystals for Use in Low-Cost Photovoltaics. *J. Am. Chem. Soc.* **2009,** *131* (35), 12554-+; Prabhakar, T.; Nagaraju, J. In *Device parameters of Cu2ZnSnS4 thin film solar cell*, Photovoltaic Specialists Conference (PVSC), 2011 37th IEEE, 19-24 June 2011; 2011; pp

001346-001351; Ahmed, S.; Reuter, K. B.; Gunawan, O.; Guo, L.; Romankiw, L. T.; Deligianni, H., A High Efficiency Electrodeposited Cu2ZnSnS4 Solar Cell. *Advanced Energy Materials* **2012,** *2* (2), 253-259; Shin, B.; Gunawan, O.; Zhu, Y.; Bojarczuk, N. A.; Chey, S. J.; Guha, S., Thin film solar cell with 8.4% power conversion efficiency using an earth-abundant Cu2ZnSnS4 absorber. *Progress in Photovoltaics: Research and Applications* **2013,** *21* (1), 72-76; Tatsuo, F.; Shin, T.; Tadayoshi, I., Enhancement of Conversion Efficiency of Cu 2 ZnSnS 4 Thin Film Solar Cells by Improvement of Sulfurization Conditions. *Applied Physics Express* **2013,** *6* (6), 062301.

13. Sato, N.; Ichimura, M.; Arai, E.; Yamazaki, Y., Characterization of electrical properties and photosensitivity of SnS thin films prepared by the electrochemical deposition method. *Solar Energy Materials and Solar Cells* **2005,** *85* (2), 153-165; Mathews, N. R.; Anaya, H. B. M.; Cortes-Jacome, M. A.; Angeles-Chavez, C.; Toledo-Antonio, J. A., Tin Sulfide Thin Films by Pulse Electrodeposition: Structural, Morphological, and Optical Properties. *Journal of The Electrochemical Society* **2010,** *157* (3), H337-H341; Caballero-Briones, F.; Palacios-Padrós, A.; Sanz, F., CuInSe2 films prepared by three step pulsed electrodeposition. Deposition mechanisms, optical and photoelectrochemical studies. *Electrochimica Acta* **2011,** *56* (26), 9556-9567.

14. Liu, F.; Huang, C.; Lai, Y.; Zhang, Z.; Li, J.; Liu, Y., Preparation of Cu(In,Ga)Se2 thin films by pulse electrodeposition. *Journal of Alloys and Compounds* **2011,** *509* (8), L129-L133.

15. Gosavi, S. R.; Deshpande, N. G.; Gudage, Y. G.; Sharma, R., Physical, optical and electrical properties of copper selenide (CuSe) thin films deposited by solution growth technique at room temperature. *Journal of Alloys and Compounds* **2008,** *448* (1–2), 344-348; Liu, K.; Liu, H.; Wang, J.; Shi, L., Synthesis and characterization of Cu2Se prepared by hydrothermal co-reduction. *Journal of Alloys and Compounds* **2009,** *484* (1–2), 674-676.

16. Yahia, I. S.; Fadel, M.; Sakr, G. B.; Shenouda, S. S., Memory switching of ZnGa2Se4 thin films as a new material for phase change memories (PCMs). *Journal of Alloys and Compounds* **2010,** *507* (2), 551-556; Ramesh, K.; Bharathi, B.; Thanikaikarasan, S.; Mahalingam, T.; Sebastian, P., Growth and Characterization of Electroplated Copper Selenide Thin Films. *Journal Of New Materials For Electrochemical Systems* **2013,** *16* (2), 127-132.

17. Bosio, A.; Romeo, N.; Mazzamuto, S.; Canevari, V., Polycrystalline CdTe thin films for photovoltaic applications. *Progress in Crystal Growth and Characterization of Materials* **2006,** *52* (4), 247-279; Jafarov, M. A.; Nasirov, E. F. In *Properties of the thin-film solar cells with heterojunctions Cu2S-Cd1-xZnxS and Cu2Se-Cd1-xZnxSe*, 2012; pp 84700I-84700I-5.

18. Deng, Z.; Mansuripur, M.; Muscat, A. J., Synthesis of two-dimensional single-crystal berzelianite nanosheets and nanoplates with near-infrared optical absorption. *Journal of Materials Chemistry* **2009,** *19* (34), 6201-6206.

19. D. W. Suggs, I. V., B.W. Gregory, J.L. Stickney, Formation of CdTe and GaAs by electrochemical atoimc layer epitaxy (ECALE). *Mat. Res. Soc. Symp. Proc.* **1991,** *222*, 283; Colletti, L. P.; Stickney, J. L., II-VI compound semiconductor

thin-film electrodeposition by ECALE. *Book of Abstracts, 210th ACS National Meeting, Chicago, IL, August 20-24* **1995,** (Pt. 1), INOR-297; Colletti, L. P.; Flowers, B. H.; Stickney, J. L., Formation of Thin-Films of CdTe, CdSe, and CdS by Electrochemical ALE. *JECS* **1997**; Colletti, L. P.; Slaughter, R.; Stickney, J. L., ZnS thin film formation by electrochemical ALE: preliminary doping studies. *Proceedings - Electrochemical Society* **1997,** *97-20* (Photoelectrochemistry), 1-10; Perdue, B.; Czerniawski, J.; Anthony, J.; Stickney, J., Optimization of Te Solution Chemistry in the Electrochemical Atomic Layer Deposition Growth of CdTe. *Journal of The Electrochemical Society* **2014,** *161* (7), D3087-D3092.

20. Banga, D.; Jarayaju, N.; Sheridan, L.; Kim, Y.-G.; Perdue, B.; Zhang, X.; Zhang, Q.; Stickney, J., Electrodeposition of CuInSe2 (CIS) via Electrochemical Atomic Layer Deposition (E-ALD). *Langmuir* **2012,** *28* (5), 3024-3031.

21. Kolb, D. M., Physical and Electrochemical Properties of Metal Monolayers on Metallic Substrates. In *Advances in Electrochemistry and Electrochemical Engineering*, Gerischer, H.; Tobias, C. W., Eds. John Wiley: New York, 1978; Vol. 11, p 125; Juttner; K.; Lorenz; W.J., *Z. Phys. Chem. N. F.* **1980,** *122,* 163; Adzic, R. R., Electrocatalytic Properties of the Surfaces Modified by Foreign Metal Ad Atoms. In *Advances in Electrochemistry and Electrochemical Engineering*, Gerishcher, H.; Tobias, C. W., Eds. Wiley-Interscience: New York, 1984; Vol. 13, p 159; Gewirth, A. A.; Niece, B. K., Electrochemical applications of in situ scanning probe microscopy. *Chem. Rev.* **1997,** *97,* 1129-1162.

22. Vaidyanathan, R.; Mathe, M. K.; Sprinkle, P.; Cox, S. M.; Happek, U.; Stickney, J. L., Electrodeposition of Cu2Se thin films by electrochemical atomic layer

epitaxy (EC-ALE). *Materials Research Society Symposium Proceedings* **2003,** *744* (Progress in Semiconductors II--Electronic and Optoelectronic Applications), 289-294.

23. Turner, A. K.; Woodcock, J. M.; Ozsan, M. E.; Cunningham, D. W.; Johnson, D. R.; Marshall, R. J.; Mason, N. B.; Oktik, S.; Patterson, M. H.; Ransome, S. J.; Roberts, S.; Sadeghi, M.; Sherborne, J. M.; Sivapathasundaram, D.; Walls, I. A., Bp Solar Thin-Film Cdte Photovoltaic Technology. *Sol. Energy Mater.* **1994,** *35* (1-4), 263-270.

24. Öznülüer, T.; Erdoğan, İ.; Şişman, İ.; Demir, Ü., Electrochemical Atom-by-Atom Growth of PbS by Modified ECALE Method. *Chemistry of Materials* **2005,** *17* (5), 935-937; Öznülüer, T.; Erdoğan, İ.; Demir, Ü., Electrochemically Induced Atom-by-Atom Growth of ZnS Thin Films: A New Approach for ZnS Co-deposition. *Langmuir* **2006,** *22* (9), 4415-4419.

25. Loizos, Z.; Mitsis, A.; Spyrellis, N.; Froment, M.; Maurin, G., Cadmium chalcogenide semiconducting thin films prepared by electrodeposition from boiling aqueous electrolytes. *Thin Solid Films* **1993,** *235* (1-2), 51-56.

26. Kazacos, M. S.; Miller, B., Studies in Selenious Acid Reduction and CdSe Film Deposition. *Journal of The Electrochemical Society* **1980,** *127* (4), 869-873; Skyllas Kazacos, M.; Miller, B., Electrodeposition of CdSe Films from Selenosulfite Solution. *Journal of The Electrochemical Society* **1980,** *127* (11), 2378-2381; Houston, G. J.; McCann, J. F.; Haneman, D., Optimising the photoelectrochemical performance of electrodeposited CdSe semiconductor electrodes. *Journal of Electroanalytical Chemistry and Interfacial*

Electrochemistry **1982,** *134* (1), 37-47; Tomkiewicz, M.; Ling, I.; Parsons, W. S., Morphology, Properties, and Performance of Electrodeposited n - CdSe in Liquid Junction Solar Cells. *Journal of The Electrochemical Society* **1982,** *129* (9), 2016-2022; Skyllas-Kazacos, M., Electrodeposition of CdSe and CdSe+CdTe thin films from cyanide solutions. *Journal of Electroanalytical Chemistry and Interfacial Electrochemistry* **1983,** *148* (2), 233-239; Wei, C.; Bose, C. S. C.; Rajeshwar, K., Compositional analysis of electrosynthesized semiconductor thin films by electrochemical quartz crystal microgravimetry: Application to the Cd + Se system. *Journal of Electroanalytical Chemistry* **1992,** *327* (1–2), 331-336.

27. Kressin, A. M.; Doan, V. V.; Klein, J. D.; Sailor, M. J., Synthesis of stoichiometric CdSe films via sequential monolayer electrodeposition. *Chem. Mater.* **1991,** *3*, 1015-1020.

28. Ham, D.; Mishra, K. K.; Rajeshwar, K., Anodic electrosynthesis of CdSe thin-films: Characterization and comparison with the passive/transpassive behavior of the CdX (X= S, Te) counterparts. *J. Electrochem. Soc.* **1991,** *138*, 100.

29. Cocivera, M.; Darkowski, A.; Love, B., Thin Film CdSe Electrodeposited from Selenosulfite Solution. *Journal of The Electrochemical Society* **1984,** *131* (11), 2514-2517; Loizos, Z.; Spyrellis, N.; Maurin, G.; Pottier, D., Semiconducting CdSex, Te1−x thin films prepared by electrodeposition. *Journal of Electroanalytical Chemistry and Interfacial Electrochemistry* **1989,** *269* (2), 399-410; Krishnan, V.; Ham, D.; Mishra, K. K.; Rajeshwar, K., Electrosynthesis of thin films of CdZnSe: composition modulation and bandgap engineering in the ternary system. *J. Electrochem. Soc.* **1992,** *139*, 23; Krishnan, V.; Ham, D.;

Mishra, K. K.; Rajeshwar, K., Electrosynthesis of Thin Films of CdZnSe : Composition Modulation and Bandgap Engineering in the Ternary System. *Journal of The Electrochemical Society* **1992,** *139* (1), 23-27.

30. Ayvazian, T.; van der Veer, W. E.; Xing, W.; Yan, W.; Penner, R. M., Electroluminescent, Polycrystalline Cadmium Selenide Nanowire Arrays. *ACS Nano* **2013,** *7* (10), 9469-9479.

31. Lee, Y.-C.; Kuo, T.-J.; Hsu, C.-J.; Su, Y.-W.; Chen, C.-C., Fabrication of 3D Macroporous Structures of II−VI and III−V Semiconductors Using Electrochemical Deposition. *Langmuir* **2002,** *18* (25), 9942-9946.

32. Swaminathan, V.; Murali, K. R., Influence of pulse reversal on the PEC performance of pulse-plated CdSe films. *Solar Energy Materials and Solar Cells* **2000,** *63* (2), 207-216; Tang, P. T., Pulse reversal plating of nickel and nickel alloys for microgalvanics. *Electrochimica Acta* **2001,** *47* (1–2), 61-66; Chandrasekar, M. S.; Pushpavanam, M., Pulse and pulse reverse plating—Conceptual, advantages and applications. *Electrochimica Acta* **2008,** *53* (8), 3313-3322; Lin, J.-Y.; Tsai, Y.-T.; Tai, S.-Y.; Lin, Y.-T.; Wan, C.-C.; Tung, Y.-L.; Wu, Y.-S., Pulse-Reversal Deposition of Cobalt Sulfide Thin Film as a Counter Electrode for Dye-Sensitized Solar Cells. *Journal of The Electrochemical Society* **2013,** *160* (2), D46-D52.

33. Banga, D.; Lensch-Falk, J. L.; Medlin, D. L.; Stavila, V.; Yang, N. Y. C.; Robinson, D. B.; Sharma, P. A., Periodic Modulation of Sb Stoichiometry in Bi2Te3/Bi2–xSbxTe3 Multilayers Using Pulsed Electrodeposition. *Crystal Growth & Design* **2012,** *12* (3), 1347-1353.

34. Lister, T. E.; Huang, B. M.; Herrick, R. D.; Stickney, J. L., Electrochemical Formation of Se Atomic Layers On Au(100). *Journal of Vacuum Science & Technology B* **1995,** *13* (3), 1268; Lister, T. E.; Stickney, J. L., Atomic level studies of selenium electrodeposition on gold (111) and gold (110). *Journal of Physical Chemistry* **1996,** *100* (50), 19568-19576; Huang, B. M.; Lister, T. E.; Stickney, J. L., Se adlattices formed on Au (100), studies by LEED, AES, STM and electrochemistry. *Surface Science* **1997,** *392* (1-3), 27.

35. Lister, T. E.; Stickney, J. L., Atomic Level Studies of Selenium Electrodeposition on Gold(111) and Gold(110). *The Journal of Physical Chemistry* **1996,** *100* (50), 19568-19576.

36. Sorenson, T. A.; Lister, T. E.; Huang, B. M.; Stickney, J. L., A Comparison of Atomic Layers Formed by Electrodeposition of Selenium and Tellurium Scanning Tunneling Microscopy Studies on Au(100) and Au(111). *Journal of The Electrochemical Society* **1999,** *146* (3), 1019-1027.

37. Pauling, L., *The Nature of the Chemical Bond and the Structure of Molecules and Crystals: An Introduction to Modern Structural Chemistry*. Cornell University Press: 1960.

38. Thompson, A. C.; Vaughan, D.; optics, C. f. X.-r.; source, a. l., *X-ray Data Booklet*. Lawrence Berkeley Laboratory: 2001.

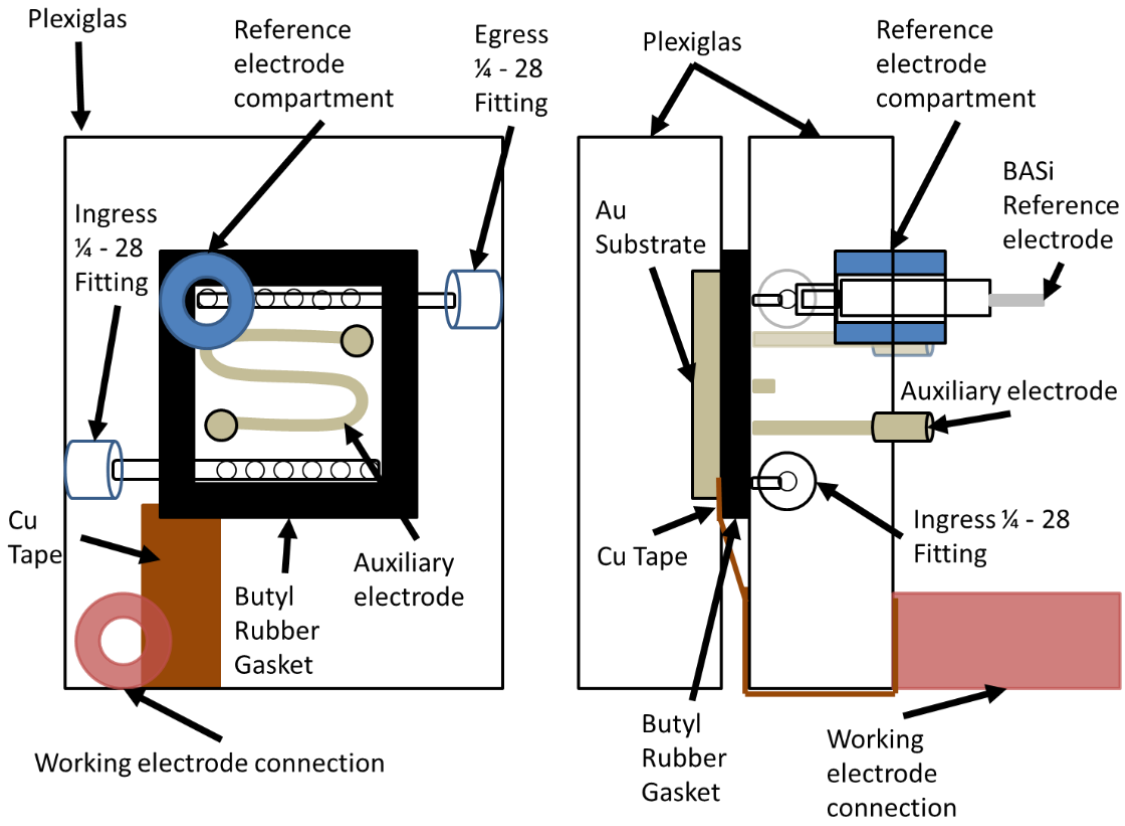

Figure 2.1: Schematic of the electrochemical flow cell, Z cell, as the solution enters left to right through the bottom row of holes, and exits the cell left to right through the top row of holes. Simulations have shown this configuration to result in a fairly homogeneous flow field.

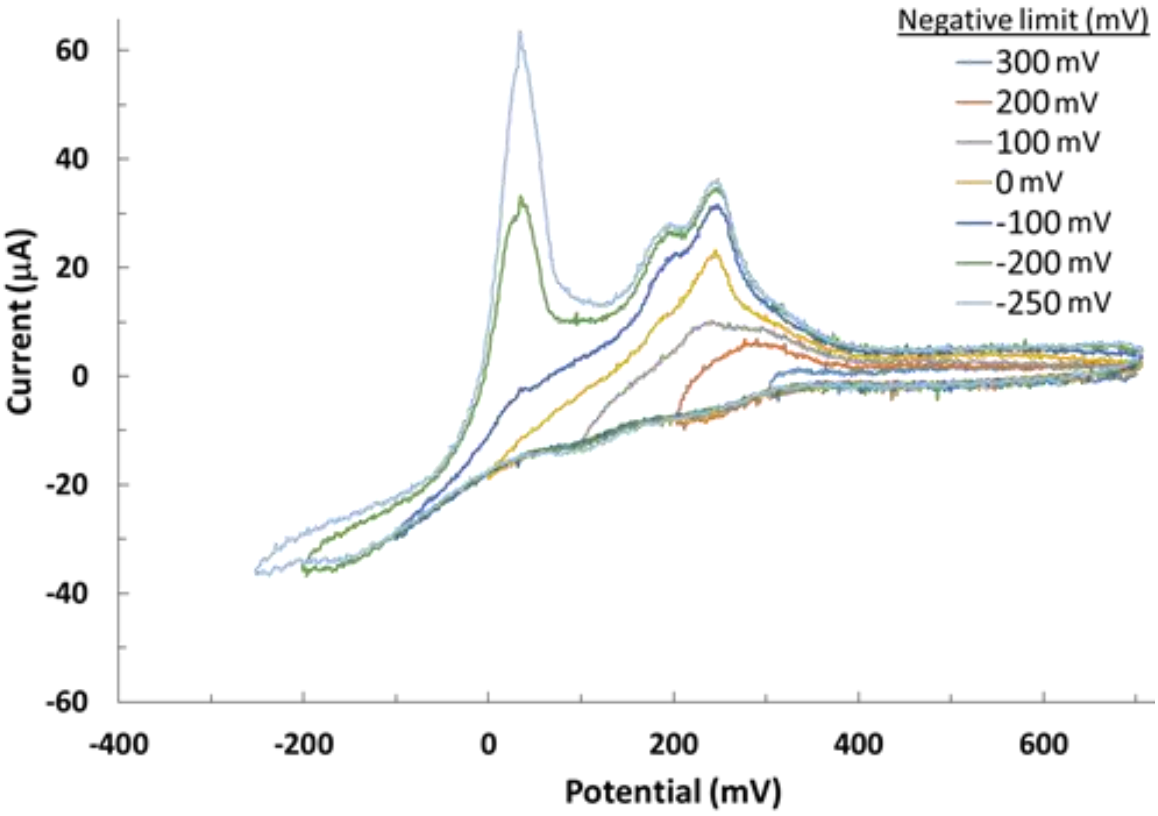

Figure 2.2a: CVs for a 1.82 cm^2 Au electrode in 0.1mM $Cu(ClO_4)_2$, pH 3, vs. a Ag/AgCl reference electrode, at a scan rate of 10 mV/sec. The flow rate was 0.5 mL/min.

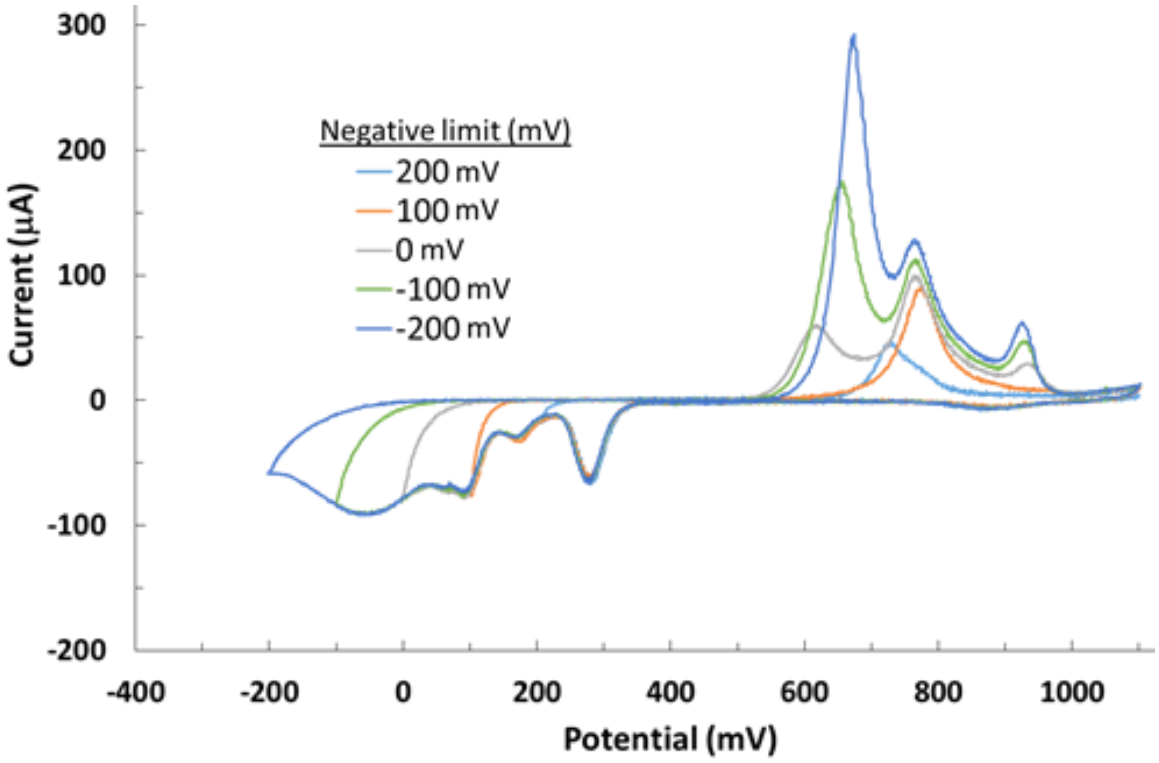

Figure 2.2b: CVs for a 1.82 cm^2 Au electrode in 0.1 mM SeO_2, pH 3, vs. an Ag/AgCl reference electrode, at a scan rate of 10 mV/sec. The flow rate 0.5 mL/min.

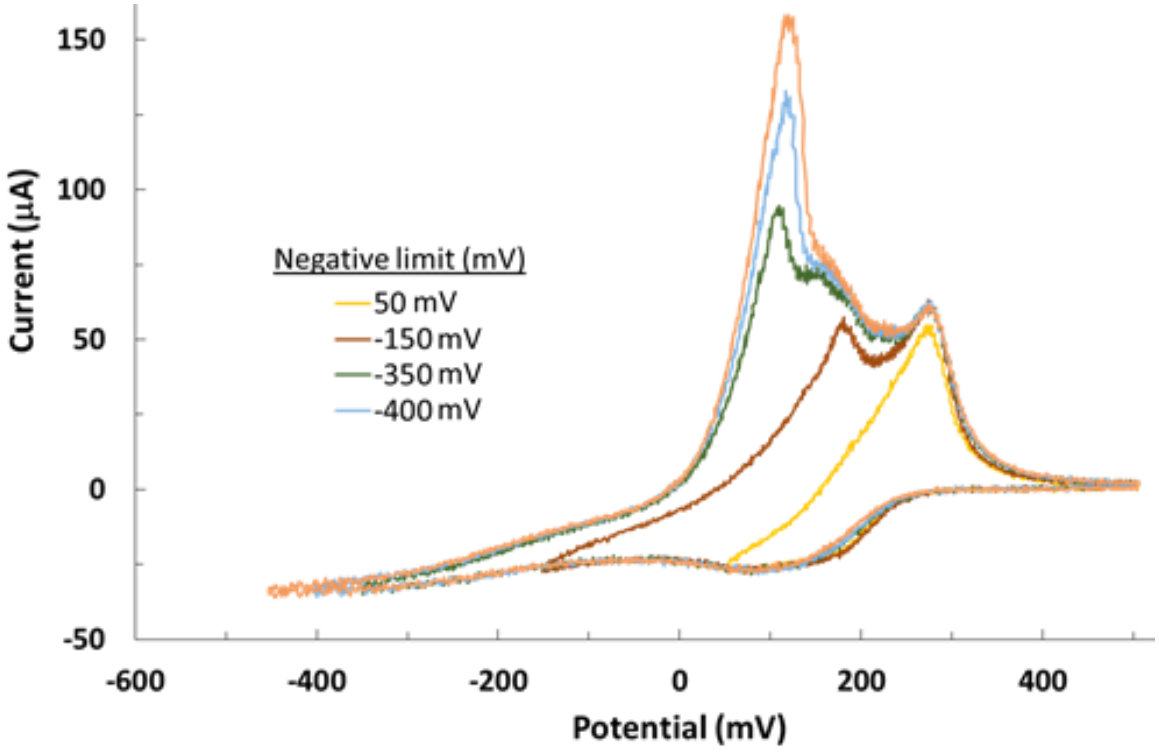

Figure 2.2c: CVs for a 1.82 cm^2 Au electrode, coated with a 0.6 ML of Se, in 0.1mM $Cu(ClO_4)_2$, pH 3, vs. an Ag/AgCl reference electrode, at a scan rate of 10 mV/sec. The flow rate was 0.5 mL/min.

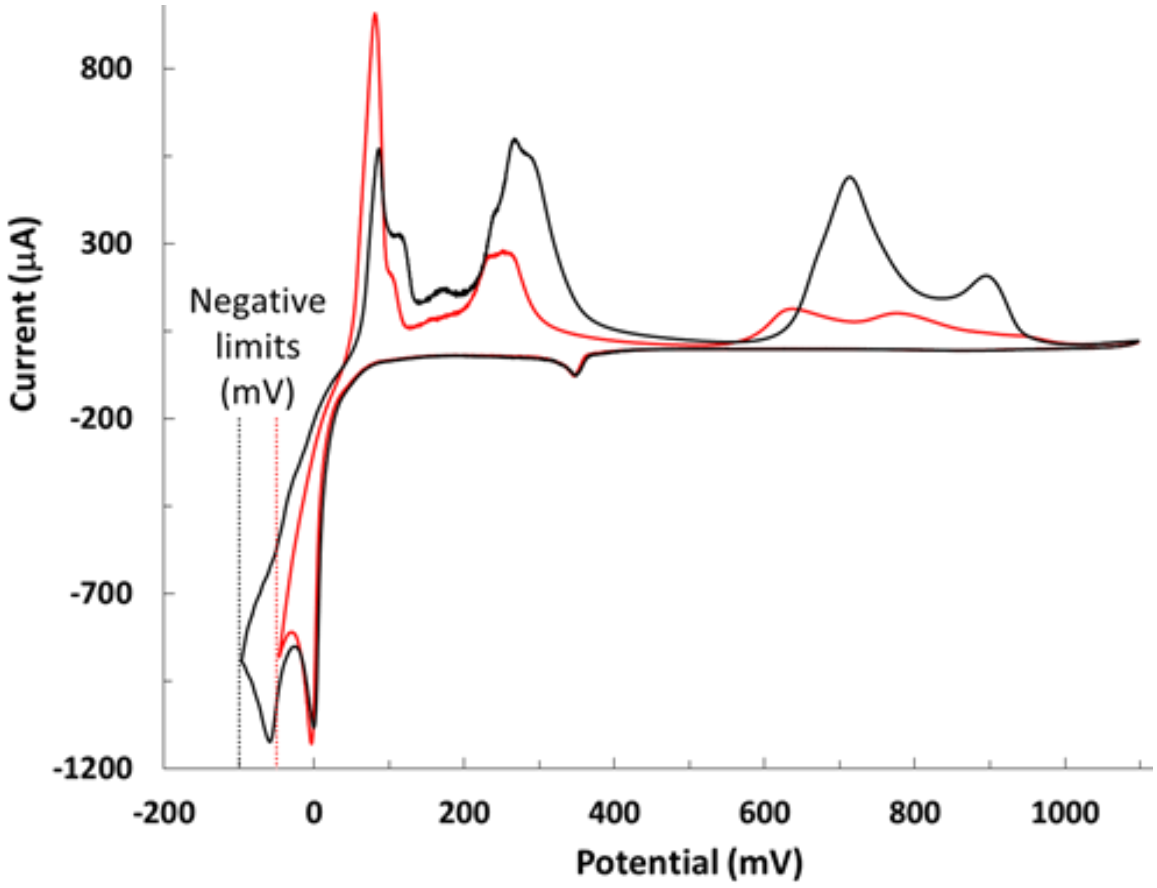

Figure 2.2d: CVs for a 2.1 cm^2 Au electrode in 1.5 mM $Cu(ClO_4)_2$, 1.5 mM SeO_2 and 0.5 M $NaClO_4$, at pH 3, vs. an Ag/AgCl reference electrode, at a scan rate of 10 mV/sec. The flow rate was 4 mL/min.

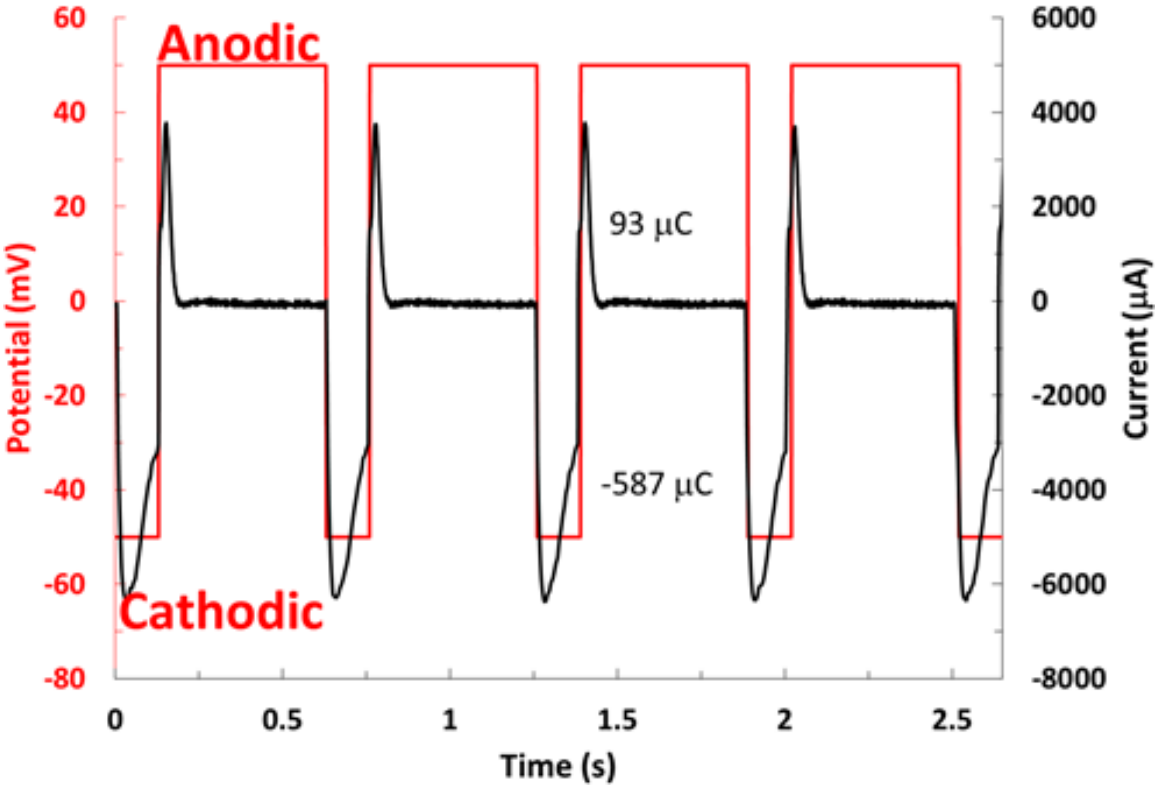

Figure 2.3: Potential (red) and current (black) profiles for 5 PP-ALD cycles. The cycle begins with the Cathodic potential, -50 mV, for 0.13 sec. Fractions of a monolayer of Se and Cu were deposited. The potential was then stepped to the Anodic potential, +50 mV, where excess Cu was oxidatively stripped.

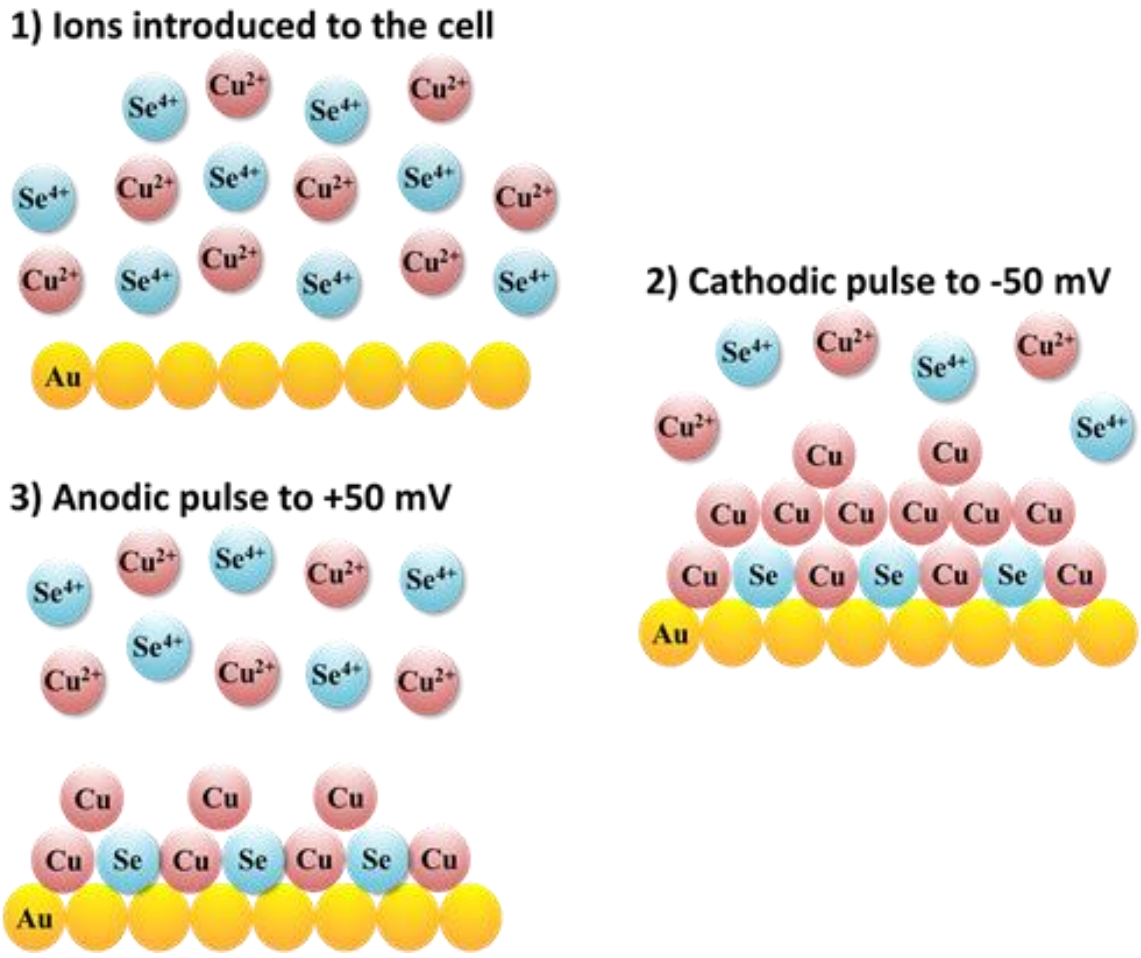

Figure 2.4: PP-ALD Diagram. 1) Cu^{2+} (red) and Se^{4+} (blue) ions are introduced into the cell at OCP. 2) The potential was then pulsed to -50 mV for 0.13 s, resulting in the deposition of less than a monolayer of Se and excess Cu. 3) The potential was then stepped to +50 mV for 0.5 s, removing excess Cu from the deposit.

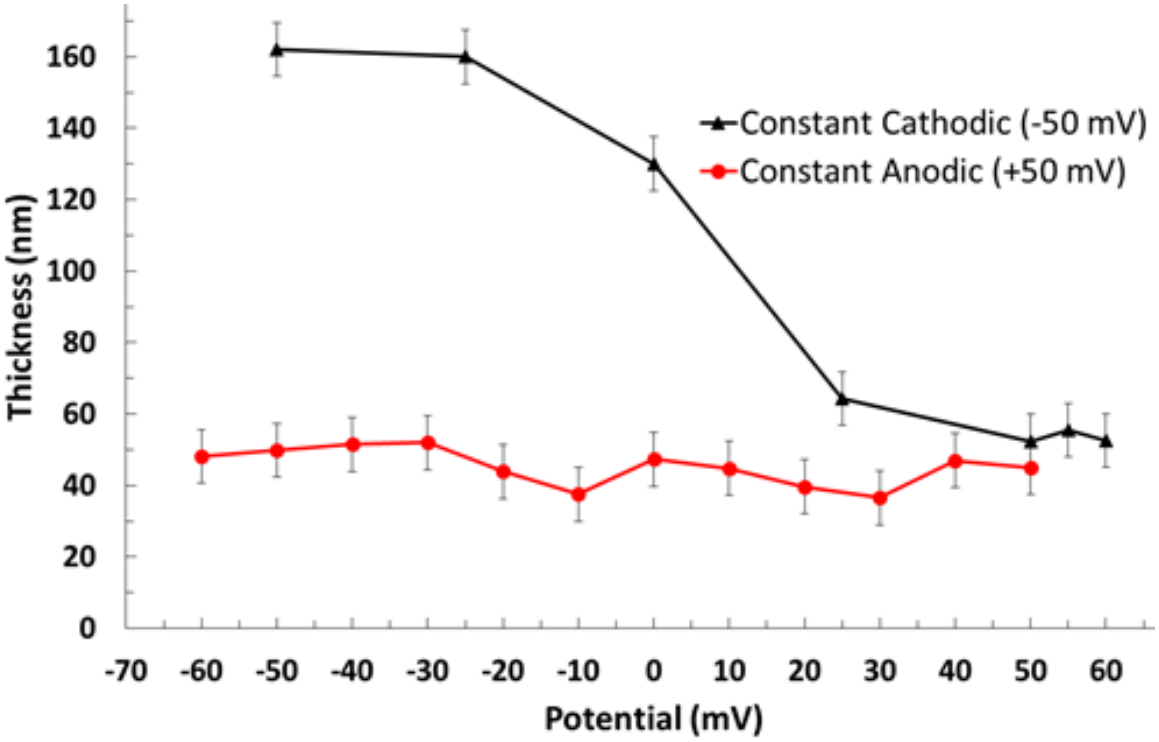

Figure 2.5: Potential vs. thickness under constant Cathodic (blue, -50 mV) and constant Anodic (red, +50 mV) conditions. Each deposit was formed with 3300 pulses.

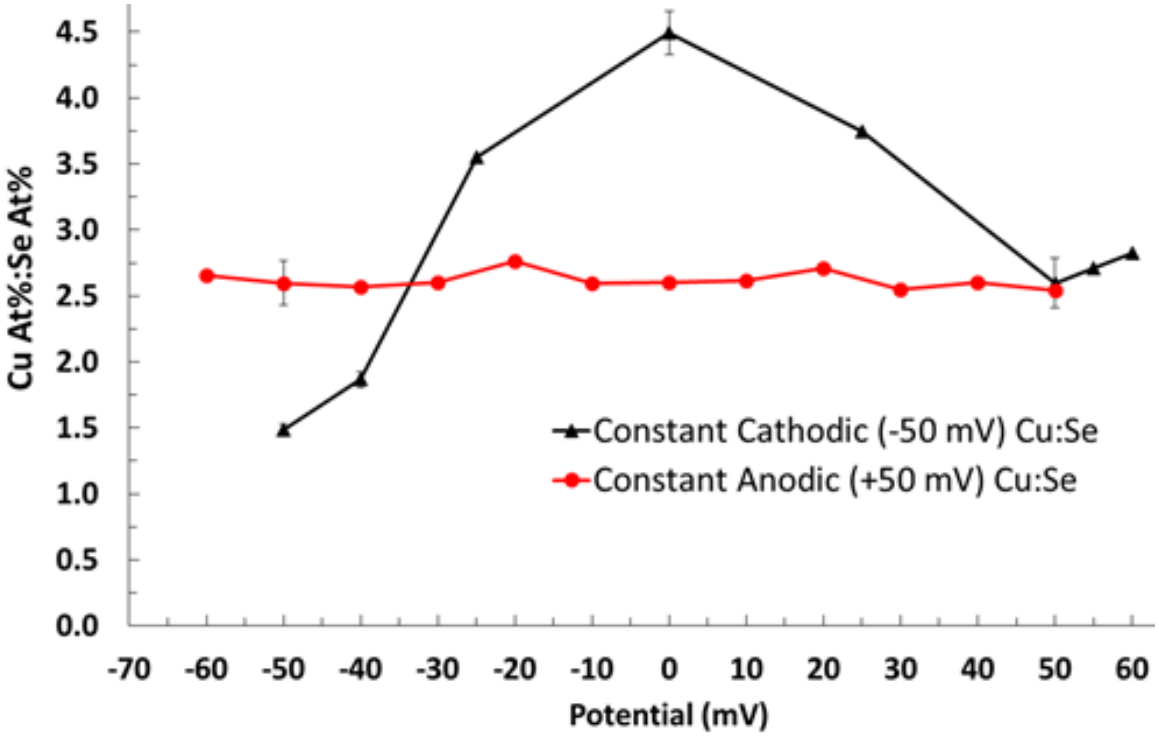

Figure 2.6: Stoichiometry, determined using EPMA, of deposits made under constant Cathodic (blue, -50 mV) and constant Anodic (red, +50 mV) potentials. In the blue curve, the Anodic potential was varied, while in the red curve, the Cathodic potential was varied. Each deposit was formed using 3300 cycles.

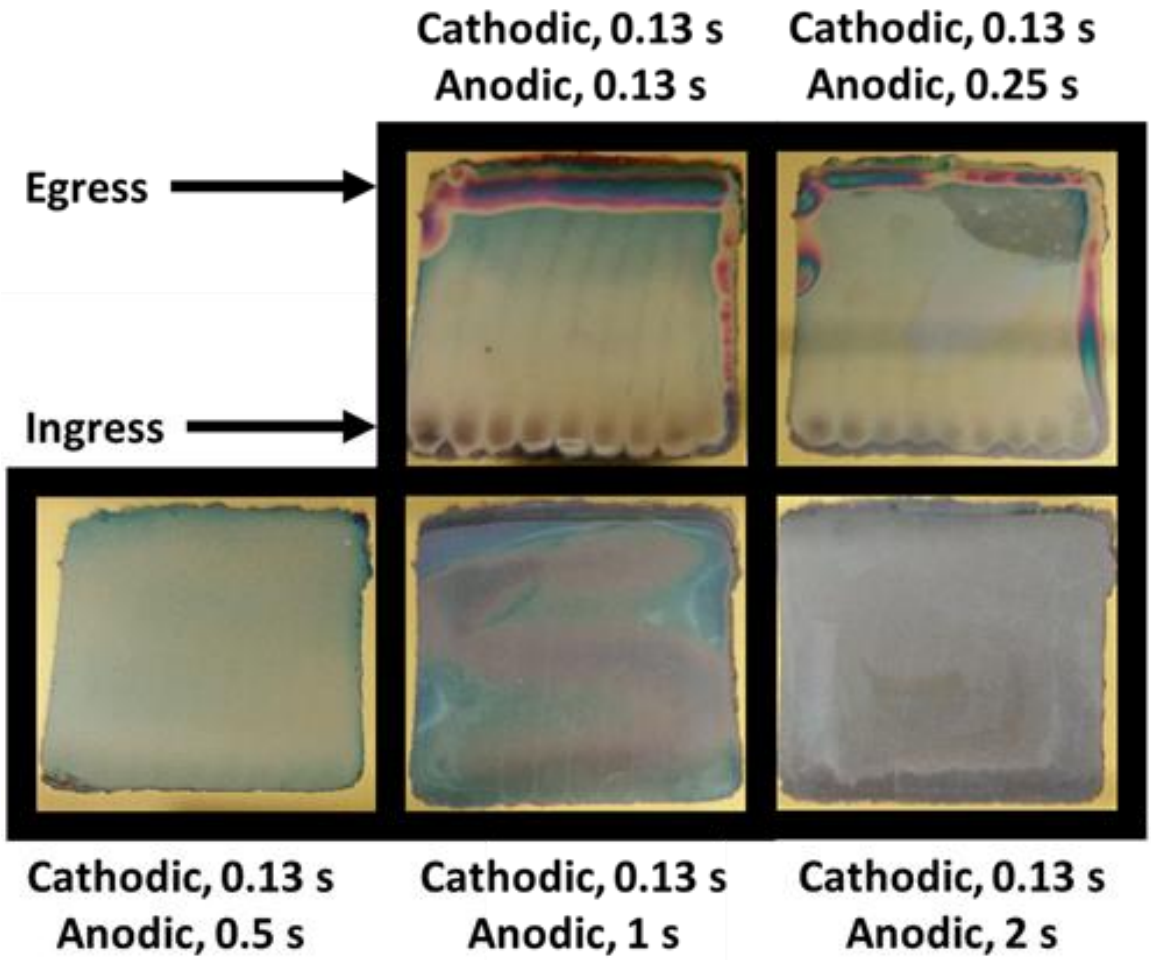

Figure 2.7: Five 3300 cycle deposits made by varying the time spent at the Anodic potential (+50 mV), while keeping the Cathodic potential (-50 mV) constant at 0.13 sec. The total time for the deposit was thus systematically increased as the Anodic pulse time increased (the 0.13 sec pulse resulted in a 15 min deposit, while the 2 sec pulse resulted in a 120 min deposit). As will become clear below, some deposition took place during both the Cathodic and Anodic pulses. The total deposition times are shown in Table 2.1.

Table 2.1: Anodic pulse time and resulting total deposition time

Anodic Pulse Time (s)	Total Deposition Time (min)
2	117
1	62
0.5	35
0.25	21
0.13	14

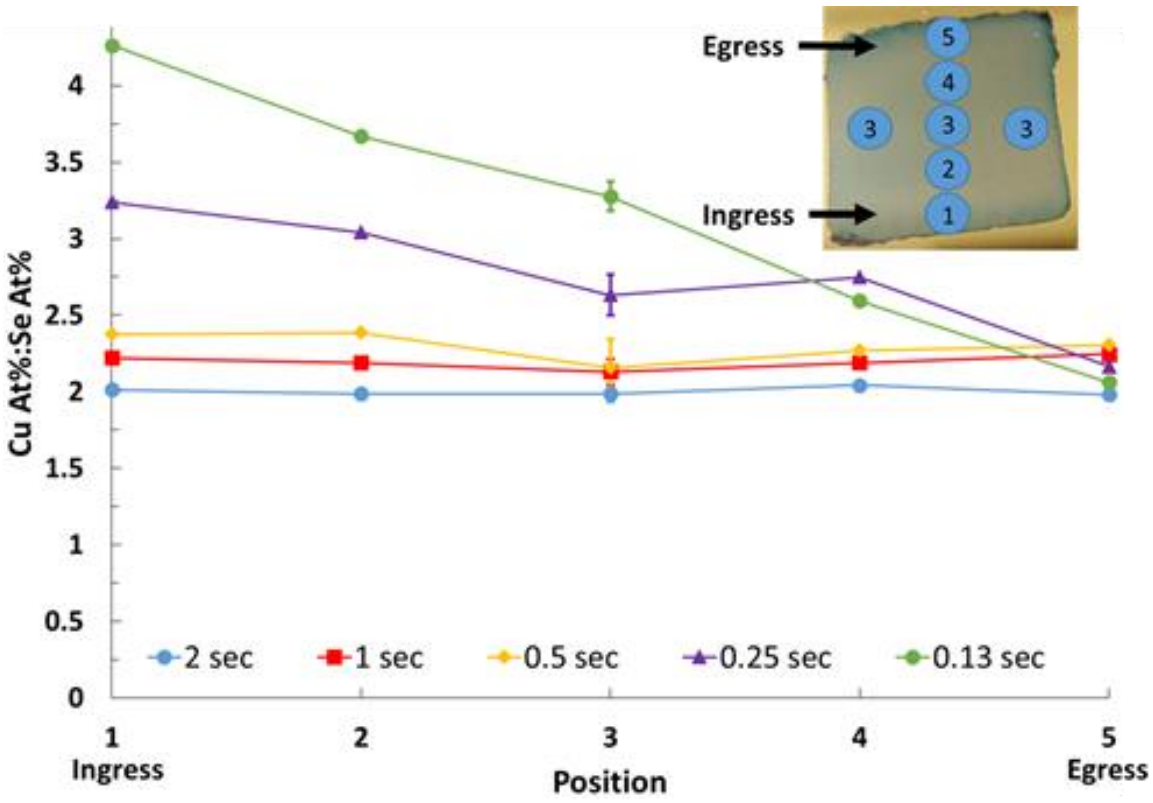

Figure 2.8: The ratio of Cu At%/Se At% collected from EPMA for the deposits in Figure 2.7 (Total deposition times are reported in Table 2.1), where the Anodic pulse times were varied. Inset indicates positions probed.

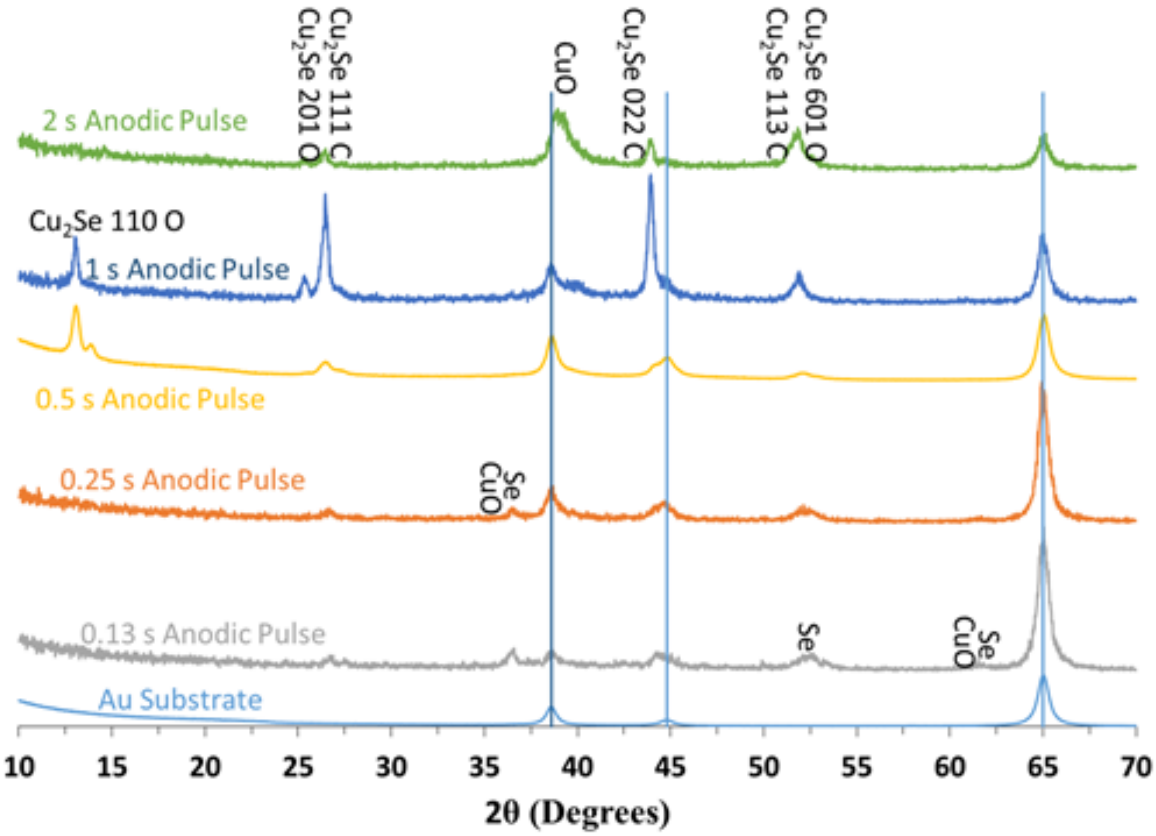

Figure 2.9: XRD patterns obtained for the samples shown in Figure 2.7. Each deposit was formed using 3300 cycles. The Cathodic pulse times were all 0.13 s, while the Anodic pulse times were varied. The total deposition times are shown in Table 2.1.

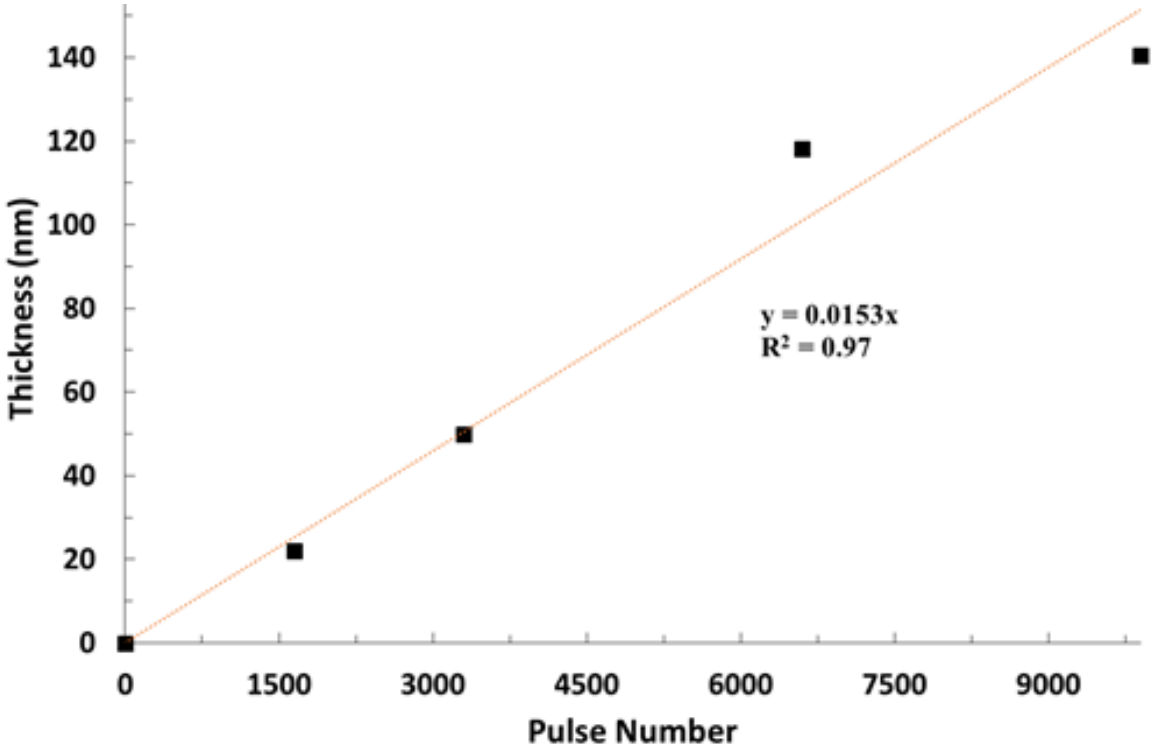

Figure 2.10: Thickness vs. Pulse Number (Anodic pulse = +50 mV, Cathodic pulse = -50 mV).

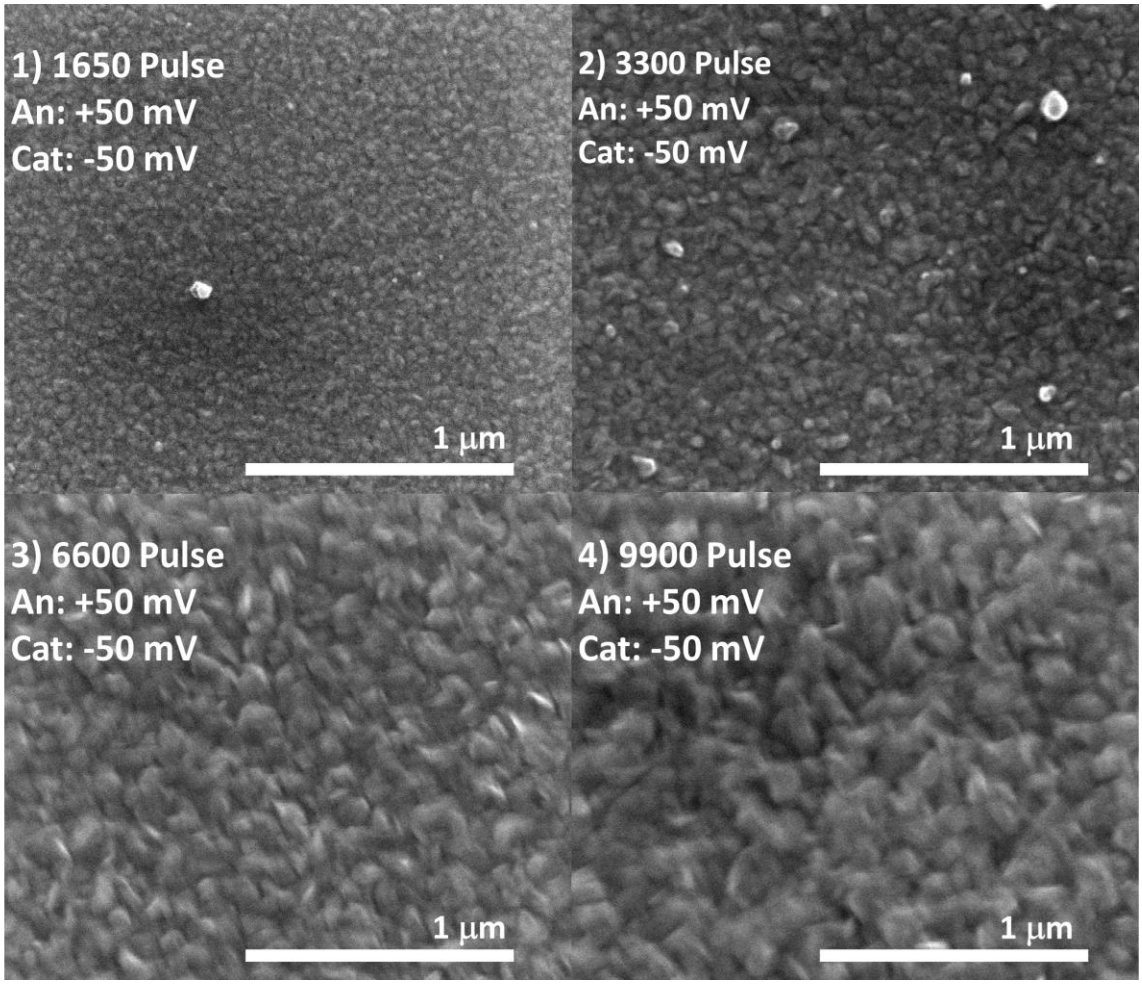

Figure 2.11: SEM of deposits formed with an increasing number of cycles. Cycle potentials were 50 mV for the Anodic and -50 mV for the Cathodic. 1) 1650 pulses = 22 nm, 2) 3300 pulse = 50 nm, 3) 6600 pulse = 118 nm, 4) 9900 pulse = 140 nm. The acceleration voltage used was 20.00 kV, and the magnification was 120,000 x objective.

CHAPTER 3

POTENTIAL PULSE ATOMIC LAYER DEPOSITION (PP-ALD) OF In_2Se_3[2]

[2] J. M. Czerniawski, J. L. Stickney, To be submitted to *Journal of the Electrochemical Society (2015)*

Abstract

Indium (III) selenide, In_2Se_3, thin films were electrodeposited at room temperature from an aqueous solution, containing ionic precursors for both In and Se, using potential pulse atomic layer deposition (PP-ALD). Cyclic voltammetry (CV) was used to determine approximate cycle potentials, and anodic and cathodic potentials were systematically examined to optimize the potential pulse program for In_2Se_3. Electron probe microanalysis (EPMA) was used to follow the In:Se atomic ratio as a function of the cycle conditions. Annealing studies were performed on stoichiometric deposits. Film thickness was a function of both the Anodic and Cathodic potentials. The optimum growth rate was consistent with previous PP-ALD studies where similar concentrations and pulse times were employed, 0.02 nm/cycle. The use of the potential pulse cycle for film growth resulted in surface limited control over the deposit stoichiometry each cycle, and thus a layer-by-layer growth process.

Introduction

$CuInSe_2$ (CIS) is a highly stable, chalcopyrite semiconductor with potential applications in p-type photovoltaics, light-emitting diodes, optoelectronics, and nonlinear optical devices.[1-4] CIS has a direct bandgap around 1.08[1, 4] and a high absorption coefficient (a ~ 10^5 cm^{-1}) leading to laboratory efficiencies as high as 15%.[2-5] CIS has been formed using techniques such as coevaporation,[6] flash evaporation,[7] chemical vapor deposition,[8] chemical spray pyrolysis,[9] chemical synthesis,[10] selenization of sputtered,[11] evaporated,[6] or electrodeposited[12] Cu and In stacked layers,[13] electrochemical codeposition,[14] and pulse electrodeposition.[1-3, 15]

This ternary compound could be manufactured by sequential electrochemical codeposition of binary selenides, such as indium selenide. In_2Se_3 is an n-type, visible light-driven semiconductor material with a direct bandgap around 1.62 eV[16] that has potential applications as an absorber layer in photovoltaic devices.[17] In_2Se_3 has been formed using numerous techniques including chemical bath deposition,[18] sputtering,[19] MOCVD,[20] spray pyrolysis,[21] magnetron sputtering,[19] and electrochemical deposition.[17]

Electrodeposition is generally considered a low cost, low temperature technique for growing thin film materials. Materials applicable for photovoltaic (PV) devices have been successfully grown using electrodeposition since Kroger et al.'s single solution CdTe work in the 70's.[22] ALD in general refers to a group of deposition techniques where surface limited reactions are used to form deposits one atomic layer at a time. A cycle of these reactions is used to form a compound monolayer and the cycle is repeated to grow the deposit to a desired thickness. The author's group has conducted extensive studies on the development of E-ALD, the electrochemical version of atomic layer deposition (ALD), to form CdTe and other compound semiconductors.[3, 23]

The vast majority of ALD work has been performed in vacuum to form oxide nanofilms. E-ALD takes advantage of the naturally occurring phenomenon underpotential deposition (UPD), a type of electrochemical surface limited reaction where an atomic layer of a first element can be deposited on a second element at a potential prior to (under) that needed to deposit the first on itself driven by the free energy of formation of a surface compound or alloy.[24] In a typical E-ALD cycle, separate solutions containing precursors of different elements are introduced to the substrate at their UPD potentials resulting in an alternating deposition of atomic layers. After deposition of an atomic layer

of the first element, the cell is rinsed with a blank solution and a precursor solution of the second element is introduced at its UPD potential, resulting in deposition of an atomic layer. The cycle is completed by rinsing again with blank. The advantages of using E-ALD are increased control of the thickness, homogeneity, crystallinity, and quality of the deposit. The drawback is the deposition rate, due to the need for multiple solution exchanges each cycle. The technique is thus best applied when nanofilms of a carefully controlled thickness and quality are required and the total number of cycles performed is minimized.[3, 25] E-ALD is generally impractical for μm thick film growth when compared to the co-electrodeposition used by BP to form μm thick CdTe PV absorber materials.[26]

Co-electrodeposition has been used to form a large number of other compounds[27], such as CdSe.[28] Early CdSe co-electrodeposition studies indicated the presence of excess Se, for a Cd:Se ratio less than one.[29-31] Researchers were able to limit the deposition of Se by dropping the concentration or forming complex soluble species thus shifting the deposition potential more negative. In a co-electrodeposition bath, however, this indirectly increased the overpotential used to deposit Cd resulting in deposits rich in Cd.[31, 32] A solution to the excess Cd and Se was proposed by Sailor et al., where instead of choosing a constant deposition potential, or current, they performed rapid and repeated cyclic voltammetry over a small range of potentials, a technique referred to as sequential monolayer electrodeposition (SMD).[30] The idea was to cycle between a negative potential where co-electrodeposition takes place, and a positive potential where excess, bulk Cd oxidized, but the Cd bound as CdSe did not. By scanning rapidly, traces of bulk cadmium formed at the more negative potentials were oxidatively removed at the positive end of each cycle, before they were buried by depositing CdSe, avoiding a buildup of excess Cd.

SMD has been used by Penner et al. to construct nanowire photo-sensors based on CdSe[33] and Lee et al. to make 3D macroporous structures of II-VI and III-V semiconductors.[34]

Pulse-reversal (PR) deposition is similar to SMD, but instead of a potential sweep, the potential is pulsed down to an anodic potential for reduction of precursor or surface oxide, then pulsed to a cathodic potential to equilibrate the deposition layer and remove any less-stable, dendritic material from the sample.[35] PR deposition was not intended to give users atomic layer control, but instead systematically remove any imperfections resulting from diffusion limited co-electrodeposited material.

Another method proposed to control excess elemental deposition in $Bi_{2-x}Sb_xTe_3$ multilayers was described by Banga et al..[36] Pulsed potentiostatic electrodeposition (PPE) is a diffusion limited, single-bath, co-electrodeposition process where a duty cycle is established by pulsing for short periods of time (~2% duty cycle) down to a potential where a desired compound forms. The cell is then allowed to "rest" at the open-circuit potential to regenerate the diffusion layer. PPE creates highly crystalline deposits, but long resting times (2-10 s) are needed to carefully control precursor concentrations near the surface of the electrode.

This a continuation of previous findings using a compound electrodeposition methodology that combines SMD, PPE, and E-ALD, where instead of cyclic voltammetry or changing solutions each cycle, the potential is alternated. As with E-ALD, sub-monolayer amounts are deposited each cycle, controlled by the surface-limited reaction between the depositing elements, and selective stripping of any bulk elemental deposit formed. It is referred to here as potential pulse atomic layer

deposition (PP-ALD). PP-ALD has been successfully used to grow Cu_2Se deposits that were comparable to those made with co-electrodeposition.

Potential steps are performed between optimized Cathodic and Anodic potentials. Given the differences in kinetics and deposition potentials for the two elemental precursors, codeposition can be performed (usually) at a Cathodic potential for a time sufficient to plate some fraction of a monolayer. The potential can then be stepped to an Anodic potential sufficiently positive to remove any elemental deposits of the more reactive element, leaving only a stable compound. The major benefits of this methodology over E-ALD are the large increase in deposition rate, increased scalability, and the ease with which solutions can be recycled.

Experimental

The solution was pH 1, 1.5 mM $In(ClO_4)_3$ (Sigma-Aldrich), 0.1 mM SeO_2 (Alfa Æsar 99.999% pure) and 0.5 M $NaClO_4$ in 10 MΩ from a Nanopure water dispenser (Millipore Advantage 10) fed by the house DI water source. The precursor concentrations were kept in the mM range in order to limit deposited amounts to a fraction of a monolayer (ML) each cycle. A ML is defined for this report as one atom for each Au substrate surface atom, or about 1.2×10^{15} atoms per cm^2. Substrates were 100 nm thick Au films on 5 nm of Ti on glass, purchased from Evaporated Metal Films (Ithaca, NY), and were cleaned by three 5 min sonications in fresh aliquots of acetone, followed by three more of Nanopure water. They were then dipped in concentrated nitric acid for 30 sec, rinsed with nanopure water and dried with nitrogen before being placed in the electrochemical flow cell (Figure 3.1). The cell (Electrochemical ALD L.C.) was immediately flushed with 0.1 M H_2SO_4 (Fisher Scientific, certified ACS plus) and the

potential was alternated for 5 sec at a time between 1400 mV and -200 mV, four times, completing cleaning of the Au surface.

Figure 3.1 diagrams the electrochemical flow cell, where the auxiliary electrode was an Au wire inlayed into a Plexiglas cell face. A 3 M Ag/AgCl reference electrode (BASi, West Lafayette, IN) was used, and the solution was pulled from degased solution reservoirs though the cell using a Masterflex (Cole Parmer) peristaltic pump. The system was automated using a program developed in-house named SEQUENCER.

Electron probe Microanalysis (EPMA) was performed on a JEOL 8600 Superprobe with a 10 KeV accelerating voltage, 15 nA beam current and 10 μm beam diameter. X-ray diffraction was performed on a PANalytical X'PERT Pro with an open Eulerian cradle, utilizing a 1.54 Å Cu Kα1 source and a parallel plate collimator. Spectroscopic ellipsometry was performed on a J.A. Woolam M-200V.

Results and Discussion

Figure 3.2 depicts cyclic voltammetry for Au substrates in separate In (3.2a) and Se (3.2b) precursor solutions, in the In precursor solution where the substrate was precoated with 0.6 ML of Se (3.2c), and in a solution containing precursors for both In and Se (3.2d). Figure 3.2a shows a CV in $In(ClO_4)_3$ at pH 1, which displays an initial scan negative to -1000 mV, but which was off scale below -600 mV due to the hydrogen evolution reaction (HER). In UPD began near 100 mV and shows features at -100 and -400 mV, just prior to extensive hydrogen evolution. In the subsequent positive going scan there was no peak for bulk In stripping, which should occur near -600 mV, the $E^{o'}$ for In^{3+}. There was an oxidation peak at -325 mV, which is felt by the authors to be

oxidative dissolution of In from a surface alloy with the Au substrate. The peak near -100 mV is In UPD stripping. The deposition of bulk In from the pH 1 solution appears to be hindered by strong HER, in that a large fraction of the cell was filled with hydrogen bubbles, rather than solution, and it may be that they coated the surface, limiting In^{3+} access. Similar In^{3+} scans in a pH 3 solution shifted the HER negative, allowing the facile deposition of bulk In and the In/Au alloy. The reduction feature at 900 mV is Au oxide reduction.

Figure 3.2b is a CV in 0.1 mM $HSeO_3^-$, pH 1. The formal potential was believed to be near 650 mV, suggesting that all Se deposition occurred at an overpotential, consistent with its slow deposition kinetics.[37] Surface limited peaks, related to UPD, are evident at 350 and 200 mV during the negative scan, along with a small amount of bulk Se formation. Stripping of the selenium in the subsequent positive going scan began at 650 mV with a small bulk peak and finished with oxidation of Se in contact with the Au surface at 850 mV.

Figure 3.2c was also a CV in $In(ClO_4)_3$, pH 1, to -1000 mV, however the Au substrate was first coated with 0.6 ML of Se. The reduction feature starting negative of -200 mV appears to be In UPD (Figure 3.2a). Subsequent reduction below -400 mV included In reacting with Se on the surface, In/Au alloy formation, bulk In formation, and extensive HER. Comparing Figures 3.2a and 3.2c, however, indicates that the adsorbed Se increased the hydrogen overpotential, pushing it 150 mV more negative. The reduction peaks below 350 mV for Se deposition, Figure 3.2b, were not evident in Figure 3.2c, as the Se was preadsorbed. The first oxidation peak in the positive going scan, -600 mV, was bulk In stripping, agreeing with the $E^{0'}$. The extensive oxidation feature

beginning at -400 mV is consistent with In stripping from the near surface In/Au alloy. From a comparison of Figures 3.2a and 3.2c, it can be seen that there is an order of magnitude more In on, or in, the surface when Se is preadsorbed. This is consistent with the hypothesis that HER was interfering with In deposition in Figure 3.2a, and the adsorbed Se worked to increase the hydrogen overpotential, allowing In deposition, as did changing to pH 3. The shoulder at -100 mV on the de-alloying peak in Figure 3.2c, matches the UPD stripping of In, Figure 3.2a, while the oxidation peak above 800 mV matches the Se oxidation feature, Figure 3.2b.

Figure 3.2d was a CV in a pH 1 solution containing 1.5 mM In^{+3} and 0.1 mM $HSeO_3^-$, also to -1000 mV. The scan began negative from 400 mV, the open circuit potential (OCP). The first reduction feature, at 325 mV, was similar to the peak in Figure 3.2b for Se deposition. $HSeO_3^-$ reduction may also account for the current between 200 and -100 mV. The reduction peak at -250 mV is consistent with In UPD, though larger, suggesting a reaction between In and Se. The hydrogen overpotential appears still larger, the HER taking off negative of -700 mV, suggesting its suppression results from the surface being coated with a mix of In and Se. During the subsequent positive going scan, the first oxidative feature, -550 mV in Figure 3.2d, is consistent with oxidation of bulk indium. Some bulk In is expected, given the 15 fold excess of In to Se in solution. The oxidation peak for In from an In/Au alloy, at -250 mV in Figure 3.2c, is not present. Instead there is a broad range of oxidation current between -500 and 400 mV, Figure 3.2d, which appears to be In oxidation from a mixed In/Se layer. The majority of that In is more stable than it was in the In/Au alloy (Figure 3.2c), suggesting the formation of a compound with Se. The lack of current for In stripping from a In/Au alloy suggests that

the formation of a layer of some In/Se compound which has blocked diffusion of In into the Au. The large peak above 700 mV in Figure 3.2d is consistent with bulk Se oxidation, left after oxidative stripping of In. The shoulder at 900 mV corresponds to oxidation of the last layer of Se from the Au substrate.

Figure 3.3 is a potential time diagram for 5 PP-ALD cycles, such as used in the present study. The cycle begins with 0.13 s at -1000 mV, the Cathodic potential, where fractions of monolayers of Se and In are deposited. The potential was then stepped to -70 mV for 0.5 s, the Anodic potential, where any excess In is removed to create the stoichiometric deposit. Figure 3.4 is a schematic diagram of one PP-ALD cycle.

Two studies were performed to investigate the dependence of the deposit on the Anodic and Cathodic cycle potentials. Figure 3.5 displays the deposit thickness after 3300 cycle, measured using spectroscopic ellipsometry, where the Cathodic potential was held constant (blue) at -1000 mV and the Anodic was varied. Figure 3.6 displays the stoichiometry, Se/In ratio, for the deposits under the same conditions as Figure 3.5. The trend was for the thickness to slowly decrease as the Anodic potential was increased from -400 mV to 50 mV. At -400 mV, bulk In should have been removed (Figure 3.2d), however, from Figure 3.6 is can be seen that the In/Se ratio was about 1.35 rather than the 1.5 expected for In_2Se_3, indicating that In was in excess. Not removing all excess In at -400 mV is also consistent with a thicker deposit (Figure 3.5). As the Anodic potential was increased, more In was removed and the stoichiometry moved closer to the expected 1.5 (Figure 3.6). By 50 mV, all In was removed and only Se remained.

From above, an Anodic potential of -70 mV was selected as near optimal, and a study varying the Cathodic potential was performed (Figure 3.5, orange). The orange

points show that the deposit thickness decreased as the Cathodic potential was raised, though the stoichiometry remained 1.5 up to -800 mV (Figure 3.6, blue). Visible inspection (Figure 3.5, orange) of deposits formed using a Cathodic potential above -1000 mV displayed a gradient in color, white to blue to orange from ingress to egress (bottom to top), with color being closely related to thickness. White corresponds to thicker areas, while orange deposits are very thin. The near laminar flow in the cell can result in a pattern, thickness gradient, across the deposit when it is at least partially controlled by convective mass transfer. On the other hand, there was little variation in thickness (Figure 3.5) when -1000 mV was used as the Cathodic potential and -200 or -70 mV was used as the Anodic. In those cases deposition was controlled by surface limited reactions, the Anodic potential functioning as a UPD potential to achieve conformal growth and maintain the deposit stoichiometry using the energetics of compound formation.

The stoichiometry did not change dramatically as the deposition potentials were varied (Figure 3.6). Deposits formed using a constant Anodic potential of -70 mV (blue), and a Cathodic potential of -700 mV or above, were rich in Se since little In was deposited so close to its formal potential. For deposits formed using -1000 mV for the Cathodic potential (Figure 3.6, grey), using more positive Anodic potentials also resulted in Se rich deposits, as more In was oxidatively stripped. All In stripped above -70 mV.

Figure 3.7 displays XRD patterns recorded for the Au substrate (grey), an as deposited In_2Se_3 film, and a In_2Se_3 film annealed for 30 min at 300^oC. The two peaks originating from the Au substrate are marked with vertical lines. Under the conditions used in these studies, XRD peaks for In_2Se_3 were not observed in the as deposited

samples. However, after annealing for 30 min at 300ºC a number of diffraction peaks were observed and correlated with hexagonal In_2Se_3 (card: In_2Se_3 hex 00-023-0294).

Conclusion

Sixty nm thick In_2Se_3 films were formed using PP-ALD. PP-ALD is an electrochemical form of ALD, where the surface limited reactions are achieved using short cycle times, so that each cycle results in less than a compound ML, and two potentials: a cathodic potential for depositing and an anodic, UPD, potential to achieve conformal growth and a stoichiometric deposit. In this report, the anodic potential was used to remove excess In by oxidative stripping at a potential where the energetics of compound formation controlled the stoichiometry. The advantage of this pulsed form of ALD, relative to previous E-ALD, is that solutions do not have to be exchanged each cycle, and so PP-ALD is faster. In theory, increasing the concentrations by two orders of magnitude should increase the rate of deposition by the same. The deposit stoichiometry remained constant over a range of conditions, with a Se:In ratio of 1.5. No XRD pattern was obtained from the as deposited films, though annealing to 300°C for 30 min produced a pattern consistent with hexagonal polycrystalline In_2Se_3. The deposition rate was 0.02 nm/cycle under the conditions used here.

Acknowledgements

Support from the National Science Foundation, DMR #1410109, is gratefully acknowledged. Thanks to Chris Fleisher and the UGA Microprobe lab. Thanks to the Integrated Bioscience and Nanotechnology Cleanroom for the use of their facilities.

References

1. Hu, S.-Y.; Lee, W.-H.; Chang, S.-C.; Cheng, Y.-L.; Wang, Y.-L., Pulsed Electrodeposition of CuInSe2 Thin Films onto Mo-Glass Substrates. *Journal of The Electrochemical Society* **2011,** *158* (5), B557-B561.
2. Caballero-Briones, F.; Palacios-Padrós, A.; Sanz, F., CuInSe2 films prepared by three step pulsed electrodeposition. Deposition mechanisms, optical and photoelectrochemical studies. *Electrochimica Acta* **2011,** *56* (26), 9556-9567.
3. Banga, D.; Jarayaju, N.; Sheridan, L.; Kim, Y.-G.; Perdue, B.; Zhang, X.; Zhang, Q.; Stickney, J., Electrodeposition of CuInSe2 (CIS) via Electrochemical Atomic Layer Deposition (E-ALD). *Langmuir* **2012,** *28* (5), 3024-3031.
4. Hamrouni, S.; AlKhalifah, M. S.; Boujmil, M. F.; Saad, K. B., Preparation and characterization of CuInSe2 electrodeposited thin films annealed in vacuum. *Applied Surface Science* **2014,** *292* (0), 231-236.
5. Fangyang, L.; Ying, L.; Zhian, Z.; Yanqing, L.; Jie, L.; Yexiang, L., Preparation of Chalcopyrite Cuinse2 Thin Films by Pulse-Plating Electrodeposition and Annealing Treatment. In *Proceedings of ISES World Congress 2007 (Vol. I – Vol. V)*, Goswami, D. Y.; Zhao, Y., Eds. Springer Berlin Heidelberg: 2009; pp 1316-1320.
6. Guillén, C.; Herrero, J., Structure, morphology and photoelectrochemical activity of CuInSe2 thin films as determined by the characteristics of evaporated metallic precursors. *Solar Energy Materials and Solar Cells* **2002,** *73* (2), 141-149.

7. Ashida, A.; Hachiuma, Y.; Yamamoto, N.; Ito, T.; Cho, Y., CuInSe2 thin films prepared by quasi-flash evaporation of In2Se3 and Cu2Se. *Journal of Materials Science Letters* **1994,** *13* (16), 1181-1184.

8. Jones, P. A.; Jackson, A. D.; Lickiss, P. D.; Pilkington, R. D.; Tomlinson, R. D., The plasma enhanced chemical vapour deposition of CuInSe2. *Thin Solid Films* **1994,** *238* (1), 4-7.

9. Shirakata, S.; Murakami, T.; Kariya, T.; Isomura, S., Preparation of CuInSe2 Thin Films by Chemical Spray Pyrolysis. *Japanese Journal of Applied Physics* **1996,** *35* (1R), 191; Tomoaki Terasako; Sho Shirakata; Shigehiro Isomura, Photoacoustic Spectra of CuInSe 2 Thin Films Prepared by Chemical Spray Pyrolysis. *Japanese Journal of Applied Physics* **1999,** *38* (8R), 4656.

10. de Kergommeaux, A.; Fiore, A.; Bruyant, N.; Chandezon, F.; Reiss, P.; Pron, A.; de Bettignies, R.; Faure-Vincent, J., Synthesis of colloidal CuInSe2 nanocrystals films for photovoltaic applications. *Solar Energy Materials and Solar Cells* **2011,** *95, Supplement 1* (0), S39-S43.

11. Guillén, C.; Martínez, M. A.; Herrero, J., CuInSe2 thin films obtained by a novel electrodeposition and sputtering combined method. *Vacuum* **2000,** *58* (4), 594-601.

12. Guillén, C.; Herrero, J., Improved Selenization Procedure to Obtain CulnSe2 Thin Films from Sequentially Electrodeposited Precursors. *Journal of The Electrochemical Society* **1996,** *143* (2), 493-498.

13. Liang, D.; Unveroglu, B.; Zangari, G., Electrodeposition of Cu-In Alloys as Precursors of Chalcopyrite Absorber Layers. *Journal of The Electrochemical Society* **2014,** *161* (12), D613-D619.

14. Bhattacharya, R. N., Solution Growth and Electrodeposited CuInSe2Thin Films. *Journal of The Electrochemical Society* **1983,** *130* (10), 2040-2042; Kaupmees, L.; Altosaar, M.; Volubujeva, O.; Mellikov, E., Study of composition reproducibility of electrochemically co-deposited CuInSe2 films onto ITO. *Thin Solid Films* **2007,** *515* (15), 5891-5894; Hernández-Pagán, E. A.; Wang, W.; Mallouk, T. E., Template Electrodeposition of Single-Phase p- and n-Type Copper Indium Diselenide (CuInSe2) Nanowire Arrays. *ACS Nano* **2011,** *5* (4), 3237-3241.

15. Palacios-Padrós, A.; Caballero-Briones, F.; Sanz, F., Enhancement in as-grown CuInSe2 film microstructure by a three potential pulsed electrodeposition method. *Electrochemistry Communications* **2010,** *12* (8), 1025-1029.

16. Qasrawi, A. F., Temperature dependence of the band gap, refractive index and single-oscillator parameters of amorphous indium selenide thin films. *Optical Materials* **2007,** *29* (12), 1751-1755.

17. Yadav, A. A.; Salunke, S. D., Photoelectrochemical properties of In2Se3 thin films: Effect of substrate temperature. *Journal of Alloys and Compounds* **2015,** (0).

18. Asabe, M. R.; Chate, P. A.; Delekar, S. D.; Garadkar, K. M.; Mulla, I. S.; Hankare, P. P., Synthesis, characterization of chemically deposited indium selenide thin films at room temperature. *Journal of Physics and Chemistry of*

Solids **2008,** *69* (1), 249-254; Pathan, H. M.; Kulkarni, S. S.; Mane, R. S.; Lokhande, C. D., Preparation and characterization of indium selenide thin films from a chemical route. *Materials Chemistry and Physics* **2005,** *93* (1), 16-20.

19. Li, S.; Yan, Y.; Zhang, Y.; Ou, Y.; Ji, Y.; Liu, L.; Yan, C.; Zhao, Y.; Yu, Z., Monophase γ-In2Se3 thin film deposited by magnetron radio-frequency sputtering. *Vacuum* **2014,** *99* (0), 228-232; Yan, Y.; Li, S.; Yu, Z.; Liu, L.; Yan, C.; Zhang, Y.; Zhao, Y., Influence of indium concentration on the structural and optoelectronic properties of indium selenide thin films. *Optical Materials* **2014,** *38* (0), 217-222; Yan, Y.; Li, S.; Ou, Y.; Ji, Y.; Liu, L.; Yan, C.; Zhang, Y.; Yu, Z.; Zhao, Y., In-situ annealing of In–Se amorphous precursors sputtered at low temperature. *Journal of Alloys and Compounds* **2014,** *614* (0), 368-372.
20. Choi, H.; Nicolaescu, R.; Paek, S.; Ko, J.; Kamat, P. V., Supersensitization of CdS Quantum Dots with a Near-Infrared Organic Dye: Toward the Design of Panchromatic Hybrid-Sensitized Solar Cells. *ACS Nano* **2011,** *5* (11), 9238-9245.
21. Aydin, E.; Sankir, M.; Sankir, N. D., Influence of silver incorporation on the structural, optical and electrical properties of spray pyrolyzed indium sulfide thin films. *Journal of Alloys and Compounds* **2014,** *603* (0), 119-124; Reyes-Figueroa, P.; Painchaud, T.; Lepetit, T.; Harel, S.; Arzel, L.; Yi, J.; Barreau, N.; Velumani, S., Structural properties of In2Se3 precursor layers deposited by spray pyrolysis and physical vapor deposition for CuInSe2 thin-film solar cell applications. *Thin Solid Films* (0).
22. Kröger, F. A., Cathodic Deposition and Characterization of Metallic or Semiconducting Binary Alloys or Compounds. *Journal of The Electrochemical*

Society **1978,** *125* (12), 2028-2034; Panicker, M. P. R.; Knaster, M.; Kroger, F. A., Cathodic Deposition Of CdTe From Aqueous-Electrolytes. *Journal of the Electrochemical Society* **1978,** *125* (4), 566-572.

23. D. W. Suggs, I. V., B.W. Gregory, J.L. Stickney, Formation of CdTe and GaAs by electrochemical atoimc layer epitaxy (ECALE). *Mat. Res. Soc. Symp. Proc.* **1991,** *222*, 283; Colletti, L. P.; Stickney, J. L., II-VI compound semiconductor thin-film electrodeposition by ECALE. *Book of Abstracts, 210th ACS National Meeting, Chicago, IL, August 20-24* **1995,** (Pt. 1), INOR-297; Colletti, L. P.; Flowers, B. H.; Stickney, J. L., Formation of Thin-Films of CdTe, CdSe, and CdS by Electrochemical ALE. *JECS* **1997**; Colletti, L. P.; Slaughter, R.; Stickney, J. L., ZnS thin film formation by electrochemical ALE: preliminary doping studies. *Proceedings - Electrochemical Society* **1997,** *97-20* (Photoelectrochemistry), 1-10; Perdue, B.; Czerniawski, J.; Anthony, J.; Stickney, J., Optimization of Te Solution Chemistry in the Electrochemical Atomic Layer Deposition Growth of CdTe. *Journal of The Electrochemical Society* **2014,** *161* (7), D3087-D3092.

24. Kolb, D. M., Physical and Electrochemical Properties of Metal Monolayers on Metallic Substrates. In *Advances in Electrochemistry and Electrochemical Engineering*, Gerischer, H.; Tobias, C. W., Eds. John Wiley: New York, 1978; Vol. 11, p 125; Juttner; K.; Lorenz; W.J., *Z. Phys. Chem. N. F.* **1980,** *122*, 163; Adzic, R. R., Electrocatalytic Properties of the Surfaces Modified by Foreign Metal Ad Atoms. In *Advances in Electrochemistry and Electrochemical Engineering*, Gerishcher, H.; Tobias, C. W., Eds. Wiley-Interscience: New York,

1984; Vol. 13, p 159; Gewirth, A. A.; Niece, B. K., Electrochemical applications of in situ scanning probe microscopy. *Chem. Rev.* **1997,** *97*, 1129-1162.

25. Vaidyanathan, R.; Mathe, M. K.; Sprinkle, P.; Cox, S. M.; Happek, U.; Stickney, J. L., Electrodeposition of Cu2Se thin films by electrochemical atomic layer epitaxy (EC-ALE). *Materials Research Society Symposium Proceedings* **2003,** *744* (Progress in Semiconductors II--Electronic and Optoelectronic Applications), 289-294.

26. Turner, A. K.; Woodcock, J. M.; Ozsan, M. E.; Cunningham, D. W.; Johnson, D. R.; Marshall, R. J.; Mason, N. B.; Oktik, S.; Patterson, M. H.; Ransome, S. J.; Roberts, S.; Sadeghi, M.; Sherborne, J. M.; Sivapathasundaram, D.; Walls, I. A., BP Solar Thin-Film Cdte Photovoltaic Technology. *Solar Energy Materials and Solar Cells* **1994,** *35* (1-4), 263-270; Cunningham, D.; Rubcich, M.; Skinner, D., Cadmium telluride PV module manufacturing at BP Solar. *Progress in Photovoltaics* **2002,** *10* (2), 159-168.

27. Öznülüer, T.; Erdoğan, İ.; Şişman, İ.; Demir, Ü., Electrochemical Atom-by-Atom Growth of PbS by Modified ECALE Method. *Chemistry of Materials* **2005,** *17* (5), 935-937; Öznülüer, T.; Erdoğan, İ.; Demir, Ü., Electrochemically Induced Atom-by-Atom Growth of ZnS Thin Films: A New Approach for ZnS Co-deposition. *Langmuir* **2006,** *22* (9), 4415-4419.

28. Loizos, Z.; Mitsis, A.; Spyrellis, N.; Froment, M.; Maurin, G., Cadmium chalcogenide semiconducting thin films prepared by electrodeposition from boiling aqueous electrolytes. *Thin Solid Films* **1993,** *235* (1-2), 51-56.

29. Kazacos, M. S.; Miller, B., Studies in Selenious Acid Reduction and CdSe Film Deposition. *Journal of The Electrochemical Society* **1980,** *127* (4), 869-873; Skyllas Kazacos, M.; Miller, B., Electrodeposition of CdSe Films from Selenosulfite Solution. *Journal of The Electrochemical Society* **1980,** *127* (11), 2378-2381; Houston, G. J.; McCann, J. F.; Haneman, D., Optimising the photoelectrochemical performance of electrodeposited CdSe semiconductor electrodes. *Journal of Electroanalytical Chemistry and Interfacial Electrochemistry* **1982,** *134* (1), 37-47; Tomkiewicz, M.; Ling, I.; Parsons, W. S., Morphology, Properties, and Performance of Electrodeposited n - CdSe in Liquid Junction Solar Cells. *Journal of The Electrochemical Society* **1982,** *129* (9), 2016-2022; Skyllas-Kazacos, M., Electrodeposition of CdSe and CdSe+CdTe thin films from cyanide solutions. *Journal of Electroanalytical Chemistry and Interfacial Electrochemistry* **1983,** *148* (2), 233-239; Wei, C.; Bose, C. S. C.; Rajeshwar, K., Compositional analysis of electrosynthesized semiconductor thin films by electrochemical quartz crystal microgravimetry: Application to the Cd + Se system. *Journal of Electroanalytical Chemistry* **1992,** *327* (1–2), 331-336.

30. Kressin, A. M.; Doan, V. V.; Klein, J. D.; Sailor, M. J., Synthesis of stoichiometric CdSe films via sequential monolayer electrodeposition. *Chem. Mater.* **1991,** *3*, 1015-1020.

31. Ham, D.; Mishra, K. K.; Rajeshwar, K., Anodic electrosynthesis of CdSe thin-films: Characterization and comparison with the passive/transpassive behavior of the CdX (X= S, Te) counterparts. *J. Electrochem. Soc.* **1991,** *138*, 100.

32. Cocivera, M.; Darkowski, A.; Love, B., Thin Film CdSe Electrodeposited from Selenosulfite Solution. *Journal of The Electrochemical Society* **1984,** *131* (11), 2514-2517; Loizos, Z.; Spyrellis, N.; Maurin, G.; Pottier, D., Semiconducting CdSex, Te1−x thin films prepared by electrodeposition. *Journal of Electroanalytical Chemistry and Interfacial Electrochemistry* **1989,** *269* (2), 399-410; Krishnan, V.; Ham, D.; Mishra, K. K.; Rajeshwar, K., Electrosynthesis of thin films of CdZnSe: composition modulation and bandgap engineering in the ternary system. *J. Electrochem. Soc.* **1992,** *139*, 23; Krishnan, V.; Ham, D.; Mishra, K. K.; Rajeshwar, K., Electrosynthesis of Thin Films of CdZnSe : Composition Modulation and Bandgap Engineering in the Ternary System. *Journal of The Electrochemical Society* **1992,** *139* (1), 23-27.

33. Liu, F.; Huang, C.; Lai, Y.; Zhang, Z.; Li, J.; Liu, Y., Preparation of Cu(In,Ga)Se2 thin films by pulse electrodeposition. *Journal of Alloys and Compounds* **2011,** *509* (8), L129-L133; Ayvazian, T.; van der Veer, W. E.; Xing, W.; Yan, W.; Penner, R. M., Electroluminescent, Polycrystalline Cadmium Selenide Nanowire Arrays. *ACS Nano* **2013,** *7* (10), 9469-9479.

34. Lee, Y.-C.; Kuo, T.-J.; Hsu, C.-J.; Su, Y.-W.; Chen, C.-C., Fabrication of 3D Macroporous Structures of II−VI and III−V Semiconductors Using Electrochemical Deposition. *Langmuir* **2002,** *18* (25), 9942-9946.

35. Swaminathan, V.; Murali, K. R., Influence of pulse reversal on the PEC performance of pulse-plated CdSe films. *Solar Energy Materials and Solar Cells* **2000,** *63* (2), 207-216; Tang, P. T., Pulse reversal plating of nickel and nickel alloys for microgalvanics. *Electrochimica Acta* **2001,** *47* (1–2), 61-66; Lin, J.-Y.;

Tsai, Y.-T.; Tai, S.-Y.; Lin, Y.-T.; Wan, C.-C.; Tung, Y.-L.; Wu, Y.-S., Pulse-Reversal Deposition of Cobalt Sulfide Thin Film as a Counter Electrode for Dye-Sensitized Solar Cells. *Journal of The Electrochemical Society* **2013,** *160* (2), D46-D52; Chandrasekar, M. S.; Pushpavanam, M., Pulse and pulse reverse plating—Conceptual, advantages and applications. *Electrochimica Acta* **2008,** *53* (8), 3313-3322.

36. Banga, D.; Lensch-Falk, J. L.; Medlin, D. L.; Stavila, V.; Yang, N. Y. C.; Robinson, D. B.; Sharma, P. A., Periodic Modulation of Sb Stoichiometry in Bi2Te3/Bi2–xSbxTe3 Multilayers Using Pulsed Electrodeposition. *Crystal Growth & Design* **2012,** *12* (3), 1347-1353.

37. Lister, T. E.; Huang, B. M.; Herrick, R. D.; Stickney, J. L., Electrochemical Formation of Se Atomic Layers On Au(100). *Journal of Vacuum Science & Technology B* **1995,** *13* (3), 1268; Lister, T. E.; Stickney, J. L., Atomic level studies of selenium electrodeposition on gold (111) and gold (110). *Journal of Physical Chemistry* **1996,** *100* (50), 19568-19576; Huang, B. M.; Lister, T. E.; Stickney, J. L., Se adlattices formed on Au (100), studies by LEED, AES, STM and electrochemistry. *Surface Science* **1997,** *392* (1-3), 27.

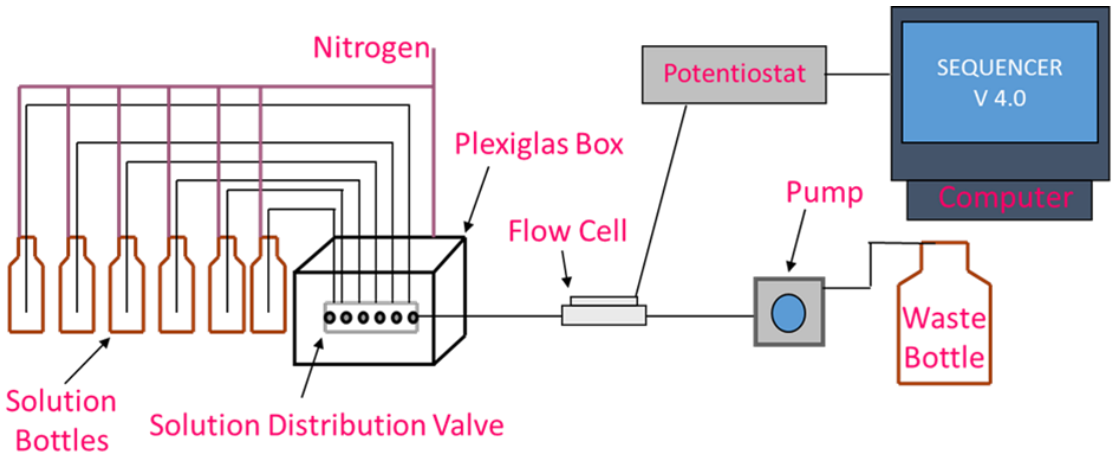

Figure 3.1: Schematic of the electrochemical flow system. Solution enters left to right drawn from nitrogen purged solution bottles by a pump through the solution distribution valve, housed in a nitrogen purged Plexiglas box, and "Z" configuration flow cell.

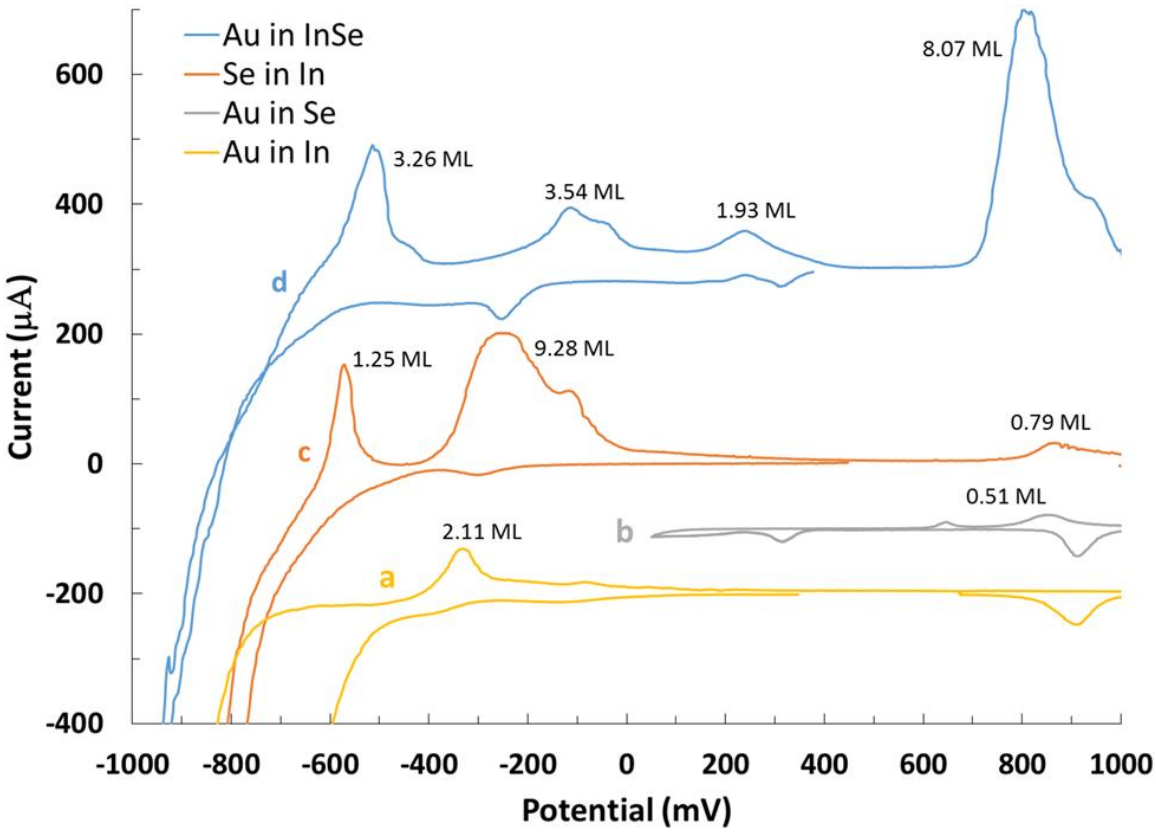

Figure 3.2: Cyclic voltammogram of a) Au in 1.5 mM $In(ClO_4)_3$ b) Au in 0.1 mM SeO_2 c) ~0.6ML Se in 1.5 mM $In(ClO_4)_3$ and d) Au in 1.5 mM $In(ClO_4)_3$ and 0.1 mM SeO_2. All solutions were pH 1. Potential was measured vs. the Ag/AgCl reference electrode with a scan rate of 10 mV/sec. The flow rate was 4 mL/min. The electrode area was 0.79 cm^2.

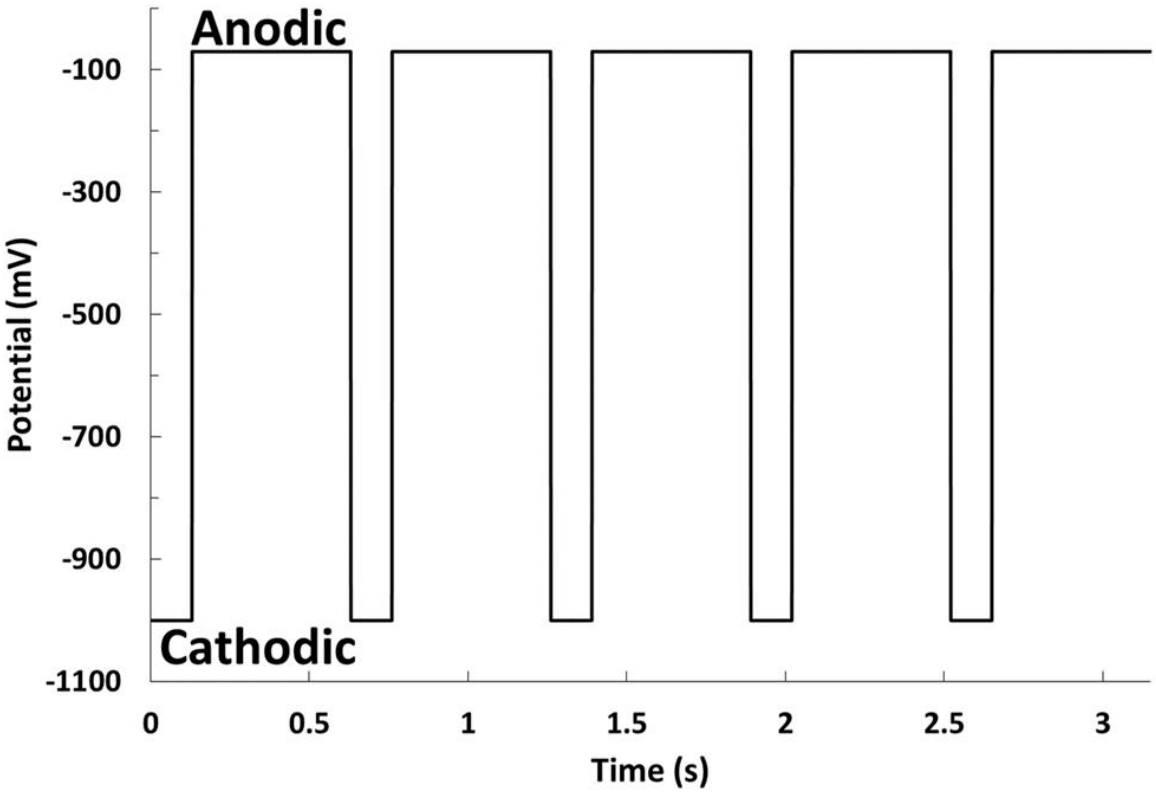

Figure 3.3: Potential profile for 5 PP-ALD cycles. The cycle begins at -1000 mV, the Cathodic potential, for 0.13 sec. Fractions of a monolayer of Se and In were deposited. The potential was then stepped to -70 mV, the Anodic potential, and any excess In was removed from the deposit.

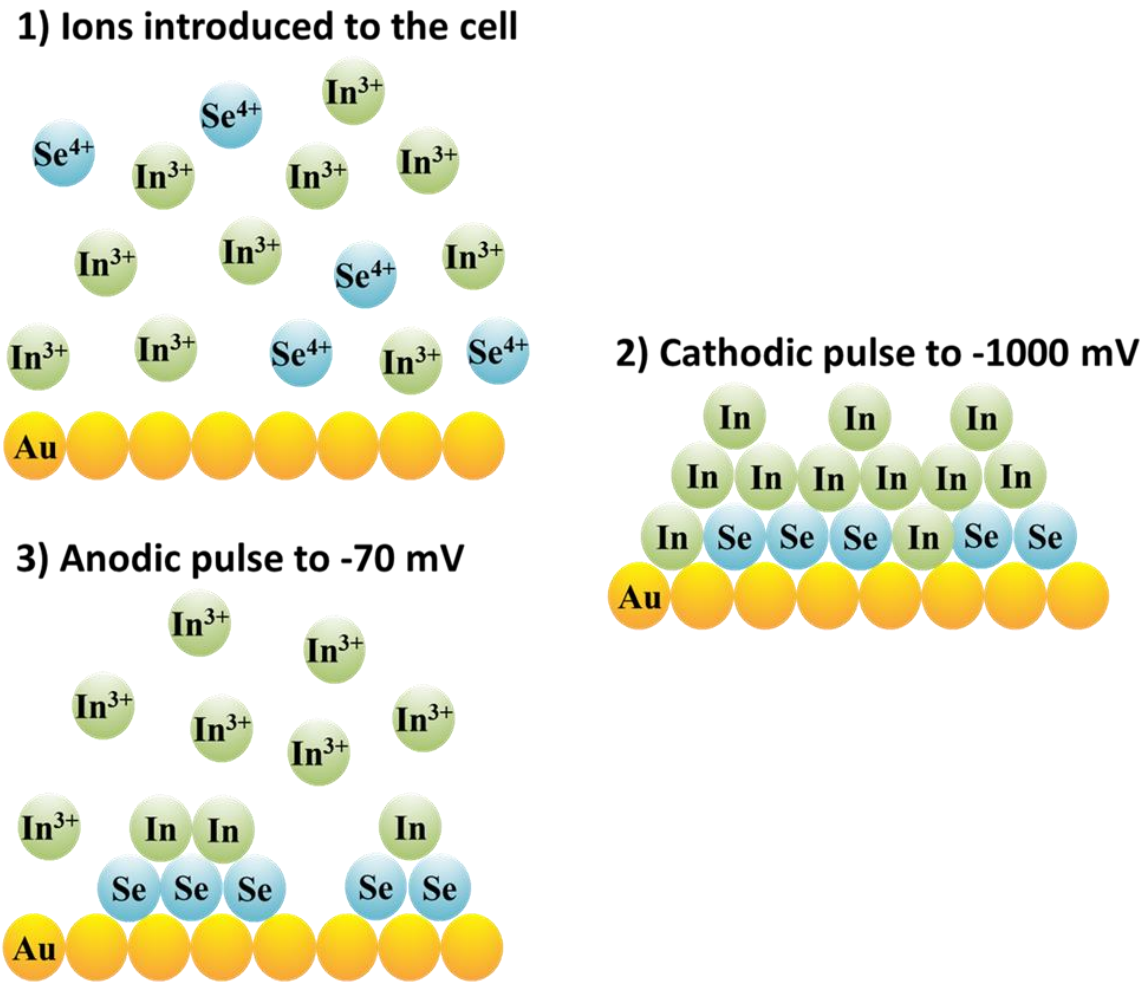

Figure 3.4: PP-ALD cartoon 1) In^{3+} (green) and Se^{4+} (blue) ions are introduced into the cell at the open circuit potential. 2) The potential is pulsed to -1000 mV for 0.13 s, resulting in the deposition of less than a monolayer of Se and excess In. 3) The potential was then stepped to -70 mV for 0.5 s, removing any excess Cu from the deposit.

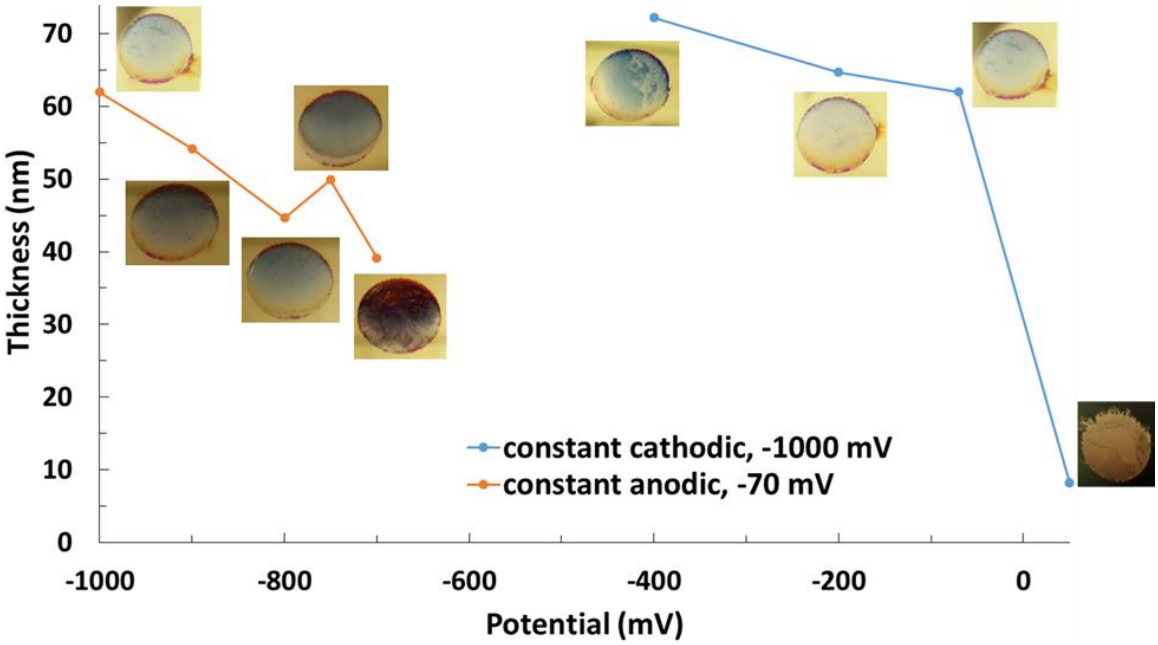

Figure 3.5: Potential vs thickness under constant Cathodic (blue, -1000 mV) and constant Anodic (orange, -70 mV) conditions. Each deposit was formed with 3300 pulses.

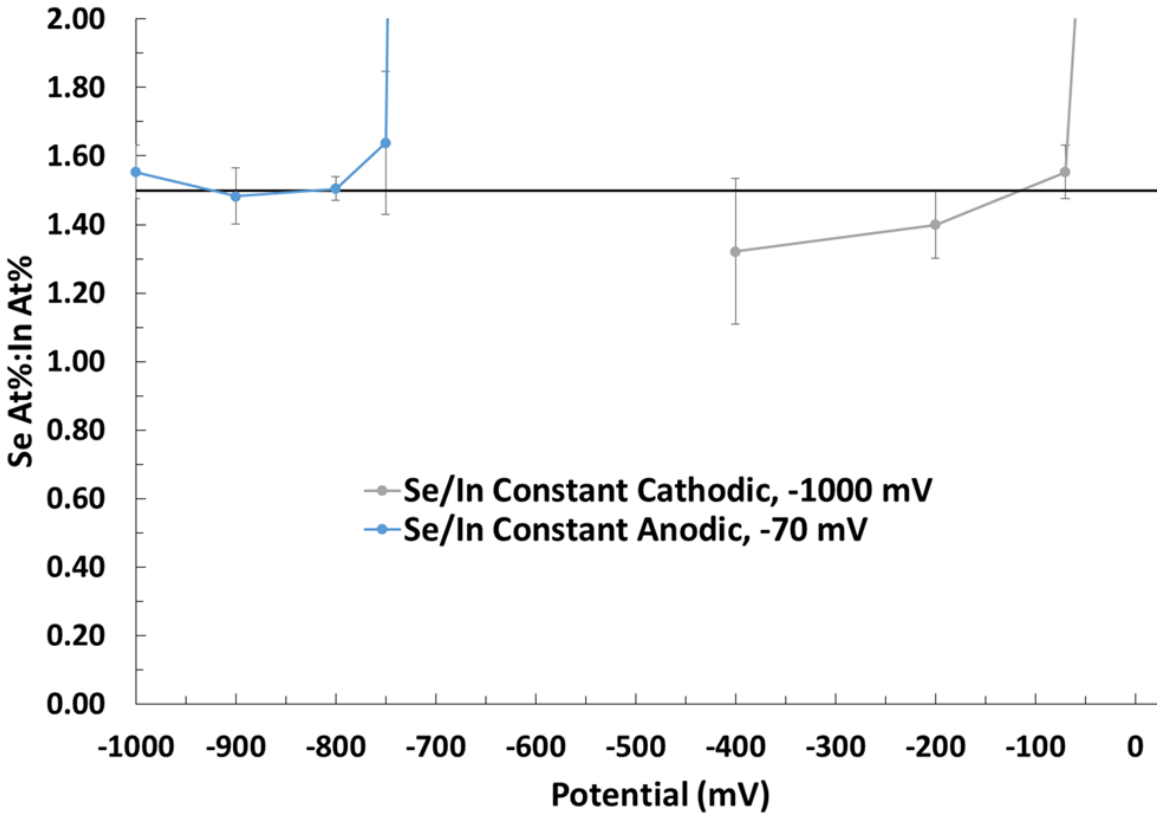

Figure 3.6: Deposit stoichiometry, determined by EPMA, of deposits made under constant Cathodic (grey, -1000 mV) and constant Anodic (blue, -70 mV) potentials. In the grey curve, the Anodic potential was varied. In the blue curve, the Cathodic potential was varied. Each deposit was formed using 3300 cycles.

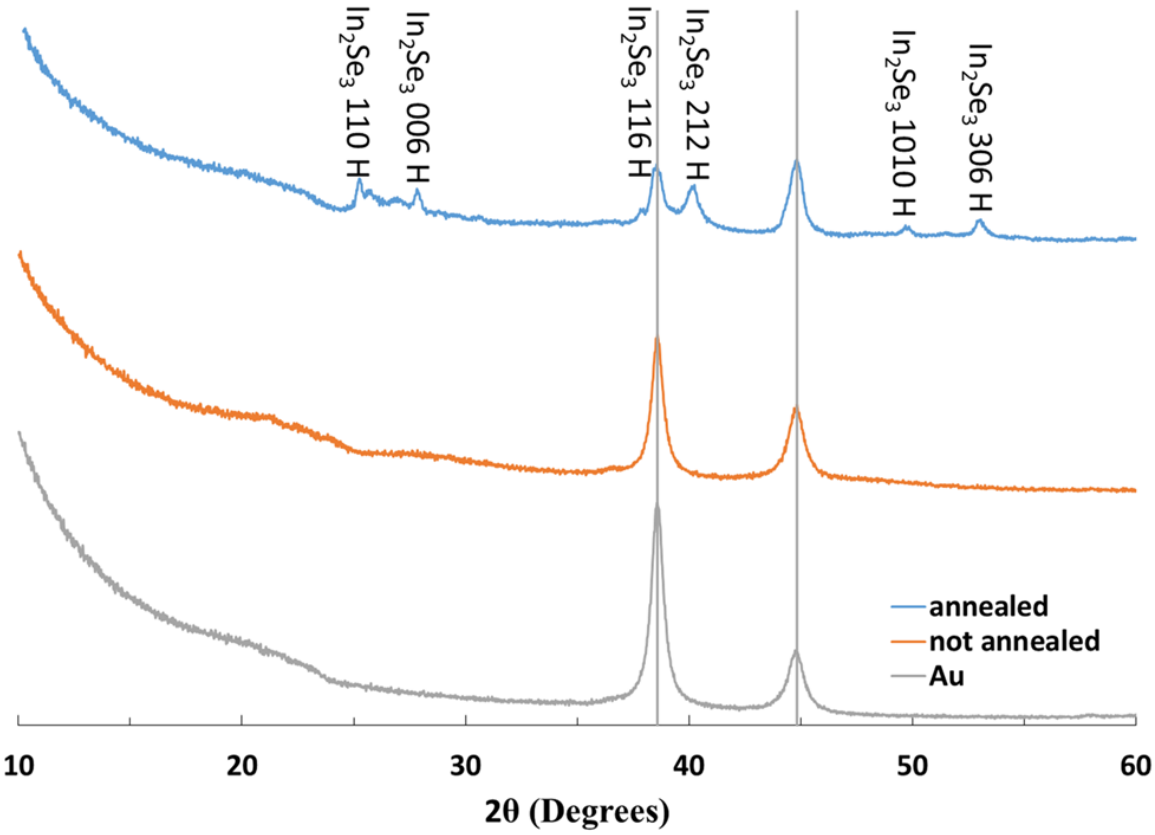

Figure 3.7: XRD pattern of Au, In_2Se_3 as deposited, and In_2Se_3 after annealing for 30 min at 300°C.

CHAPTER 4

INVESTIGATION OF PRECURSOR SOLUTION PH ON INSE THIN FILMS DEPOSITED BY POTENTIAL PULSE ATOMIC LAYER DEPOSITION (PP-ALD)[3]

[3] J. M. Czerniawski, J. L. Stickney, To be submitted to *Journal of the Electrochemical Society (2015)*

Abstract

Indium (III) selenide, In_2Se_3, thin films were deposited at room temperature from a pH 3 and pH 1 aqueous solution containing both In^{+3} and Se^{+4} ions using potential pulse atomic layer deposition (PP-ALD) in order to determine optimum solution pH. Cyclic voltammetry (CV) was used to determine approximate deposition potentials for In and Se. Electron probe microanalysis (EPMA) was used to follow the In:Se atomic ratios as a function of Anodic and Cathodic potentials. Films made with a pH 3 precursor were thin and did not adhere to the substrate. In pH 1 conditions, thin films with an ideal stoichiometric composition of 2:3 In to Se could be grown. No crystallographic patterns could be obtained from the thin films.

Introduction

In_2Se_3 is an n-type, visible light-driven semiconductor material with a direct bandgap around 1.62 eV[1] that has potential applications as an absorber layer in photovoltaic devices.[2] In_2Se_3 has been formed using numerous techniques including chemical bath deposition,[3] sputtering,[4] MOCVD,[5] spray pyrolysis,[6] magnetron sputtering,[4] and electrochemical deposition.[2]

Electrodeposition is generally considered a low cost, low temperature technique for growing thin film materials. Materials applicable for photovoltaic (PV) devices have been successfully grown using electrodeposition since Kroger et al.'s single solution CdTe work in the 70's.[7] ALD in general refers to a group of deposition techniques where surface limited reactions are used to form deposits one atomic layer at a time. A cycle of these reactions is used to form a compound monolayer and the cycle is repeated to grow

the deposit to a desired thickness. The author's group has conducted extensive studies on the development of E-ALD, the electrochemical version of atomic layer deposition (ALD), to form CdTe and other compound semiconductors.[8, 9]

The vast majority of ALD work has been performed in vacuum to form oxide nanofilms. E-ALD takes advantage of the naturally occurring phenomenon underpotential deposition (UPD), a type of electrochemical surface limited reaction where an atomic layer of a first element can be deposited on a second element at a potential prior to (under) that needed to deposit the first on itself driven by the free energy of formation of a surface compound or alloy.[10] In a typical E-ALD cycle, separate solutions containing precursors of different elements are introduced to the substrate at their UPD potentials resulting in an alternating deposition of atomic layers. After deposition of an atomic layer of the first element, the cell is rinsed with a blank solution and a precursor solution of the second element is introduced at its UPD potential, resulting in deposition of an atomic layer. Rinsing again with blank completes the cycle. The advantages of using E-ALD are increased control of the thickness, homogeneity, crystallinity, and quality of the deposit. The drawback is the deposition rate, due to the need for multiple solution exchanges each cycle. The technique is thus best applied when nanofilms of a carefully controlled thickness and quality are required and the total number of cycles performed is minimized.[9, 11] E-ALD is generally impractical for μm thick film growth when compared to the co-electrodeposition used by BP to form μm thick CdTe PV absorber materials.[12]

Co-electrodeposition has been used to form a large number of other compounds[13], such as CdSe.[14] Early CdSe co-electrodeposition studies indicated the presence of excess Se, for a Cd:Se ratio less than one.[15-17] Researchers were able to limit the deposition of Se

by dropping the concentration or forming complex soluble species thus shifting the deposition potential more negative. In a co-electrodeposition bath, however, this indirectly increased the overpotential used to deposit Cd resulting in deposits rich in Cd.[17, 18] A solution to the excess Cd and Se was proposed by Sailor et al., where instead of choosing a constant deposition potential, or current, they performed rapid and repeated cyclic voltammetry over a small range of potentials, a technique referred to as sequential monolayer electrodeposition (SMD).[16] The idea was to cycle between a negative potential where co-electrodeposition takes place, and a positive potential where excess, bulk Cd oxidized, but the Cd bound as CdSe did not. By scanning rapidly, traces of bulk cadmium formed at the more negative potentials were oxidatively removed at the positive end of each cycle, before they were buried by depositing CdSe, avoiding a buildup of excess Cd. SMD has been used by Penner et al. to construct nanowire photo-sensors based on CdSe[19] and Lee et al. to make 3-D macroporous structures of II-VI and III-V semiconductors.[20]

Another method proposed to control excess elemental deposition in $Bi_{2-x}Sb_xTe_3$ multilayers was described by Banga et al..[21] Pulsed potentiostatic electrodeposition (PPE) is a diffusion limited, single-bath, co-electrodeposition process where a duty cycle is established by pulsing for short periods of time (~2% duty cycle) down to a potential where a desired compound forms. The cell is then allowed to "rest" at the open-circuit potential to regenerate the diffusion layer. PPE creates highly crystalline deposits, but long resting times (2-10 s) are needed to carefully control precursor concentrations near the surface of the electrode.

This is an investigation into optimum precursor solution pH for a compound electrodeposition methodology that combines SMD, PPE, and E-ALD, where instead of cyclic voltammetry or changing solutions each cycle, the potential is alternated. As with E-ALD, sub-monolayer amounts are deposited each cycle, controlled by the surface-limited reaction between the depositing elements, and selective stripping of any bulk elemental deposit formed. It is referred to here as potential pulse atomic layer deposition (PP-ALD). PP-ALD has been successfully used to grow Cu_2Se deposits that were comparable to those made with co-electrodeposition. Those conditions were the foundation for a precursor which contained In and Se ions that could be used to develop a PP-ALD program to create the In_2Se_3 compound.

Potential steps are performed between optimized Cathodic and Anodic potentials. Given the differences in kinetics and deposition potentials for the two elemental precursors, codeposition can be performed (usually) at a Cathodic potential for a time sufficient to plate some fraction of a monolayer. The potential can then be stepped to an Anodic potential sufficiently positive to remove any elemental deposits of the more reactive element, leaving only a stable compound. The major benefits of this methodology over E-ALD are the large increase in deposition rate, increased scalability, and the ease with which solutions can be recycled.

Experimental

The solutions were 1.5 mM $In(ClO_4)_3$ (Sigma-Aldrich) with 0.1 mM SeO_2 (Alfa Æsar 99.999% pure) and 0.5 M $NaClO_4$ in 10 MΩ nanopure water (Millipore Advantage 10), fed by the house DI water source. The solution was then adjusted to pH 3 or pH 1 using $HClO_4$.

Precursor concentrations were kept in the mM range in order to help limit deposited amounts to a fraction of a monolayer (ML) each cycle. A ML is defined for this report as one atom for each Au substrate surface atom, or about 1.2 X 10^{15} atoms per cm^2. Substrates were 100 nm Au films on 5 nm of Ti on glass, purchased from Evaporated Metal Films (Ithaca, NY), and were first cleaned by three 5 min sonications in fresh aliquots of acetone, followed by three more sonications in aliquots of nanopure water. The substrates were then dipped in concentrated nitric acid for 30 sec, rinsed with nanopure water and dried with nitrogen before being placed in the electrochemical flow cell (Figure 4.1). The cell (Electrochemical ALD L.C.) was immediately flushed with 0.1 M H_2SO_4 (Fisher Scientific, certified ACS plus) and the potential was then held alternately for 5 sec at a time, between +1400 mV and -200 mV, four times to complete cleaning of the Au surface.

Figure 4.1 diagrams the electrochemical flow cell, where the auxiliary electrode was an Au wire inlayed into a Plexiglas cell face. Cu tape was used to connect the working electrode to its connection post. A 3 M Ag/AgCl reference electrode (BASi, West Lafayette, IN) was used, and the solution was pulled from degased solution reservoirs though the cell from the ingress up through the cell to the egress using a Masterflex (Cole Parmer) peristaltic pump.

Electron probe Microanalysis (EPMA) was performed on a JEOL 8600 Superprobe with a 10 KeV accelerating voltage, 15 nA beam current and 10 um beam diameter and spectroscopic ellipsometry was performed on a J.A. Woolam M-200V.

Results and Discussion

Figure 4.2 depicts cyclic voltammograms of pH 3 solutions used to determine deposition potentials for Se on Au (4.2a), In on Au (4.2b), and In on Se (4.2c).

In Figure 4.2a is a CV of pH 3 Se solution on an Au substrate. The reduction peak at 200 mV is the reduction of Se UPD. The higher coverage UPD reduction occurs at 100 mV. The reduction that occurs at 0 mV is the beginning of bulk Se reduction. The oxidation that begins at 600 mV is bulk Se oxidation. The second oxidation feature around 800 mV is the higher Se UPD. The oxidation peak positive of 600 mV corresponded to bulk stripping, while that at 775 mV was to surface limited stripping of Se. The oxidation peak at 925 mV demonstrates a fairly unique behavior. Normally, the most positive peak is associated with stripping the atoms most strongly bound to the surface, however the 925 mV oxidation peak only appeared when the potential was scanned to 0 mV or below. The surface structure for electrodeposited Se on Au is known to change with increasing coverage.[22, 23] Previous work using in-situ EC-STM showed that a low coverage $(\sqrt{3}X\sqrt{3})R30°$ structure was formed on Au(111) with triangular defects at 1/3 ML, where the Se atoms were separated at distances near their van der Waals diameter, 0.50 nm.[22, 23, 24] At lower potentials a higher coverage structure, composed of eight member rings of Se, were formed with a coverage closer to 0.89 ML.[23] That is, at more negative potentials the adsorbed Se structure undergoes a phase change to a more densely packed, more stable structure. Such a phase change might explain the appearance of the peak at 925 mV and its apparent increased stability.

Figure 4.2b is a CV of Au in a pH 3 In solution. The reduction beginning at -75 mV is the UPD of In. -475 mV is the beginning of alloy formation and the oxidation at -450 mV is the removal of alloy from the substrate. The oxidation feature at 100 mV is

UPD stripping from the surface. No peak for In bulk appears since the In/Au alloy has not saturated the Au bulk.

Figure 4.2c is a CV of a ~0.6 ML Se coated Au electrode in a pH 3 In solution. The reduction of UPD In occurs at a more negative potential since Se resides on the surface. The amount of In present is larger, seen in the oxidation feature which begins around -250 mV, since the In reacts with both the Au surface and the Se to form a compound. The oxidation feature beginning at 600 is similar to the one seen in 4.3a but is larger since a small amount of In was able to alloy with the Au but was not able to be oxidized until the Se layer protecting it was removed.

Figure 4.3 depicts cyclic voltammograms used to determine deposition potentials for In (4.3a) and Se (4.3b) separately, for In on Se (4.3c), and a CV of Au in a solution containing both In and Se precursor (4.3d) pH 1.

Figure 4.3a shows a potential scan down to -1 V of a gold substrate in $In(ClO_4)_3$, pH 1 solution. UPD begins around 100 mV and peaks around -150 mV. Bulk In begins around -300 mV until the reduction of water to form hydrogen gas begins at -500 mV. Due to excessive hydrogen evolution, an insufficient amount of time was spent at -1 V to get an adequate stripping peak for the bulk In, given the $E^{0'}$ for In is believed to be -600 mV. The oxidation feature that occurs at -400 mV is most likely the first layer of In alloy stripping from the deposit. Since this layer is at the surface, bound to both Au and In residing under the surface, it is bound more strongly than bulk In but weaker than UPD In. The oxidation of UPD begins at -250 mV and -100 mV. The reduction feature at 900 mV is Au oxide reduction.

Figure 4.3b is a potential scan of a gold substrate in 0.1 mM $HSeO_3^-$ pH 1 solution. The formal potential here is believed to be near 650 mV, suggesting that all Se deposition occurs at an overpotential, indicative of slow kinetics.[25] Surface limited peaks related to UPD are evident at 350, and 200 mV during the reduction scans. Stripping of the surface limited peak occurs at 850 mV. No peak above 850 is present since the scan was reversed above 0 mV. The reduction feature at 900 mV is the reduction of Au oxide.

Figure 4.3c shows a potential scan down to -1 V of a 0.6 ML Se pre-layer in $In(ClO_4)_3$, pH 1 solution. The reduction feature starting at -200 mV is the beginning of In reduction (4.3a) until a peak shows up at -300 mV corresponding to the reduction of Se^0 to Se^{2-}. The subsequent reduction at -400 mV is the reduction of In bulk (4.3a) and the beginning of the hydrogen evolution can be seen at -500 mV. Since the surface was modified with Se, the kinetics for hydrogen evolution slowed down, seen in the delay and shift of the sharp reduction feature. Note the reduction of Se UPD is not seen at 350 mV (Figure 4.3b) since the surface was preconditioned earlier with a Se layer. The first oxidation peak at -600 mV is the oxidation of In bulk, which agrees with the $E^{0'}$ discussed earlier. The oxidation beginning at -400 mV is consistent with the procedural stripping of the alloy from the surface of the substrate seen in Figure 4.3a. The shoulder that occurs around -100 mV matches the UPD stripping of In seen in Figure 4.3a. The oxidation beginning at 800 mV matches the oxidation feature seen in Figure 4.3b for Se UPD oxidation.

The potential scan in Figure 4.3d goes to -1 V and is representative of a gold electrode in a solution containing 1.5 mM In^{+3} and 0.1 mM $HSeO_3^-$. The open circuit potential (OCP) was around 400 mV and, starting negative, the first reduction feature

seen at -325 mV is similar to the Se reduction peak seen in Figure 4.3b. Again, the peak was not present in 4.3c since the 0.6 ML pre-layer of Se was formed without the presence of In precursor. Se^{4+} reduction can also account for the reduction between 200 and -80 mV though a small amount of the reduction between 0 and -80 mV could be attributed to In reduction seen in Figure 4.3a. The reduction feature that peaks around -240 mV is the reduction of Se^{0} to Se^{2-} and was seen in window opening CV of a gold substrate in Se^{+4} precursor (not pictured). The reduction beginning at -320 mV is In bulk reduction until finally at -530 mV hydrogen evolution occurs but the kinetics are slowed since the substrate surface has been modified. The oxidation feature seen at -600 mV is similar to the one seen in 4.3b, which is attributed to bulk In oxidation. The oxidation feature at -350 is surface alloy and In UPD stripping similar to that seen in Figure 4.3c. The feature is smaller in size since the compound is forming and prevents In from alloying as severely with the Au. This stabilization with not only the surface alloy but also the compound explains the shift to a more positive potential. The shoulder around -100 mV matches that in Figure 4.3a for In UPD. The oxidation feature occurring at 150 mV is In stripping from indium selenide compound. The peak beginning at 650 mV is the oxidation of bulk Se from the substrate and the shoulder that peaks at 950 mV is Se UPD oxidation. Figure 4.4 displays and example pulse profile for 5 cycles of a PP-ALD program used to make the deposits.

Figure 4.5 displays a study of thickness under constant anodic (orange) and constant cathodic (blue) conditions for 3300 cycle deposits made with pH 3 precursor. In the orange curve (anodic potential, 200 mV) the thickness increases as the cathodic potential is stepped progressively more negative. This trend can be explained by excess

material codepositing at the Cathodic pulse resulting in thicker deposits. The overall thickness, however, is thinner than expected for a 3300-pulse deposit, which is usually around 50 nm. It is possible that at pH 3, In is not stable and precipitates as an insoluble oxide or undergoes hydrolysis over time, seen as a white powder in precursor solution bottles.[26] It is possible that at pH 3 the solubility of In is greatly reduced since it is close to the conditions needed to form In_2O_3.[27] Since less precursor is available, a larger over potential is needed to deposit significant amounts of material. As the anodic potential is stepped more positive (blue, constant cathodic, -800 mV) the deposit becomes thinner and thinner correlating to greater and grater oxidation of the deposit. The deposits made with pH 3 precursor were red and did not adhere to the surface, removing easily with a wipe.

The same study was done for an pH 1 InSe precursor solution. Figure 4.6 displays the deposit thickness, from spectroscopic ellipsometry, after 3300 cycles where the Cathodic pulse potential was held constant (blue) and the Anodic pulse potential was varied. As the anodic potential is increased from -400 mV to +50 mV, deposit thickness decreases. At -400 mV bulk In is partially removed but creates a rough deposit as compound bi-layers are grown, increasing the resulting thickness since more surface area is available. As the Anodic potential is increased, more of the bulk In is removed until, at +50 mV, all In is removed from the deposit and only Se remains. When the potential is stepped back down to -1000 mV, most of the bulk Se strips as Se^{2-} and a thin red deposit is left at the end of deposition.

When the Cathodic pulse potential is varied and the Anodic pulse is held constant at -70 mV (orange) the thickness increases as the deposition potential becomes more

negative due to an increase in the overpotential. The inlay photos of each deposit show homogeneity increases macroscopically as more material is deposited. Deposits made with pH 1 solution acted as an interference filter, displaying a pale blue hue at the desired thickness, and adhered well to the substrate.

Figure 4.7 shows the ratio of Se/In of 3300 cycle deposits made under constant cathodic (blue) and constant anodic (orange) conditions from pH 3 precursor. Under constant cathodic conditions (blue) as the anodic potential is stepped positive, more In is removed from the surface making until all In is removed above 200 mV. Under constant anodic conditions (orange) the more negative the deposition potential the more In is deposited on the surface. Above -800 mV the potential is not negative enough to deposit In and so the ratio is high in Se.

In Figure 4.8, the stoichiometry does not change dramatically as the deposition potential is varied (blue, constant Anodic, -70 mV). Deposits made above a deposition potential of -750 mV are rich in Se since In deposition does not take place above this potential (data point not on scale). As the anodic potential becomes more positive (grey, constant Cathodic -1000 mV) the amount of In decrease since In is oxidized to a greater extent until all the indium is removed at potentials above -100 mV (data point is not on scale).

Conclusion

Because of solution stability and more predictable thin film growth, an In solution made with a pH of 1 was more desirable than solution made with a pH of 3. PP-ALD In_2Se_3 deposits made with pH 1 solution were 60 nm thick and those made using pH 3

were 10 to 20 nm unless a significant overpotential is used. Deposit thickness increased as the deposition potential was investigated at more and more negative potentials since more In can be deposited. In the pH 1 solution, the thickness was not significantly affected as the oxidation potential was moved more positive since the In oxidized should only be less stable bulk. In the pH 3 solution though, the In amount of oxidized was linear until all In was removed from the surface above 200 mV. The ratio of Se:In remained consistent at 1.5 unless the deposition potential was not negative enough to reduce In or the oxidation potential was too positive and oxidized all the In from the deposit.

Acknowledgements

Support from the National Science Foundation, DMR #1410109, is gratefully acknowledged.

References

1. Qasrawi, A. F., Temperature dependence of the band gap, refractive index and single-oscillator parameters of amorphous indium selenide thin films. *Optical Materials* **2007,** *29* (12), 1751-1755.
2. Yadav, A. A.; Salunke, S. D., Photoelectrochemical properties of In2Se3 thin films: Effect of substrate temperature. *Journal of Alloys and Compounds* **2015,** (0).
3. Asabe, M. R.; Chate, P. A.; Delekar, S. D.; Garadkar, K. M.; Mulla, I. S.; Hankare, P. P., Synthesis, characterization of chemically deposited indium selenide thin films at room temperature. *Journal of Physics and Chemistry of Solids* **2008,** *69* (1), 249-254; Pathan, H. M.; Kulkarni, S. S.; Mane, R. S.; Lokhande, C. D., Preparation and characterization of indium selenide thin films from a chemical route. *Materials Chemistry and Physics* **2005,** *93* (1), 16-20.
4. Li, S.; Yan, Y.; Zhang, Y.; Ou, Y.; Ji, Y.; Liu, L.; Yan, C.; Zhao, Y.; Yu, Z., Monophase γ-In2Se3 thin film deposited by magnetron radio-frequency sputtering. *Vacuum* **2014,** *99* (0), 228-232; Yan, Y.; Li, S.; Yu, Z.; Liu, L.; Yan, C.; Zhang, Y.; Zhao, Y., Influence of indium concentration on the structural and optoelectronic properties of indium selenide thin films. *Optical Materials* **2014,** *38* (0), 217-222; Yan, Y.; Li, S.; Ou, Y.; Ji, Y.; Liu, L.; Yan, C.; Zhang, Y.; Yu, Z.; Zhao, Y., In-situ annealing of In–Se amorphous precursors sputtered at low temperature. *Journal of Alloys and Compounds* **2014,** *614* (0), 368-372.

5. Choi, H.; Nicolaescu, R.; Paek, S.; Ko, J.; Kamat, P. V., Supersensitization of CdS Quantum Dots with a Near-Infrared Organic Dye: Toward the Design of Panchromatic Hybrid-Sensitized Solar Cells. *ACS Nano* **2011,** *5* (11), 9238-9245.

6. Aydin, E.; Sankir, M.; Sankir, N. D., Influence of silver incorporation on the structural, optical and electrical properties of spray pyrolyzed indium sulfide thin films. *Journal of Alloys and Compounds* **2014,** *603* (0), 119-124; Reyes-Figueroa, P.; Painchaud, T.; Lepetit, T.; Harel, S.; Arzel, L.; Yi, J.; Barreau, N.; Velumani, S., Structural properties of In2Se3 precursor layers deposited by spray pyrolysis and physical vapor deposition for CuInSe2 thin-film solar cell applications. *Thin Solid Films* (0).

7. Kröger, F. A., Cathodic Deposition and Characterization of Metallic or Semiconducting Binary Alloys or Compounds. *Journal of The Electrochemical Society* **1978,** *125* (12), 2028-2034; Panicker, M. P. R.; Knaster, M.; Kroger, F. A., Cathodic Deposition Of CdTe From Aqueous-Electrolytes. *Journal of the Electrochemical Society* **1978,** *125* (4), 566-572.

8. D. W. Suggs, I. V., B.W. Gregory, J.L. Stickney, Formation of CdTe and GaAs by electrochemical atoimc layer epitaxy (ECALE). *Mat. Res. Soc. Symp. Proc.* **1991,** *222*, 283; Colletti, L. P.; Stickney, J. L., II-VI compound semiconductor thin-film electrodeposition by ECALE. *Book of Abstracts, 210th ACS National Meeting, Chicago, IL, August 20-24* **1995,** (Pt. 1), INOR-297; Colletti, L. P.; Flowers, B. H.; Stickney, J. L., Formation of Thin-Films of CdTe, CdSe, and CdS by Electrochemical ALE. *JECS* **1997**; Colletti, L. P.; Slaughter, R.; Stickney, J. L., ZnS thin film formation by electrochemical ALE: preliminary doping studies.

Proceedings - Electrochemical Society **1997,** *97-20* (Photoelectrochemistry), 1-10; Perdue, B.; Czerniawski, J.; Anthony, J.; Stickney, J., Optimization of Te Solution Chemistry in the Electrochemical Atomic Layer Deposition Growth of CdTe. *Journal of The Electrochemical Society* **2014,** *161* (7), D3087-D3092.

9. Banga, D.; Jarayaju, N.; Sheridan, L.; Kim, Y.-G.; Perdue, B.; Zhang, X.; Zhang, Q.; Stickney, J., Electrodeposition of CuInSe2 (CIS) via Electrochemical Atomic Layer Deposition (E-ALD). *Langmuir* **2012,** *28* (5), 3024-3031.

10. Kolb, D. M., Physical and Electrochemical Properties of Metal Monolayers on Metallic Substrates. In *Advances in Electrochemistry and Electrochemical Engineering*, Gerischer, H.; Tobias, C. W., Eds. John Wiley: New York, 1978; Vol. 11, p 125; Juttner; K.; Lorenz; W.J., *Z. Phys. Chem. N. F.* **1980,** *122*, 163; Adzic, R. R., Electrocatalytic Properties of the Surfaces Modified by Foreign Metal Ad Atoms. In *Advances in Electrochemistry and Electrochemical Engineering*, Gerishcher, H.; Tobias, C. W., Eds. Wiley-Interscience: New York, 1984; Vol. 13, p 159; Gewirth, A. A.; Niece, B. K., Electrochemical applications of in situ scanning probe microscopy. *Chem. Rev.* **1997,** *97*, 1129-1162.

11. Vaidyanathan, R.; Mathe, M. K.; Sprinkle, P.; Cox, S. M.; Happek, U.; Stickney, J. L., Electrodeposition of Cu2Se thin films by electrochemical atomic layer epitaxy (EC-ALE). *Materials Research Society Symposium Proceedings* **2003,** *744* (Progress in Semiconductors II--Electronic and Optoelectronic Applications), 289-294.

12. Turner, A. K.; Woodcock, J. M.; Ozsan, M. E.; Cunningham, D. W.; Johnson, D. R.; Marshall, R. J.; Mason, N. B.; Oktik, S.; Patterson, M. H.; Ransome, S. J.;

Roberts, S.; Sadeghi, M.; Sherborne, J. M.; Sivapathasundaram, D.; Walls, I. A., BP Solar Thin-Film Cdte Photovoltaic Technology. *Solar Energy Materials and Solar Cells* **1994,** *35* (1-4), 263-270; Cunningham, D.; Rubcich, M.; Skinner, D., Cadmium telluride PV module manufacturing at BP Solar. *Progress in Photovoltaics* **2002,** *10* (2), 159-168.

13. Öznülüer, T.; Erdoğan, İ.; Şişman, İ.; Demir, Ü., Electrochemical Atom-by-Atom Growth of PbS by Modified ECALE Method. *Chemistry of Materials* **2005,** *17* (5), 935-937; Öznülüer, T.; Erdoğan, İ.; Demir, Ü., Electrochemically Induced Atom-by-Atom Growth of ZnS Thin Films: A New Approach for ZnS Co-deposition. *Langmuir* **2006,** *22* (9), 4415-4419.

14. Loizos, Z.; Mitsis, A.; Spyrellis, N.; Froment, M.; Maurin, G., Cadmium chalcogenide semiconducting thin films prepared by electrodeposition from boiling aqueous electrolytes. *Thin Solid Films* **1993,** *235* (1-2), 51-56.

15. Kazacos, M. S.; Miller, B., Studies in Selenious Acid Reduction and CdSe Film Deposition. *Journal of The Electrochemical Society* **1980,** *127* (4), 869-873; Skyllas Kazacos, M.; Miller, B., Electrodeposition of CdSe Films from Selenosulfite Solution. *Journal of The Electrochemical Society* **1980,** *127* (11), 2378-2381; Houston, G. J.; McCann, J. F.; Haneman, D., Optimising the photoelectrochemical performance of electrodeposited CdSe semiconductor electrodes. *Journal of Electroanalytical Chemistry and Interfacial Electrochemistry* **1982,** *134* (1), 37-47; Tomkiewicz, M.; Ling, I.; Parsons, W. S., Morphology, Properties, and Performance of Electrodeposited n - CdSe in Liquid Junction Solar Cells. *Journal of The Electrochemical Society* **1982,** *129* (9), 2016-

2022; Skyllas-Kazacos, M., Electrodeposition of CdSe and CdSe+CdTe thin films from cyanide solutions. *Journal of Electroanalytical Chemistry and Interfacial Electrochemistry* **1983,** *148* (2), 233-239; Wei, C.; Bose, C. S. C.; Rajeshwar, K., Compositional analysis of electrosynthesized semiconductor thin films by electrochemical quartz crystal microgravimetry: Application to the Cd + Se system. *Journal of Electroanalytical Chemistry* **1992,** *327* (1–2), 331-336.

16. Kressin, A. M.; Doan, V. V.; Klein, J. D.; Sailor, M. J., Synthesis of stoichiometric CdSe films via sequential monolayer electrodeposition. *Chem. Mater.* **1991,** *3*, 1015-1020.

17. Ham, D.; Mishra, K. K.; Rajeshwar, K., Anodic electrosynthesis of CdSe thin-films: Characterization and comparison with the passive/transpassive behavior of the CdX (X= S, Te) counterparts. *J. Electrochem. Soc.* **1991,** *138*, 100.

18. Cocivera, M.; Darkowski, A.; Love, B., Thin Film CdSe Electrodeposited from Selenosulfite Solution. *Journal of The Electrochemical Society* **1984,** *131* (11), 2514-2517; Loizos, Z.; Spyrellis, N.; Maurin, G.; Pottier, D., Semiconducting CdSex, Te1−x thin films prepared by electrodeposition. *Journal of Electroanalytical Chemistry and Interfacial Electrochemistry* **1989,** *269* (2), 399-410; Krishnan, V.; Ham, D.; Mishra, K. K.; Rajeshwar, K., Electrosynthesis of thin films of CdZnSe: composition modulation and bandgap engineering in the ternary system. *J. Electrochem. Soc.* **1992,** *139*, 23; Krishnan, V.; Ham, D.; Mishra, K. K.; Rajeshwar, K., Electrosynthesis of Thin Films of CdZnSe : Composition Modulation and Bandgap Engineering in the Ternary System. *Journal of The Electrochemical Society* **1992,** *139* (1), 23-27.

19. Liu, F.; Huang, C.; Lai, Y.; Zhang, Z.; Li, J.; Liu, Y., Preparation of Cu(In,Ga)Se2 thin films by pulse electrodeposition. *Journal of Alloys and Compounds* **2011,** *509* (8), L129-L133; Ayvazian, T.; van der Veer, W. E.; Xing, W.; Yan, W.; Penner, R. M., Electroluminescent, Polycrystalline Cadmium Selenide Nanowire Arrays. *ACS Nano* **2013,** *7* (10), 9469-9479.

20. Lee, Y.-C.; Kuo, T.-J.; Hsu, C.-J.; Su, Y.-W.; Chen, C.-C., Fabrication of 3D Macroporous Structures of II−VI and III−V Semiconductors Using Electrochemical Deposition. *Langmuir* **2002,** *18* (25), 9942-9946.

21. Banga, D.; Lensch-Falk, J. L.; Medlin, D. L.; Stavila, V.; Yang, N. Y. C.; Robinson, D. B.; Sharma, P. A., Periodic Modulation of Sb Stoichiometry in Bi2Te3/Bi2–xSbxTe3 Multilayers Using Pulsed Electrodeposition. *Crystal Growth & Design* **2012,** *12* (3), 1347-1353.

22. Lister, T. E.; Stickney, J. L., Atomic Level Studies of Selenium Electrodeposition on Gold(111) and Gold(110). *The Journal of Physical Chemistry* **1996,** *100* (50), 19568-19576.

23. Sorenson, T. A.; Lister, T. E.; Huang, B. M.; Stickney, J. L., A Comparison of Atomic Layers Formed by Electrodeposition of Selenium and Tellurium Scanning Tunneling Microscopy Studies on Au(100) and Au(111). *Journal of The Electrochemical Society* **1999,** *146* (3), 1019-1027.

24. Pauling, L., *The Nature of the Chemical Bond and the Structure of Molecules and Crystals: An Introduction to Modern Structural Chemistry*. Cornell University Press: 1960.

25. Lister, T. E.; Huang, B. M.; Herrick, R. D.; Stickney, J. L., Electrochemical Formation of Se Atomic Layers On Au(100). *Journal of Vacuum Science & Technology B* **1995,** *13* (3), 1268; Lister, T. E.; Stickney, J. L., Atomic level studies of selenium electrodeposition on gold (111) and gold (110). *Journal of Physical Chemistry* **1996,** *100* (50), 19568-19576; Huang, B. M.; Lister, T. E.; Stickney, J. L., Se adlattices formed on Au (100), studies by LEED, AES, STM and electrochemistry. *Surface Science* **1997,** *392* (1-3), 27.

26. Hattox, E. M.; Vries, T. D., The Thermodynamics of Aqueous Indium Sulfate Solutions1. *Journal of the American Chemical Society* **1936,** *58* (11), 2126-2129; Sato, T., Preparation and thermal decomposition of indium hydroxide. *Journal of Thermal Analysis and Calorimetry* **2005,** *82* (3), 775-782; Chou, W.-L.; Huang, Y.-H., Electrochemical removal of indium ions from aqueous solution using iron electrodes. *Journal of Hazardous Materials* **2009,** *172* (1), 46-53.

27. Pourbaix, M., *Atlas of Electrochemical Equilibria in Aqueous Solutions*. New York, 1974.

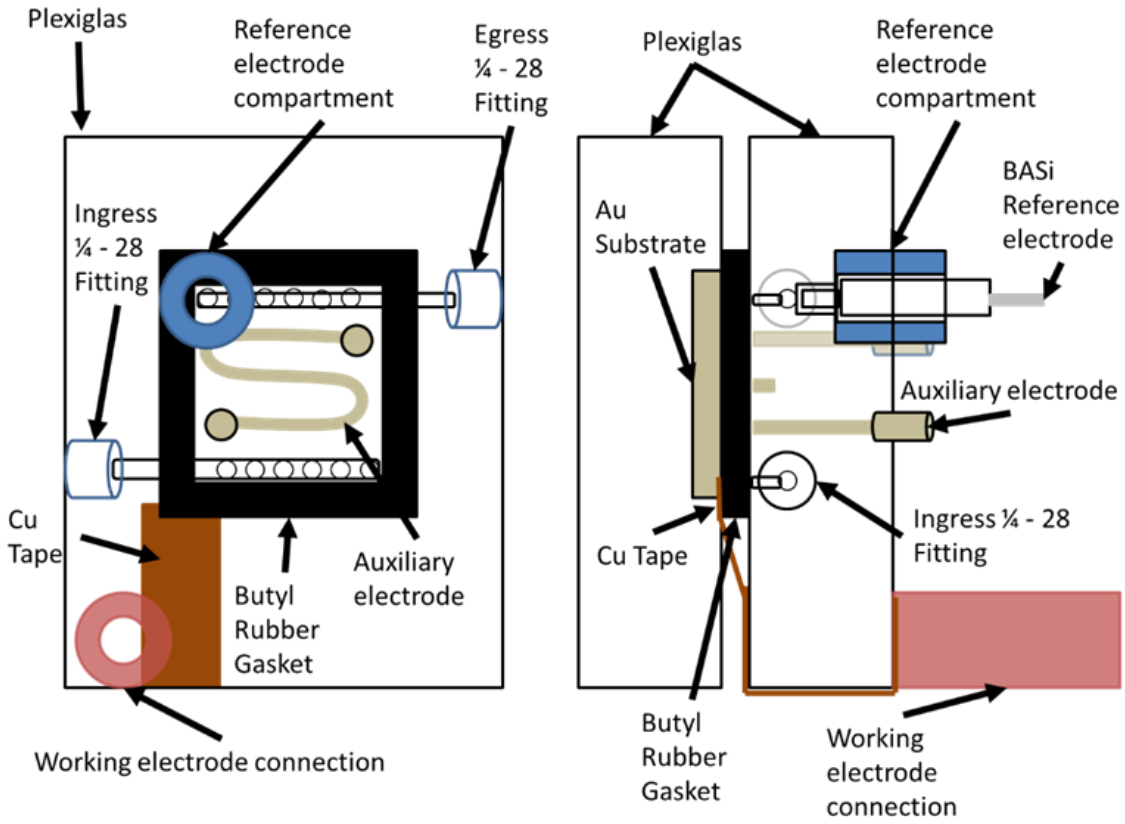

Figure 4.1: Schematic of the electrochemical flow cell, Z cell, as the solution enters left to right through the bottom row of holes, and exits the cell left to right through the top row of holes. Simulations have shown this configuration to result in a fairly homogeneous flow field.

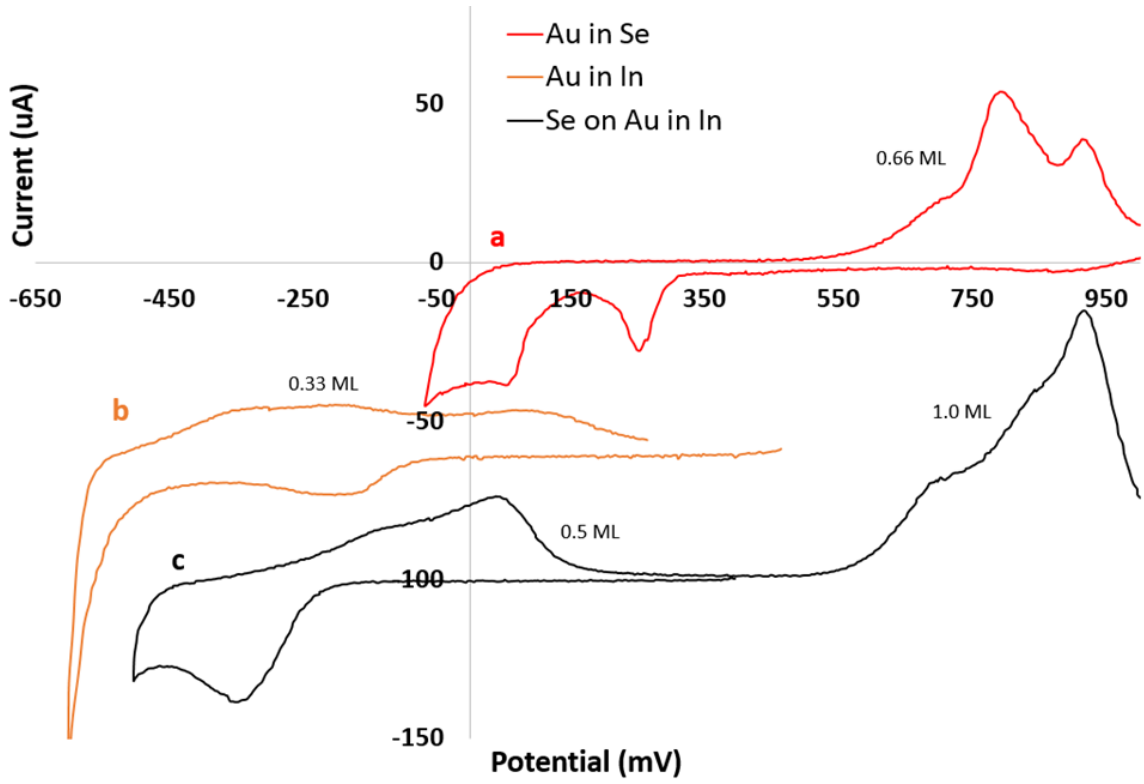

Figure 4.2: Cyclic voltammogram of a) Au in 0.1 mM SeO_2 b) Au in 1.5 mM $In(ClO_4)_3$ and c) ~0.6 ML Se in 1.5 mM $In(ClO_4)_3$. All solutions were pH 3. Potential was measured vs. the Ag/AgCl reference electrode with a scan rate of 10 mV/sec. The flow rate was 4mL/min. The electrode area was 0.79 cm^2.

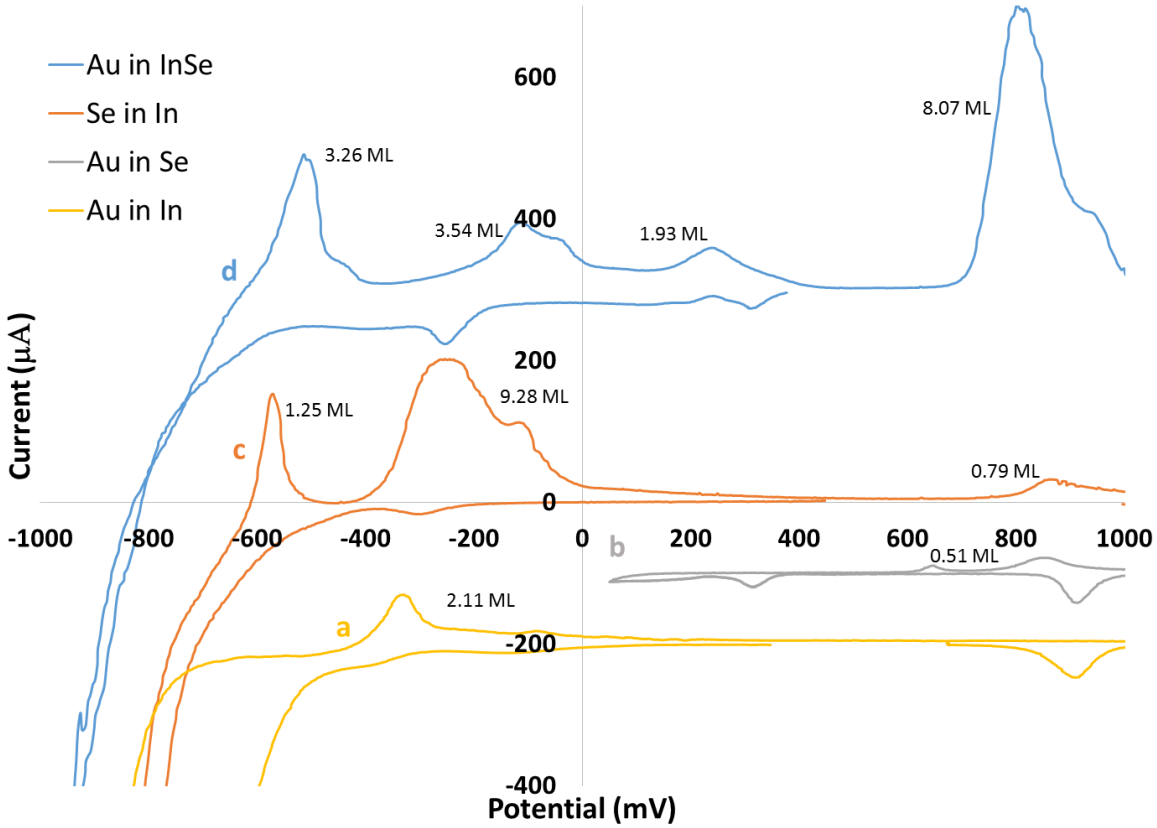

Figure 4.3: Cyclic voltammogram of a) Au in 1.5 mM $In(ClO_4)_3$ b) Au in 0.1 mM SeO_2 c) ~0.6ML Se in 1.5 mM $In(ClO_4)_3$ and d) Au in 1.5 mM $In(ClO_4)_3$ and 0.1 mM SeO_2. All solutions were pH 1. Potential was measured vs. the Ag/AgCl reference electrode with a scan rate of 10 mV/sec. The flow rate was 4 mL/min. The electrode area was 0.79 cm^2.

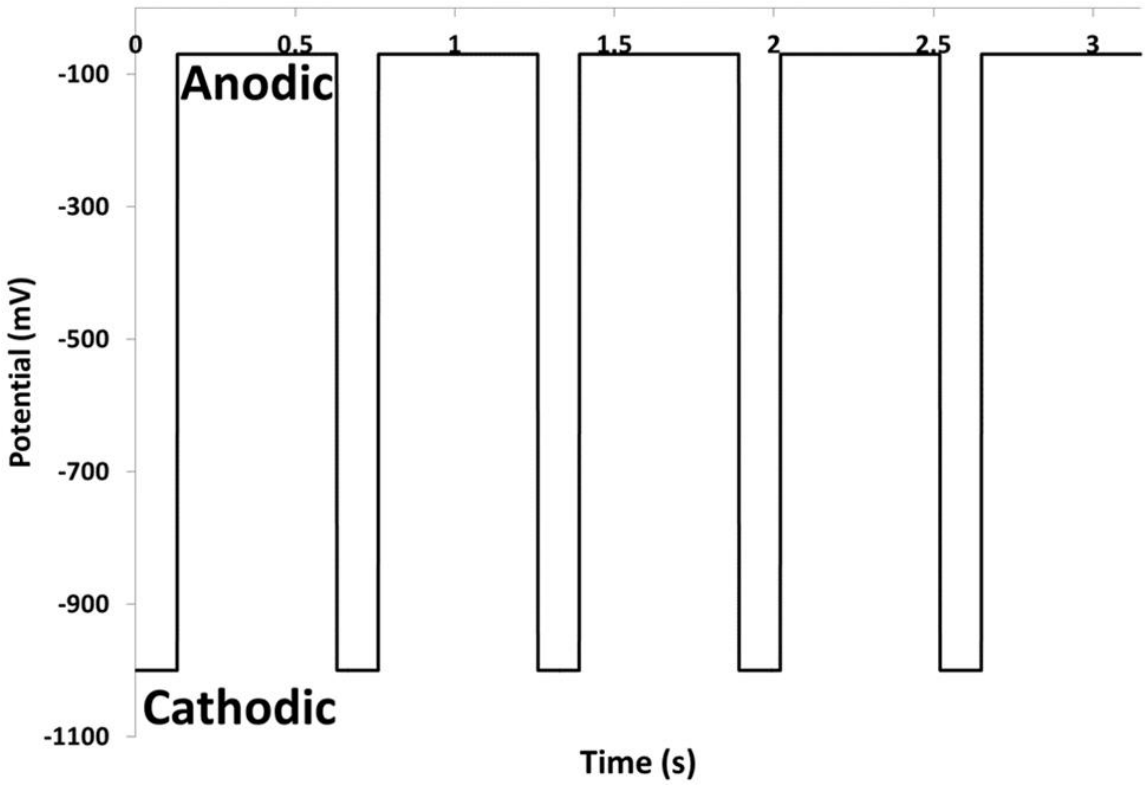

Figure 4.4: Potential profile for 5 PP-ALD cycles. The cycle begins at -1000 mV, the Cathodic potential, for 0.13 sec. Fractions of a monolayer of Se and In were deposited. The potential was then stepped to -70 mV, the Anodic potential, and any excess In was removed from the deposit.

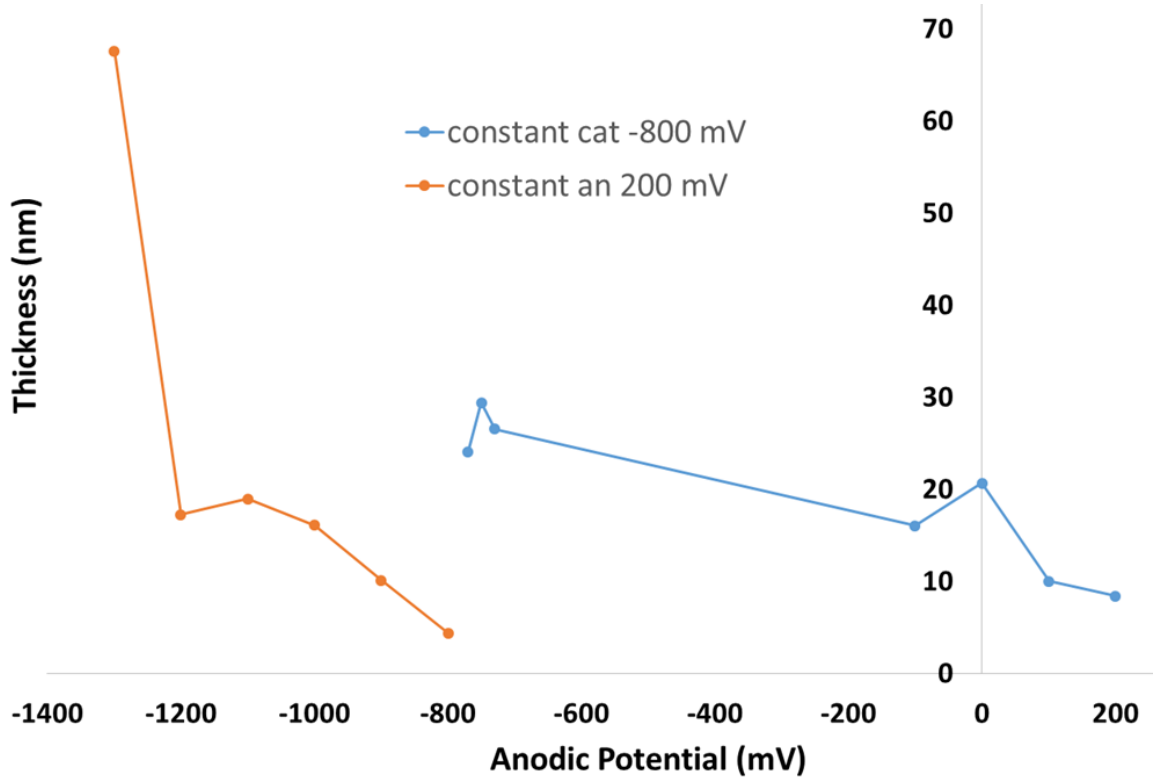

4.5 pH 3 Potential vs thickness under constant Cathodic (blue, -800 mV) and constant Anodic (orange, 200 mV) conditions. Each deposit was formed with 3300 pulses. pH 3 solution.

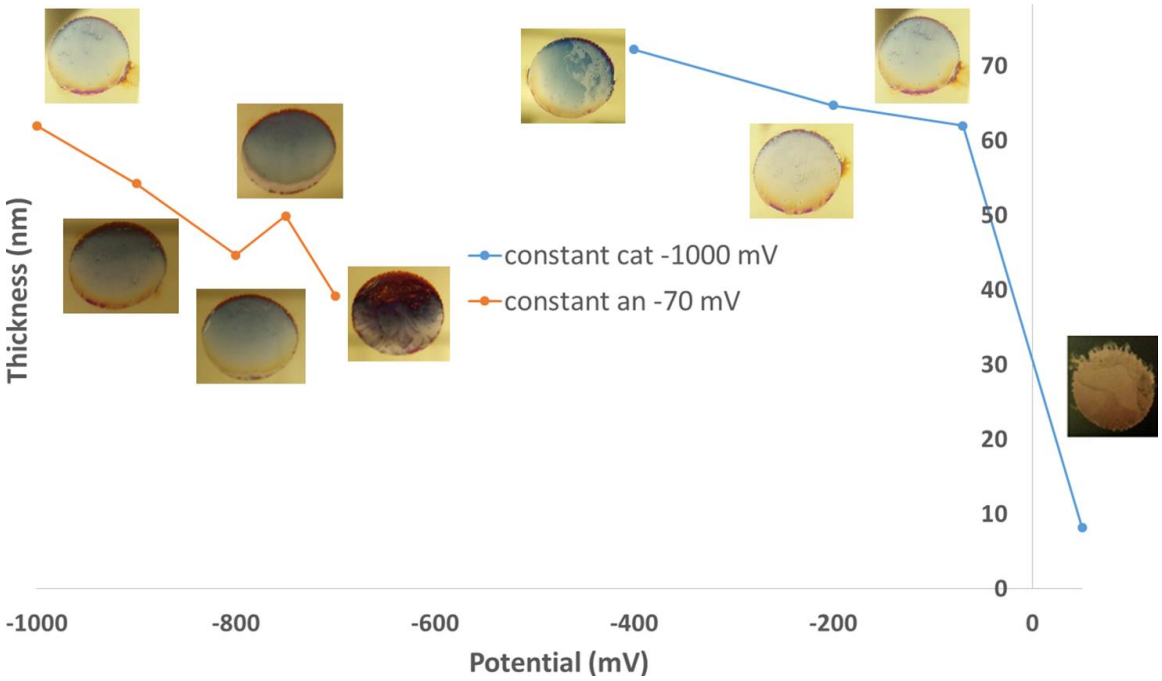

Figure 4.6: Potential vs thickness under constant Cathodic (blue, -1000 mV) and constant Anodic (orange, -70 mV) conditions. Each deposit was formed with 3300 pulses from a pH 1 solution.

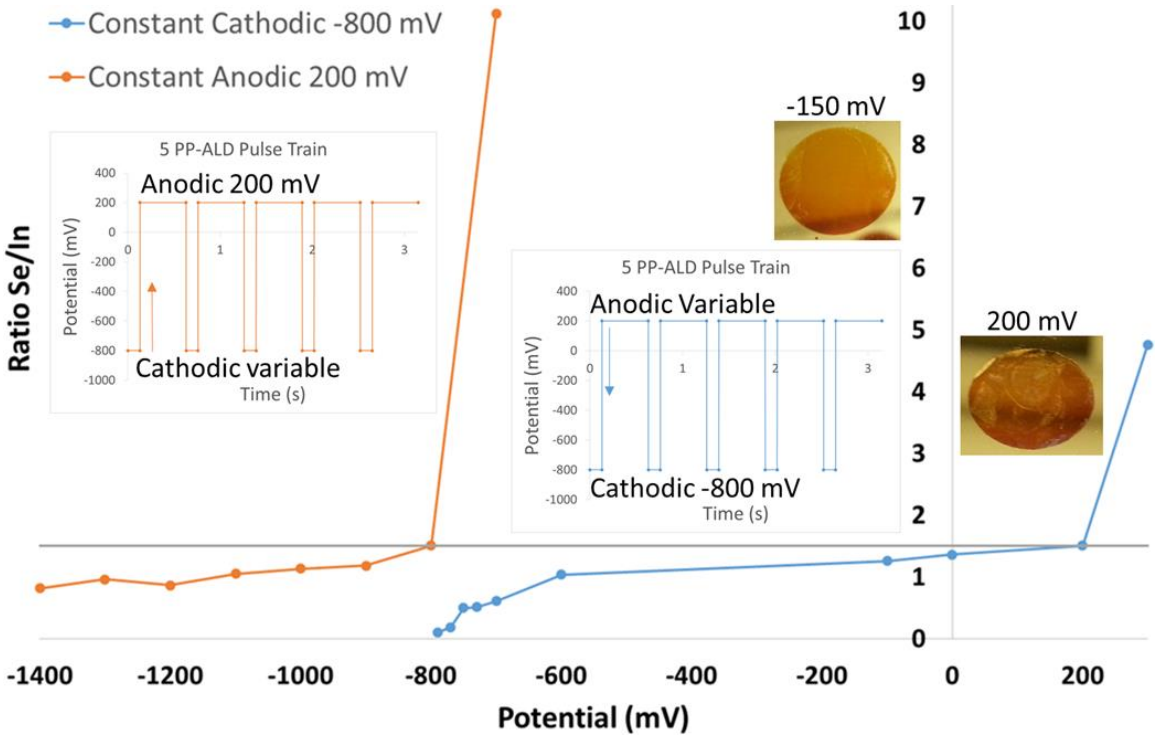

Figure 4.7: Deposit stoichiometry, determined by EPMA, of deposits made under constant Cathodic (blue, -800 mV) and constant Anodic (orange, 200 mV) potentials. In the blue curve, the Anodic potential was varied. In the orange curve, the Cathodic potential was varied. Each deposit was formed using 3300 cycles from a pH 3 solution.

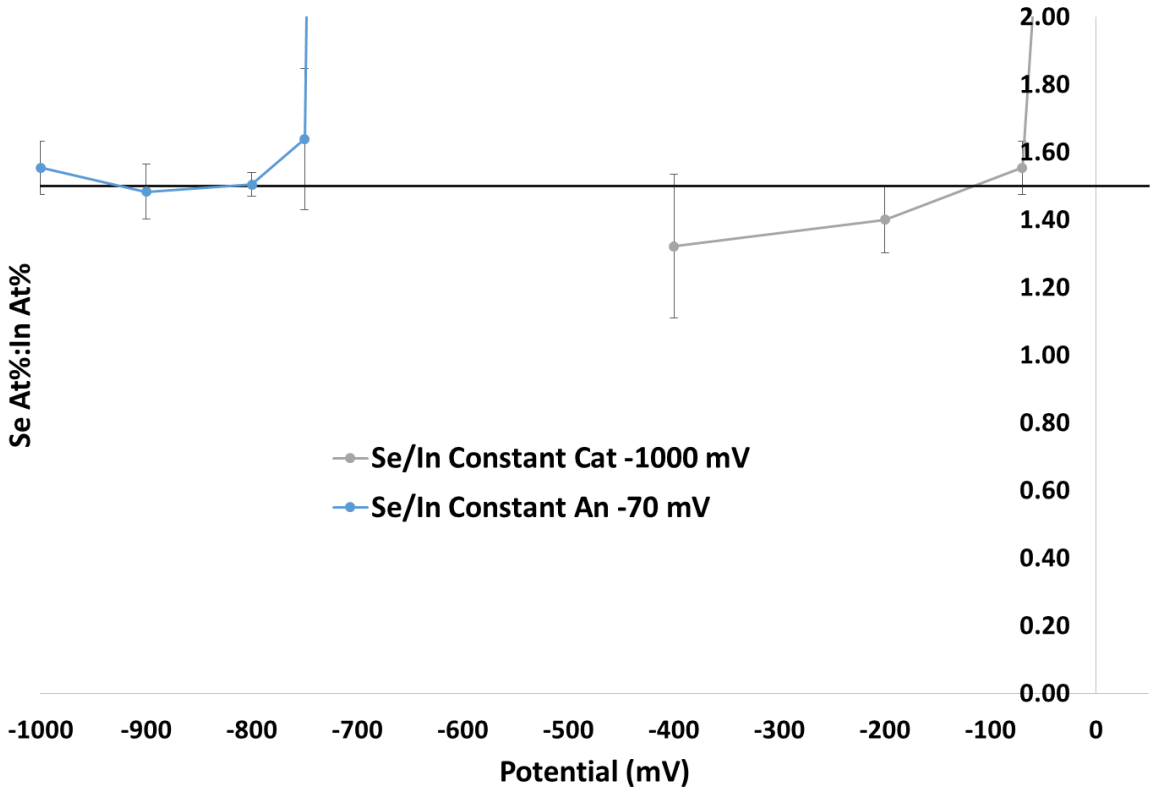

Figure 4.8: Deposit stoichiometry, determined by EPMA, of deposits made under constant Cathodic (grey, -1000 mV) and constant Anodic (blue, -70 mV) potentials. In the grey curve, the Anodic potential was varied. In the blue curve, the Cathodic potential was varied. Each deposit was formed using 3300 cycles from a pH 1 solution.

CHAPTER 5

PRELIMINARY STUDIES OF SE^{+6} ION AS A REPLACEMENT PRECURSOR FOR SE^{+4} ION[4]

[4] J. M. Czerniawski, J. L. Stickney, To be submitted to *Journal of the Electrochemical Society (2015)*

Abstract

Cyclic voltammetry (CV) was used to examine changes in the electrochemical profile for Au in Se^{+6} ions when compared to the profile of Au in Se^{+4} ions. A CV of an Au substrate treated with underpotentially deposited Cu showed the amount of Se deposited from Se^{+6} solution was slightly higher, 0.3 ML, compared to the Se amount deposited on an untreated Au surface from the same solution, 0.1 ML. While Cu appeared to have a positive effect on Se^{+6} deposition, the increase is not practical enough to consider Se^{+6} precursor a viable replacement for Se^{+4} precursor.

Introduction

Cu is commonly used to modify sorption agents, such as activated carbon, in order to improve sequestration of arsenic and selenium surface and groundwater contaminants.[1] The mechanism for Se sorption involves the formation of a surface complex with a metal oxide however, Se^{+4} forms stronger surface complexes with metal oxides than Se^{+6} requiring the integration of different materials to remove Se^{+6} contaminants.[1, 2] Electrodeposition might create energetically favorable conditions that allows for both Se^{+4} and Se^{+6} species to be removed from solution and deposited onto metal surfaces negating the need for multi-component sorption agents.

Electrodeposition is known as a low temperature, low-cost, and scalable thin film synthesis method. Cu_2Se is one well-studied compound, due to its application in the formation of photovoltaic (PV) absorber layers, that has been successfully grown using electrodeposition since the late 80's.[3] The classic electrodeposition methodology is co-electrodeposition, described for CdTe deposition by Kroger et al..[4] The

co-electrodeposition process is low-cost and simple, given the right solution chemistry. Many binary compounds have been formed using co-electrodeposition, at a controlled potential or current in a single solution containing precursors for both elements.[5] Taking advantage of the thermodynamics of co-electrodeposition might aid in the removal of Se contamination from aqueous environments.

The author's group has also conducted extensive studies on the development of E-ALD, the electrochemical version of atomic layer deposition (ALD), to form CdTe and other compound semiconductors.[6, 7] E-ALD takes advantage of electrochemical surface limited reactions where an atomic layer of a first element can be deposited on a second element at a potential prior to (under) that needed to deposit the first on itself driven by the free energy of formation of a surface compound or alloy, called UPD.[8] The advantages of using E-ALD are increased control of the thickness, homogeneity, crystallinity, and quality of the deposit. The drawback is the deposition rate, due to the need for multiple solution exchanges each cycle. The technique is thus best applied when nanofilms of a carefully controlled thickness and quality are required and the total number of cycles performed is minimized.[7, 9] E-ALD is generally impractical for µm thick film growth when compared to the co-electrodeposition used by BP to form µm thick CdTe PV absorber materials.[10] As an attempt to address the long growth cycles, potential pulse atomic layer deposition (PP-ALD) has been developed as a faster alternative. Understanding the behavior of Se^{+6} ion vs Se^{+4} might be useful for future PP-ALD studies when codeposition precursor ions are not compatible, i.e. Sn^{+2} and Se^{+4} ions.

Experimental

The solutions, adjusted to pH 1, contained either 1.5 mM $Cu(ClO_4)_2$ (98% purity from Sigma-Aldrich), 1.5 mM SeO_2 (Alfa Æsar 99.999% pure), or 1.5 mM Na_2SeO_4 (Alfa Æsar 99.9% pure) in 0.5 M $NaClO_4$ and 18 MΩ Nanopure water (Millipore Advantage 10), fed by the house DI water source. Precursor concentrations were kept in the mM range to help limit deposited amounts to a fraction of a monolayer (ML) each cycle. A ML is defined for this report as one atom for each Au substrate surface atom, or about 1.2 X 10^{15} atoms per cm^2. Substrates were 100 nm thick Au films on 5 nm of Ti on glass, purchased from Evaporated Metal Films (Ithaca, NY), and were first cleaned by three 5 min sonication in fresh aliquots of acetone, then three in aliquots of Nanopure water. They were then dipped in concentrated nitric acid for 30 sec, rinsed with Nanopure water and dried with nitrogen before being placed in the electrochemical flow cell (Figure 5.1). The cell (Electrochemical ALD L.C.) was immediately flushed with 0.1 M H_2SO_4 (Fisher Scientific, certified ACS plus) and the potential was then alternated four times between +1400 mV and -200 mV, for 5 seconds at each potential, to complete cleaning of the Au surface.

Figure 5.1 diagrams the electrochemical flow cell, where the auxiliary electrode was an Au wire inlayed into a Plexiglas cell face. Cu tape was used to connect the working electrode to its connection post. A 3 M Ag/AgCl reference electrode (BASi, West Lafayette, IN) was used, and the solution was pulled from degased solution reservoirs though the cell from the ingress up through the cell to the egress using a Masterflex (Cole Parmer) peristaltic pump.

Results and Discussion

A window opening scan of a gold substrate in 1.5 mM $HSeO_4^-$ pH 1 solutions can be seen in Figure 5.2. When compared to a scan in 1.5 mM $HSeO_3^-$ (green), thermodynamic differences between Se^{+4} and Se^{+6} can be observed. The formal potential for Se oxidation is believed to be near 600 mV, suggesting that all Se deposition occurs at an overpotential, indicative of slow kinetics.[11] Starting from the open circuit potential (OCP, 550 mV) in a Se^{+4} solution (green), the first reduction feature around 275 mV is the reduction of a low coverage UPD layer. The reduction of the higher coverage Se can be seen around 75 mV followed closely by bulk reduction at 0 mV. In the positive direction, bulk strips at 600 mV and overlays onto the low coverage UPD stripping peak at 800 mV. The peak at 900 mV only occurs when the potential is scanned below 0 mV and is attributed to a known morphological change as coverage increases.[12] The remaining scans show slightly different behavior when a Se^{+6} precursor is utilized. A small surface limited feature related to UPD began at 300 mV and continues until -200 mV when the Se deposited is reduced to a soluble Se^{2-} species. The first oxidation feature is the oxidation of S^{2-} to Se^0. The second is similar to the one seen in the green scan, that is the low coverage UPD oxidation.

The grey scan in Figure 5.3 begins in the negative direction from the OCP (500 mV). The features at 275 mV and 150 mV are deposition of Cu UPD onto the Au substrate surface, Cu $E^{0'}$ = 0 mV. The oxidation features seen in the positive direction correspond to the stripping of the different UPD layers. As the scan continues positive, no oxidation feature is seen around 800 mV since no Se was exposed to the substrate. The green scan is a ~0.5 ML Cu surface made by scanning an Au substrate negative to 150 mV in a Cu^{2+} solution. The solution was exchanged for blank then Se^{+6} precursor was

introduced at 150 mV. The potential was scanned to 0 mV and immediately turned positive at 0 mV, no hold at 0 mV. The resulting oxidation is that of Cu from the substrate and quantification indicates no Cu was lost during the process. The peak which appears around 800 mV is that of UPD Se oxidation from the surface. Having Se feature present indicates the Cu does have an effect on the removal of Se^{+6} was compared to an earlier scan of Au in Se^{+6} to 0 mV where less Se deposition was observed (Figure 5.2, purple). A precoated Cu layer was then placed into a Se^{+6} solution at 150 mV and the potential was then held for 10 min at 0 mV in the Se^{+6} solution (Figure 5.3, blue). The resulting oxidation showed, again, no change to the Cu coverage at 200 mV, but displayed a 3 fold increase in the amount of Se deposited. This was compared to the brown curve in Figure 5.3 which showed 0.1 ML of Se stripping from an Au surface after an Au substrate was held in Se^{+6} solution for 10 min at 0 mV.

Conclusion

Cyclic voltammetry (CV) exposed changes in the electrochemical profile for Au in Se^{+6} ions when compared to the profile of Au in Se^{+4} ions. Many features, such as highly packed Se layers, were not present in a Se^{+6} solution. Since a significant negative deposition potential was needed to overcome thermodynamic differences, Se^{+6} deposition began near the potential Se reduced to the soluble selenide species. A CV of an Au substrate treated with underpotentially deposited Cu showed the amount of Se deposited from Se^{+6} solution was slightly higher, 0.3 ML, compared to the Se amount deposited on an untreated Au surface from the same solution, 0.1 ML. While the presence of UPD Cu seems to have an effect on the amount of Se^{+6} removed from solution, the amount is not

beneficial to a method such as PP-ALD since growth times would need to be increased to obtain practical film thicknesses.

Acknowledgements

Support from the National Science Foundation, DMR #1410109, is gratefully acknowledged.

References

1. Jegadeesan, G.; Mondal, K.; Lalvani, S., Adsorption of Se (IV) and Se (VI) Using Copper-Impregnated Activated Carbon and Fly Ash-Extracted Char Carbon. *Water, Air, & Soil Pollution* **2015,** *226* (8), 1-12.
2. Boyle-Wight, E. J.; Katz, L. E.; Hayes, K. F., Spectroscopic Studies of the Effects of Selenate and Selenite on Cobalt Sorption to γ-Al2O3. *Environmental Science & Technology* **2002,** *36* (6), 1219-1225; Su, C.; Suarez, D. L., Selenate and Selenite Sorption on Iron Oxides An Infrared and Electrophoretic Study. *Soil Science Society of America Journal* **2000,** *64* (1), 101-111.
3. Pottier, D.; Maurin, G., Preparation of polycrystalline thin films of CuInSe2 by electrodeposition. *J. Appl. Electrochem.* **1989,** *19*, 361.
4. Panicker, M. P. R.; Knaster, M.; Kroger, F. A., Cathodic Deposition Of CdTe From Aqueous-Electrolytes. *Journal of the Electrochemical Society* **1978,** *125* (4), 566-572.
5. Hodes, G.; Engelhard, T.; Herrington, C. R.; Kazmerski, L. L.; Cahen, D., Electrodeposited layers of CuInS2, CuIn5S8, and CuInSe2. *Progr. Cryst. Growth Charact.* **1985,** *10*, 345; Hodes, G.; Cahen, D., Electrodeposition of CuInSe2 and CuInS2 films. *Solar Cells* **1986,** *16*, 245; Yuan, T.; Li, Y.; Jia, M.; Lai, Y.; Li, J.; Liu, F.; Liu, Y., Fabrication of Cu2ZnSnS4 thin film solar cells by sulfurization of electrodeposited stacked binary Cu–Zn and Cu–Sn alloy layers. *Materials Letters* **2015,** *155*, 44-47.
6. D. W. Suggs, I. V., B.W. Gregory, J.L. Stickney, Formation of CdTe and GaAs by electrochemical atoimc layer epitaxy (ECALE). *Mat. Res. Soc. Symp. Proc.*

1991, *222*, 283; Colletti, L. P.; Stickney, J. L., II-VI compound semiconductor thin-film electrodeposition by ECALE. *Book of Abstracts, 210th ACS National Meeting, Chicago, IL, August 20-24* **1995,** (Pt. 1), INOR-297; Colletti, L. P.; Flowers, B. H.; Stickney, J. L., Formation of Thin-Films of CdTe, CdSe, and CdS by Electrochemical ALE. *JECS* **1997**; Colletti, L. P.; Slaughter, R.; Stickney, J. L., ZnS thin film formation by electrochemical ALE: preliminary doping studies. *Proceedings - Electrochemical Society* **1997,** *97-20* (Photoelectrochemistry), 1-10; Perdue, B.; Czerniawski, J.; Anthony, J.; Stickney, J., Optimization of Te Solution Chemistry in the Electrochemical Atomic Layer Deposition Growth of CdTe. *Journal of The Electrochemical Society* **2014,** *161* (7), D3087-D3092.

7. Banga, D.; Jarayaju, N.; Sheridan, L.; Kim, Y.-G.; Perdue, B.; Zhang, X.; Zhang, Q.; Stickney, J., Electrodeposition of CuInSe2 (CIS) via Electrochemical Atomic Layer Deposition (E-ALD). *Langmuir* **2012,** *28* (5), 3024-3031.
8. Kolb, D. M., Physical and Electrochemical Properties of Metal Monolayers on Metallic Substrates. In *Advances in Electrochemistry and Electrochemical Engineering*, Gerischer, H.; Tobias, C. W., Eds. John Wiley: New York, 1978; Vol. 11, p 125; Juttner; K.; Lorenz; W.J., *Z. Phys. Chem. N. F.* **1980,** *122*, 163; Adzic, R. R., Electrocatalytic Properties of the Surfaces Modified by Foreign Metal Ad Atoms. In *Advances in Electrochemistry and Electrochemical Engineering*, Gerishcher, H.; Tobias, C. W., Eds. Wiley-Interscience: New York, 1984; Vol. 13, p 159; Gewirth, A. A.; Niece, B. K., Electrochemical applications of in situ scanning probe microscopy. *Chem. Rev.* **1997,** *97*, 1129-1162.

9. Vaidyanathan, R.; Mathe, M. K.; Sprinkle, P.; Cox, S. M.; Happek, U.; Stickney, J. L., Electrodeposition of Cu2Se thin films by electrochemical atomic layer epitaxy (EC-ALE). *Materials Research Society Symposium Proceedings* **2003,** *744* (Progress in Semiconductors II--Electronic and Optoelectronic Applications), 289-294.

10. Turner, A. K.; Woodcock, J. M.; Ozsan, M. E.; Cunningham, D. W.; Johnson, D. R.; Marshall, R. J.; Mason, N. B.; Oktik, S.; Patterson, M. H.; Ransome, S. J.; Roberts, S.; Sadeghi, M.; Sherborne, J. M.; Sivapathasundaram, D.; Walls, I. A., BP Solar Thin-Film Cdte Photovoltaic Technology. *Solar Energy Materials and Solar Cells* **1994,** *35* (1-4), 263-270; Cunningham, D.; Rubcich, M.; Skinner, D., Cadmium telluride PV module manufacturing at BP Solar. *Progress in Photovoltaics* **2002,** *10* (2), 159-168.

11. Lister, T. E.; Huang, B. M.; Herrick, R. D.; Stickney, J. L., Electrochemical Formation of Se Atomic Layers On Au(100). *Journal of Vacuum Science & Technology B* **1995,** *13* (3), 1268; Lister, T. E.; Stickney, J. L., Atomic level studies of selenium electrodeposition on gold (111) and gold (110). *Journal of Physical Chemistry* **1996,** *100* (50), 19568-19576; Huang, B. M.; Lister, T. E.; Stickney, J. L., Se adlattices formed on Au (100), studies by LEED, AES, STM and electrochemistry. *Surface Science* **1997,** *392* (1-3), 27.

12. Lister, T. E.; Stickney, J. L., Atomic Level Studies of Selenium Electrodeposition on Gold(111) and Gold(110). *The Journal of Physical Chemistry* **1996,** *100* (50), 19568-19576; Sorenson, T. A.; Lister, T. E.; Huang, B. M.; Stickney, J. L., A Comparison of Atomic Layers Formed by Electrodeposition of Selenium and

Tellurium Scanning Tunneling Microscopy Studies on Au(100) and Au(111). *J. Electrochem. Soc.* **1999,** *146* (3), 1019-1027.

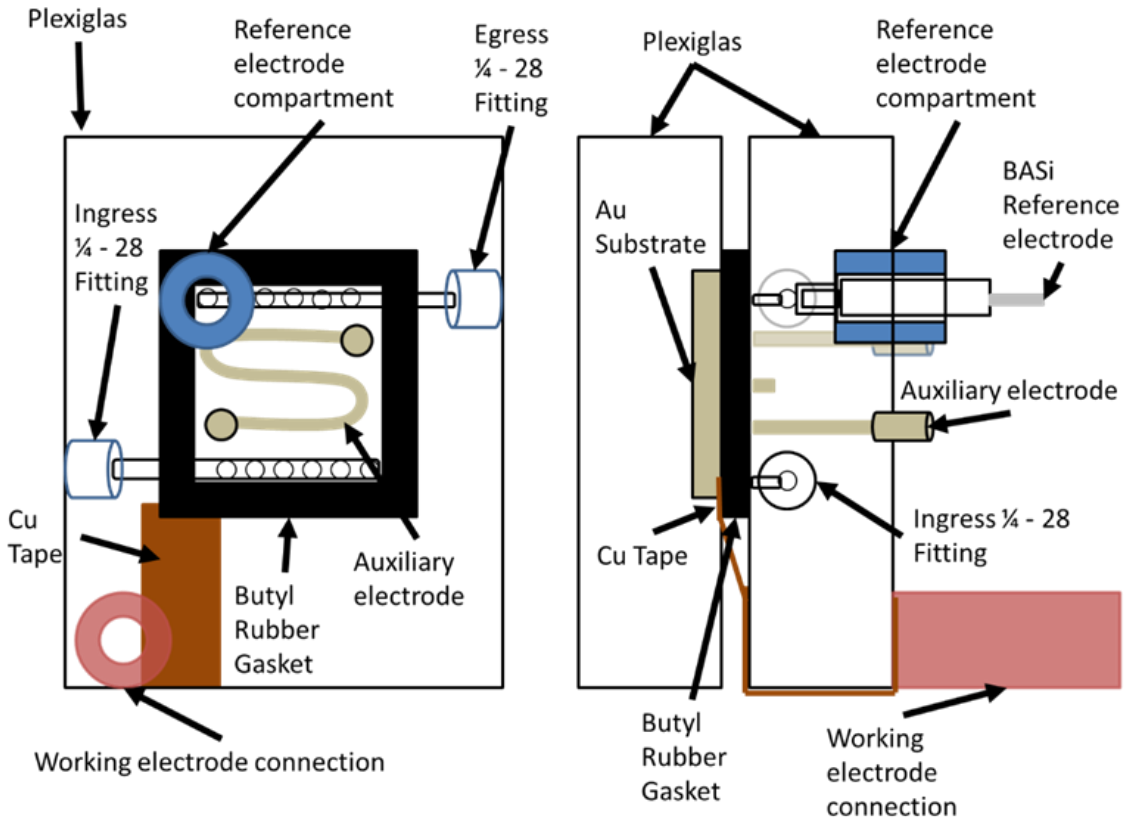

Figure 5.1: Schematic of the electrochemical flow cell, Z cell, as the solution enters left to right through the bottom row of holes, and exits the cell left to right through the top row of holes. Simulations have shown this configuration to result in a fairly homogeneous flow field.

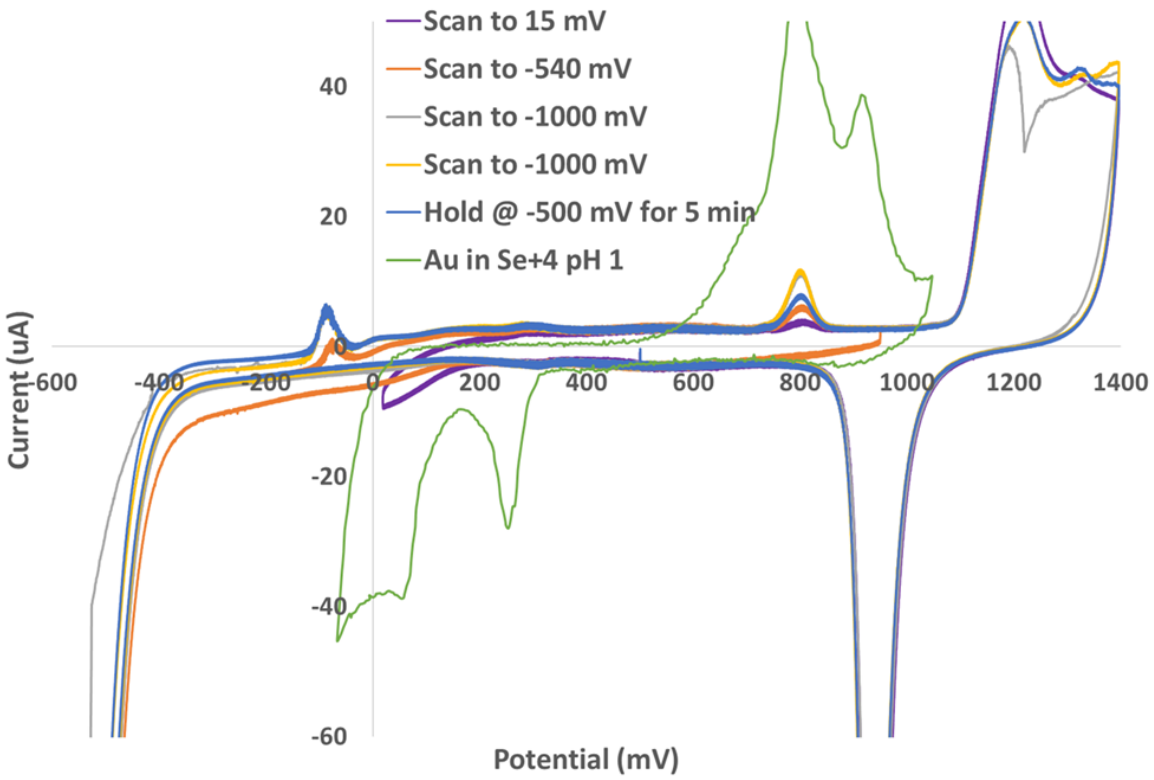

Figure 5.2: CV of 2.1 cm^2 Au electrode in (green) 1.5 mM Se^{+4} pH 1, (purple) 1.5 mM Se^{+6} negative limit 15 mV, (orange) 1.5 mM Se^{+6} negative limit -540 mV, (grey) 1.5 mM Se^{+6} negative limit -1000 mV, (yellow) 1.5 mM Se^{+6} negative limit -1000 mV, and (blue) 1.5 mM Se^{+6} 5 min hold at negative limit -500 mV. A Ag/AgCl reference electrode was utilized with a scan rate of 10 mV/sec and a pump rate of 4 mL/min.

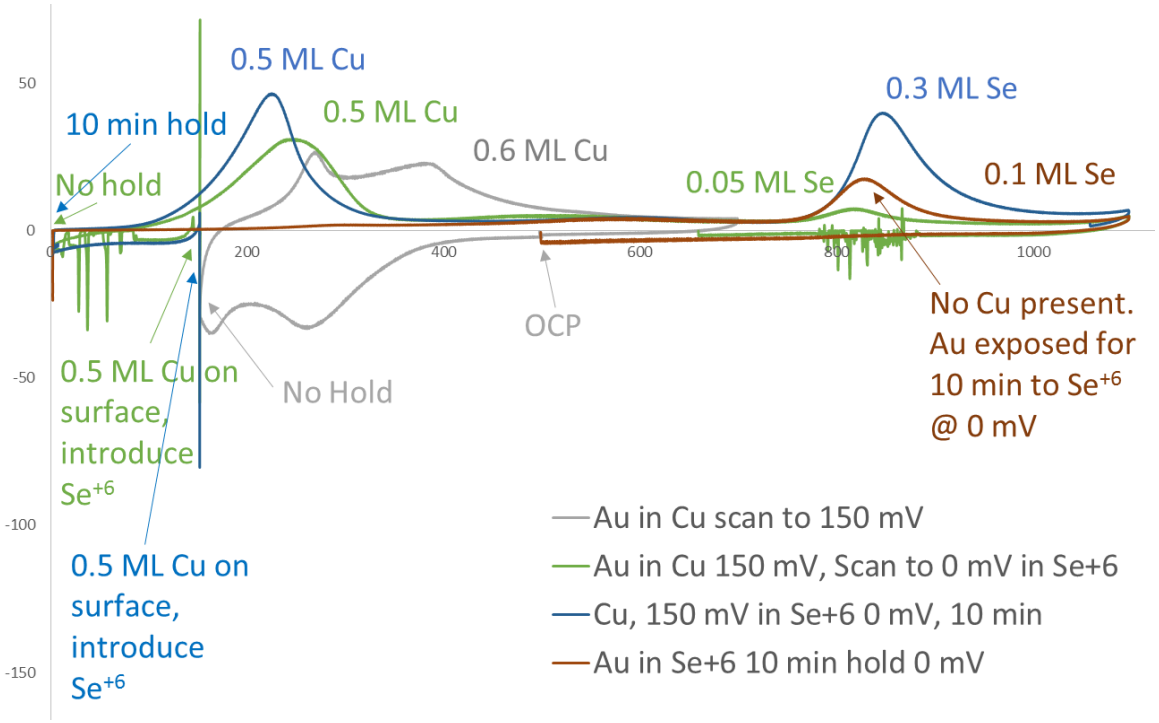

Figure 5.3: CV of (Grey) 2.1 cm^2 Au electrode in 1.5 mM Cu^{2+} pH 1. (Green) ~0.5 ML Cu pre-layer in Se^{+6} negative limit 0 mV. (Blue) 0.5 ML Cu pre-layer in Se^{+6} for 10 min, negative limit 0 mV. (Brown) 2.1 cm^2 electrode in 1.5 mM Se^{+6} for 10 min, negative limit 0 mV. An Ag/AgCl reference electrode was utilized with a scan rate of 10 mV/sec and a pump rate of 4 mL/min.

CHAPTER 6

INVESTIGATION OF METHODS TO OPTIMIZE CDTE DEPOSITS MADE USING ELECTROCHEMICAL ATOMIC LAYER DEPOSITION (E-ALD)[5]

[5] J. M. Czerniawski, J. L. Stickney, To be submitted to *Journal of the Electrochemical Society (2015)*

Abstract

Optimization studies of CdTe deposits made with E-ALD are reported here. An investigation of gasket material is presented which demonstrated butyl rubber was the best at preventing O_2 from entering the cell. Automated CO_2 cell purges were also introduced in order to remove O_2 gas and H_2 gas that accumulated inside the cell over time. Preliminary studies indicated that CO_2 cell purges followed by alkaline solution rinses were effective at removing O_2 and H_2. Finally, the deposition behavior of CdTe thin films made in acidic and basic media were investigated using layer-by-layer deposition and stripping studies to minimize any harmful defects from CO_2 purges. Cd terminated layers were not affected by the alkaline CO_2 conditions, however Te terminated layers resulted in 20% less deposition in alkaline conditions.

Introduction

Affordable solar energy has long been desired as an alternative to fossil fuels.[1] Solar energy, however, will only be economically viable for large-scale production if the cost can be reduced to \$0.33/Watts peak (Wp: watts produced at T = 25^0 C and incident radiation of 1000 Watts/m^2).[2] Current commercial 1st generation Si photovoltaic (PV) cells cost \$0.85/Wp and only deliver a photon to electron conversion efficiency of 10-11%.[3] New materials and methods must be studied until ideal production costs can be obtained.

CdTe has long been considered one of the best choices for the absorber layer in a 2nd generation heterojunction configuration due to its ~1.5 eV band gap, the ideal value for photovoltaic conversion efficiency, and chemical stability.[4] Calculations indicate

CdTe thin film solar cells have a maximum theoretical conversion efficiency of 28-30%, but to date the record observed for a CdTe cell has an actual efficiency of 21.0%.[5] CdTe is still a relevant PV absorber material but has largely been overshadowed by new, more earth-abundant multi-junction absorber materials with better light trapping mechanisms.

The losses which plague CdTe absorber layers are mostly attributed to defects in the heterojunction PV's many layers caused by the fabrication techniques used to create them. These techniques often require the use of high temperatures and low pressures. Electrodeposition, however, holds promise as a low cost, flexible, room temperature technique for the production of II-VI compound semiconductors.[6]

Electrochemical atomic layer deposition (E-ALD), the condensed phase alternative to atomic layer deposition, is a well-developed technique for the production of II-VI compound semiconductors and allows for alternating deposition of atomic layers of elements to form a variety of materials. E-ALD is based on surface limited reactions and provides superior control over thickness, homogeneity, crystallinity, and overall quality of the deposit.

Side reactions, like the hydrogen evolution reaction and oxygen reduction, can interfere with electrodeposition of elements. These effects must be minimized using a less oxygen permeable rubber gasket material such as butyl rubber[7] or taking advantage of well understood mechanisms such as CO_2 scrubbing using an alkaline solvent[8] to purge H_2 bubbles from the substrate's surface. Optimizing CdTe E-ALD growth conditions may result in increased conversion efficiency as a result of improved quality which would make the technique a viable alternative for lowering production costs.

Experimental

The solutions were 0.5 mM $CdSO_4$ (Alfa Æsar 99.999% pure) with 0.1 mM TeO_2 (Alfa Æsar 99.999% pure) and 0.5 M $NaClO_4$ in 10 MΩ nanopure water (Millipore Advantage 10), fed by the house DI water source. The solutions were adjusted to pH 3.

Precursor concentrations were kept in the mM range in order to assist with limiting deposition to a fraction of a monolayer (ML) each cycle. A ML is defined for this report as one atom for each Au substrate surface atom, or about 1.2×10^{15} atoms per cm^2. Substrates were 100 nm Au films on 5 nm of Ti on glass, purchased from Evaporated Metal Films (Ithaca, NY), and were first cleaned by three 5 min sonications in fresh aliquots of acetone, followed by three more sonications in aliquots of nanopure water. The substrates were then dipped in concentrated nitric acid for 30 sec, rinsed with nanopure water and dried with nitrogen before being placed in the electrochemical flow system (Figure 6.1). The flow cell (Electrochemical ALD L.C.) was immediately flushed with 0.1 M H_2SO_4 (Fisher Scientific, certified ACS plus) and the potential was then held alternately for 5 sec at a time, between +1400 mV and -200 mV, four times to complete cleaning of the Au surface.

Figure 6.1 diagrams the electrochemical flow system. Solution flows from nitrogen purged bottles, through a solution distribution valve, and into the flow cell using a Masterflex (Cole Parmer) peristaltic pump. The flow cell is comprised of 3 electrodes where the auxiliary electrode was an Au wire inlayed into a Plexiglas cell face. Cu tape was used to connect the working electrode to its connection post and a 3 M Ag/AgCl reference electrode (BASi, West Lafayette, IN) was used. The CO_2 distribution valves were 2 way directional valves detailed in Figure 6.2. When the valves were not powered,

solution traveled from a reservoir, through the cell and into the waste. When the valves were powered, flow direction was reversed as CO_2 gas pushed solution out of the cell and into the waste.

Results and Discussion

Previous results from this group indicate oxygen gas in the E-ALD system will inhibit deposition of CdTe. A cyclic voltammogram (CV) of an Au substrate in 0.1 M H_2SO_4 gives an indication of the O_2 levels in the cell (Figure 6.3). Oxygen reduction begins around 200 mV and the current registered at -200 mV is indicative of the total amount of O_2 reduced in the cell. When precursor bottles were not purged and a silicone rubber gasket was used (red), the amount of current registered at -200 mV was -20 μA. When solution bottles were purged with nitrogen for 1 hour to remove O_2 (green), reduction for oxygen was still present but the amount was reduced to about half. A gasket made of butyl rubber replaced the silicone rubber gasket and the solution was again degassed for 1 hour (blue). Reductive charge due to O_2 gas is suppressed when precursor solutions are purged with N_2 and a butyl rubber gasket with low O_2 permeability[7] is used. This suppression indicates successful isolation of the deposition area from atmosphere since O_2 levels are nearly nonexistent.

CdTe deposits were made using the program seen in Figure 6.4. Cd solution was introduced into the cell for 10 s (Figure 6.4 orange) at -550 mV, followed by a 15 s quiescent deposition period (yellow) at the same potential. Next, a pH 3 $NaClO_4$ black was rinsed into the cell to rinse out any remaining Cd ions (red). A similar step is then repeated to deposit a layer of Te (dark and light blue) at -800 mV. Ideally, layer-by-layer growth would be expected. Previous studies have shown depositing Cd at -550 mV would

put down less than 1 monolayer (ML) of Cd and depositing Te at -800 mV would put down 1 thermodynamically stable ML of Te and reduce the less stable bulk to H_2Te.[6] Deposits were examined with a microscope and were found to be homogeneous but holes in the surface were evident and it was hypothesized that they originated from H_2 gas evolved from the Au surface at potentials below the hydrogen evolution reaction (HER), below -200 mV for pH 3 solution, that were preventing precursor from reaching the electrode's surface. A cartoon of the CdTe E-ALD cycle can be seen in Figure 6.5.

After 5 cycles of deposition, CO_2 gas is delivered to the cell via 3 way isolation valves in order to remove any O_2 gas introduced by diffusion from the atmosphere and H_2 gas formed from at a hydrogen evolution overpotential (negative of -200 mV). Figure 6.6 depicts the steps taken in one CO_2 purge. CO_2 was injected into the cell by energizing the valves seen in Figure 6.2. Alkaline water was subsequently introduced to dissolve the CO_2, acting as a scrubber.[8] A pH 3 blank was then pumped into the cell in order to prepare for the next grouping of CdTe E-ALD cycles. After inspection with the microscope, deposits made without the CO_2 purge were homogeneous and more reproducible. Deposits made with the CO_2 purge where thin and non-uniform (Figure 6.7) indicating this step had a dramatic effect on deposition.

The effect of the CO_2 purge step (Figure 6.6) on Cd and Te were subsequently studied. Table 1 displays a series of 8 total experiments where a single layer of E-ALD Cd was deposited on an Au substrate. Four of the Cd layers were not exposed to a CO_2 purge step. The deposits were stripped and quantified by integrating the resulting charge. The average charge was 421 μC, which is ~0.5 ML. When the second set of four experiments was exposed to a CO_2 purge, the average charge observed was 432 μC,

which is also ~0.5 ML. The lack of discrepancy between the two quantified amounts suggests Cd was not the species affected by CO_2 purging.

Figure 6.7a displays 4 current time profiles of ~0.6 ML of E-ALD Te stripping in pH 3 blank. No CO_2 exposure occurred prior to oxidation. The amount quantified after oxidation matched the amount deposited ~0.6 ML. Figure 6.7b displays 4 current time profiles of ~0.6 ML Te stripping in pH 3 blank after exposure to a CO_2 purge step. The deposit exposed to a CO_2 purge was 20% thinner than the deposit not exposed suggesting Te is stripped during the CO_2 purge cycle.

A similar trend can be seen in Figure 6.8. In Figure 6.8a, one trilayer of TeCdTe was created using the E-ALD cycle described in Figure 6.4. No exposure to a CO_2 treatment occurred. When quantified, 0.6 ML of Cd were present and 1 ML of Te was preset. When the trilayer was exposed to a CO_2 purge (Figure 6.8b), the amount of Cd present remained the same (~0.6 ML) but the amount of Te decreased to ~0.8 ML, a 20% loss of Te.

Due to the pH changes required for a successful CO_2 purge, the pH dependence of Te deposition must be studied. Figure 6.9a is a CV of Au in a pH 3 Te solution. Reduction of the low coverage UPD begins around 350 mV with the high coverage UPD peaking around -200 mV. Bulk Te occurs around -300 mV and in the reverse direction oxidizes at 300 mV. The UPD oxidation peaks around 500 mV. In pH 9 Te (Figure 6.9b) various features shift to more negative potentials due to the change in pH. There seems to be a strong dependence on H^+ with the stability of Te in the deposit since the bulk Te oxidation peak occurs around +300 mV in the acidic solution and -100 mV in base. It

may be possible to protect deposits from Te loss during CO_2 exposure by holing at more negative potentials or terminating deposition with a Cd layer. Further studies are needed.

Conclusion

O_2 gas levels were reduced by purging the E-ALD system with N_2. Oxygen was excluded from the cell by using the less permeable butyl rubber. O_2 and H_2 were eliminated from the system by purging the cell with CO_2 periodically however, deposition is inhibited by exposure to the basic rinse during the purge step. Preliminary results show Cd is not affected by CO_2 purging, but a 20% loss is observed when Te is exposed to a CO_2 purge. Investigating possible Cd shielding of Te during CO_2 may reduce stripping and improve deposit quality. Further investigation of Te deposition in basic medium might improve our understanding of Te loss during CO_2 purges.

Acknowledgements

Support from the National Science Foundation, DMR #1410109, is gratefully acknowledged.

References

1. Birkmire, R. W.; Eser, E., Polycrystalline thin film solar cells: Present status and future potential. *Annual Review of Materials Science* **1997,** *27*, 625-653; Shah, A.; Torres, P.; Tscharner, R.; Wyrsch, N.; Keppner, H., Photovoltaic technology: The case for thin-film solar cells. *Science* **1999,** *285* (5428), 692-698.
2. US, D. o. E. Multi Year Program Plan 2008-2012. https://www1.eere.energy.gov/solar/pdfs/solar_program_mypp_2008-2012.pdf.
3. Wu, X., High-efficiency polycrystalline CdTe thin-film solar cells. *Solar Energy* **2004,** *77* (6), 803-814; Powalla, M.; Bonnet, D., Thin-Film Solar Cells Based on the Polycrystalline Compound Semiconductors CIS and CdTe. *Advances in OptoElectronics* **2007,** *2007*.
4. Zhou Fang, X. C. W., Hong Cai Wu, and Ce Zhou Zhao, Achievements and Challenges of CdS/CdTe Solar Cells. *International Journal of Photoenergy* **2011,** *2011*.
5. First Solar, I. First Solar Sets World Record for CdTe Solar PV Efficiency. http://investor.firstsolar.com/releasedetail.cfm?releaseID=593994 (accessed 11/1); Green, M. A.; Emery, K.; Hishikawa, Y.; Warta, W.; Dunlop, E. D., Solar cell efficiency tables (Version 45). *Progress in Photovoltaics: Research and Applications* **2015,** *23* (1), 1-9.
6. Gregory, B. W.; Stickney, J. L., Electrochemical atomic layer epitaxy (ECALE). *Journal of Electroanalytical Chemistry* **1991,** *300* (1-2), 543-561.

7. Robb, W. L., THIN SILICONE MEMBRANES-THEIR PERMEATION PROPERTIES AND SOME APPLICATIONS. *Annals of the New York Academy of Sciences* **1968,** *146* (1), 119-137.

8. Bai, H.; Yeh, A. C., Removal of CO2 Greenhouse Gas by Ammonia Scrubbing. *Industrial & Engineering Chemistry Research* **1997,** *36* (6), 2490-2493; Lackner, K. S., Capture of carbon dioxide from ambient air. *The European Physical Journal Special Topics* **2009,** *176* (1), 93-106.

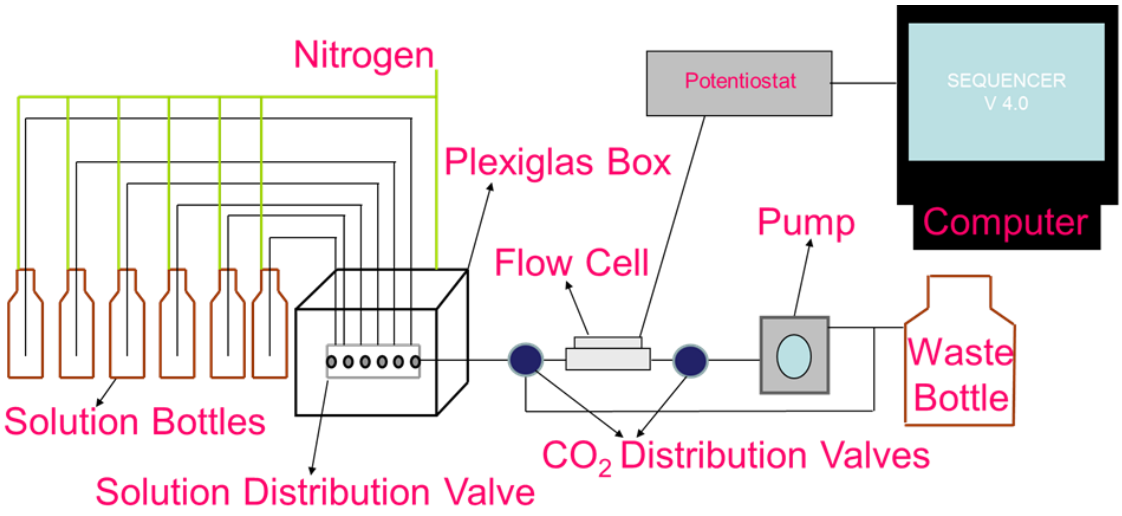

Figure 6.1: Schematic of the electrochemical flow system with "Z" cell. Solution enters left to right from the solution bottles, through the distribution valve, into the cell, and ends in a waste container. All valves and pumps are controlled by the in-house SEQUENCER program.

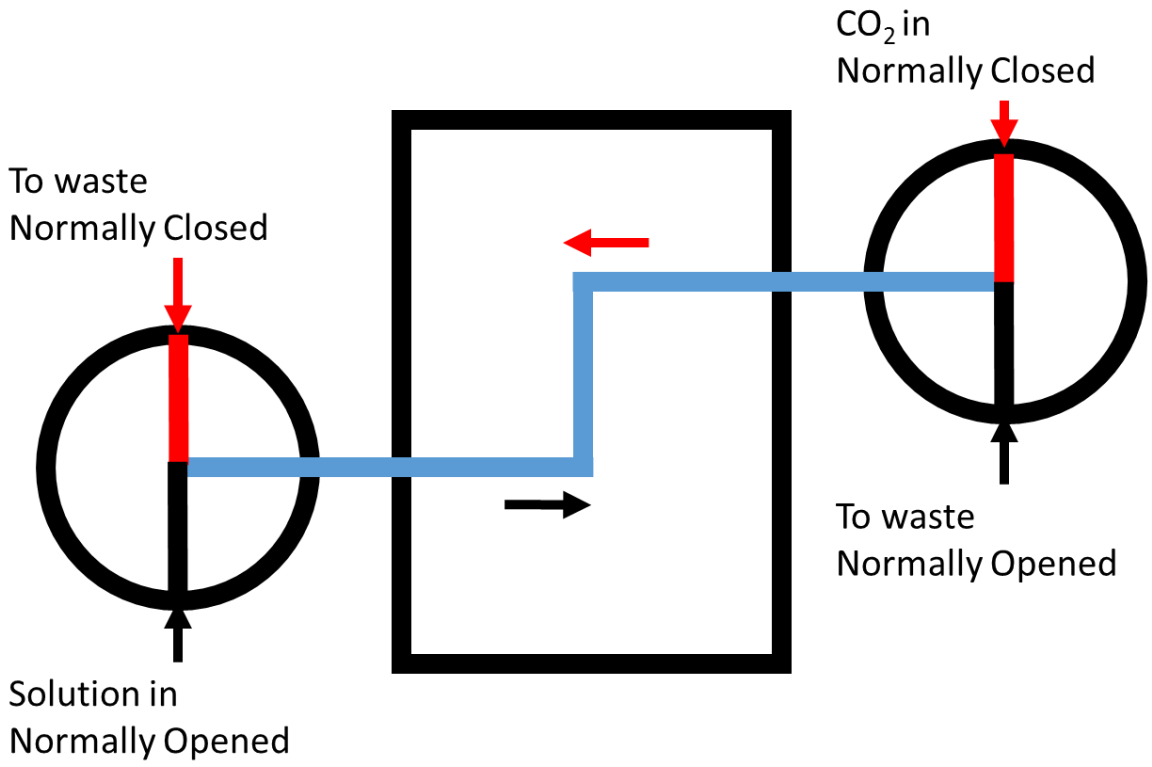

Figure 6.2: Schematic of the electrochemical "Z" flow cell with CO_2 distribution valve assembly. When the valves are not powered, solution enters the cell from left to right from the solution bottles. When powered, CO_2 gas is introduced at a high pressure from right to left, pushing solution out of the cell and into waste.

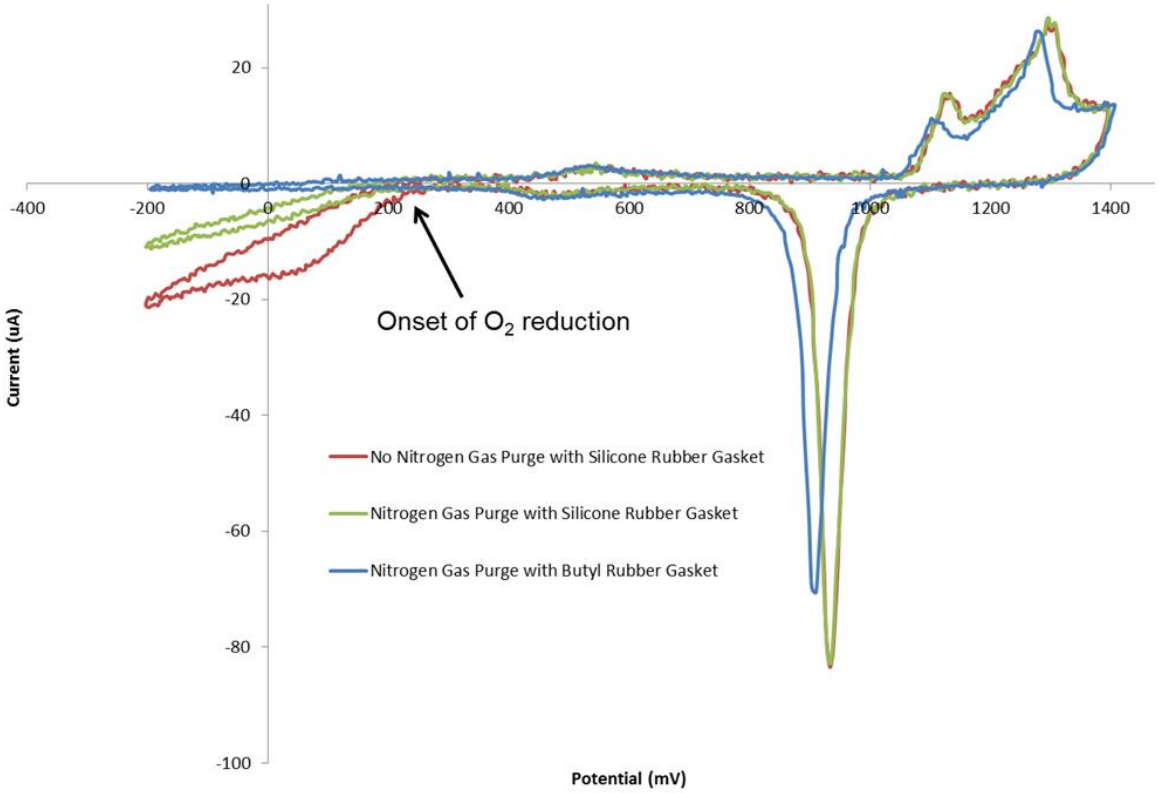

Figure 6.3: Au substrate (2.1 cm^2) CV in 0.1 M H_2SO_4 with (red) no nitrogen solution purge and a silicone rubber gasket, (green) silicone rubber gasket and nitrogen solution purge, (blue) butyl rubber gasket and nitrogen solution purge. The scan rate was 10 mV/sec and the flow rate was 4 mL/min.

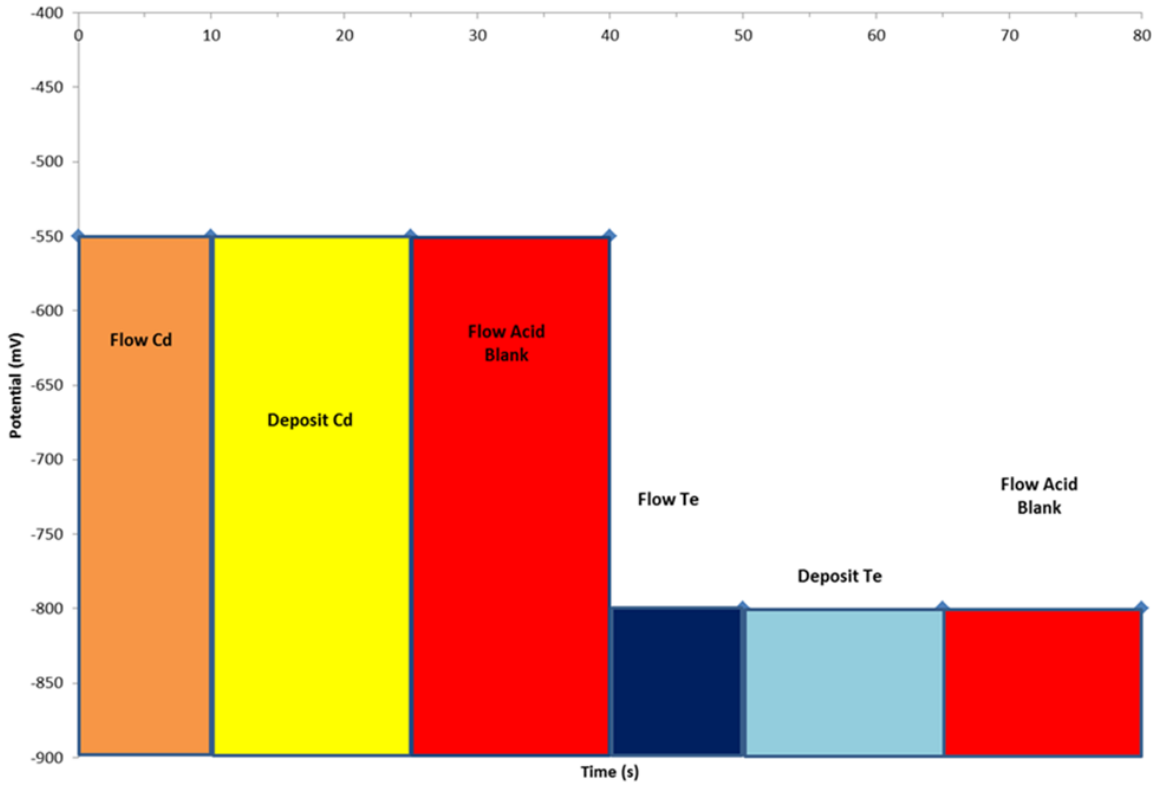

Figure 6.4: Proposed CdTe E-ALD deposition cycle. Cd is deposited at a potential of -550 and Te is deposited at a potential of -800 mV vs. Ag/AgCl reference electrode. The deposition steps are performed in quiescent solution. During solution replacement, the flow rate is 14 mL/min.

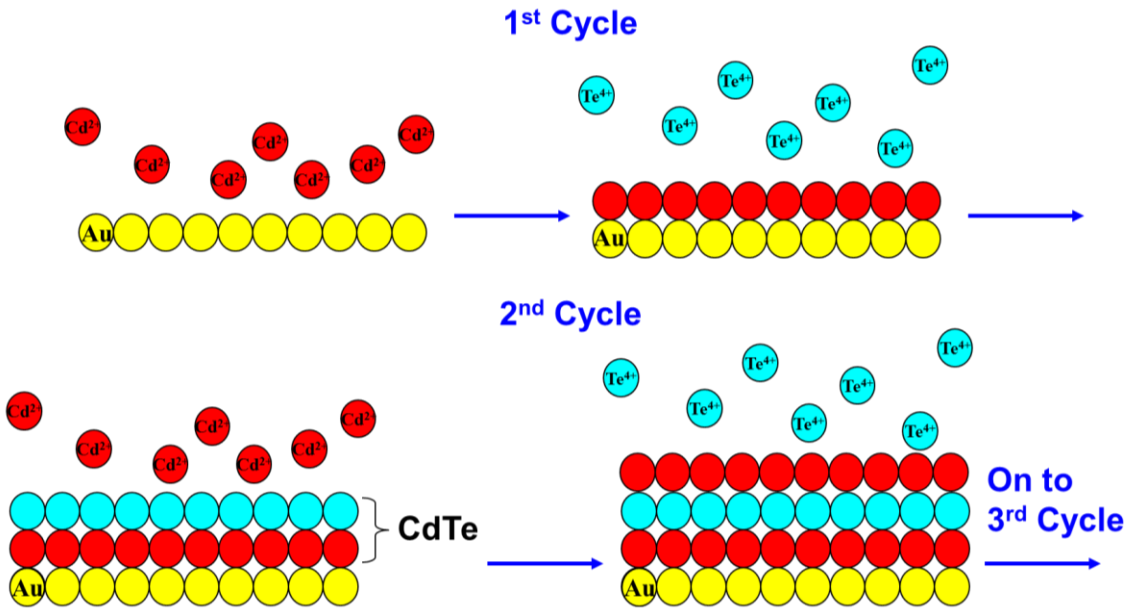

Figure 6.5: E-ALD diagram. 1) Cd precursor is introduced into the cell at a UPD potential (-550 mV) 2) After a 15 second blank rinse, Te precursor is introduced to the cell and the potential is stepped negative to -800 mV, where bulk Te is reduced and only UPD Te remains. A blank rinse follows then Cd precursor is reintroduced into the cell. This cycle is repeated until a desired film thickness is achieved.

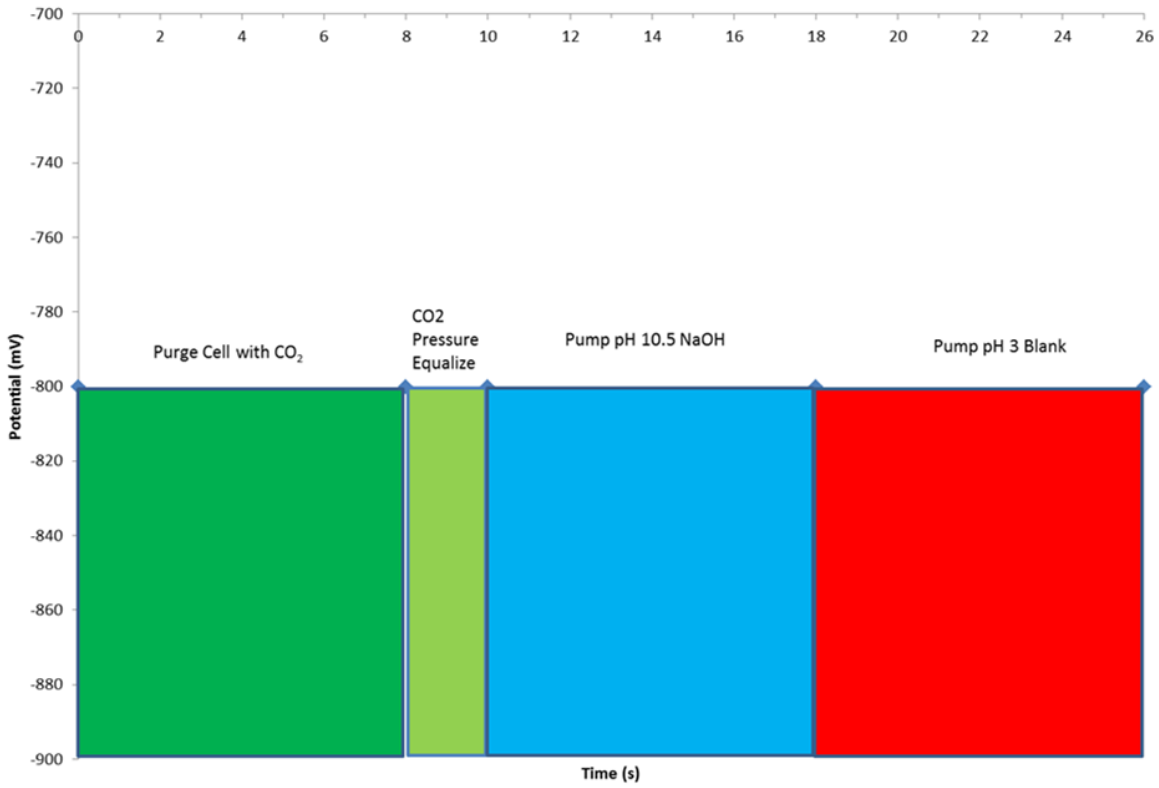

Figure 6.6: Proposed CO_2 purge cycle. After 5 CdTe deposition cycles, CO_2 gas is introduced into the cell at 10 psi to remove any O_2 or H_2 gas in the cell. The gas pressure inside the cell is then allowed to equalize to atmospheric pressure. Basic solution is pumped into the cell to dissolve the CO_2 gas. Finally, pH 3 blank is pumped into the cell and the CdTe cycles begin again.

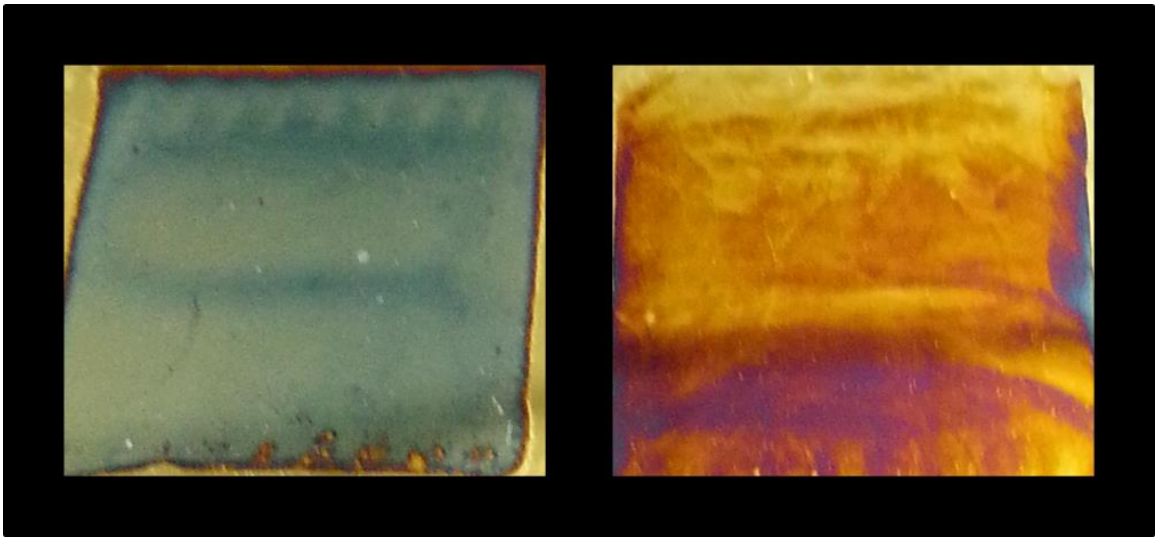

Figure 6.7: CdTe deposited (left) with no CO_2 purge step and (right) a CO_2 purge after 5 CdTe deposition cycles.

Table 6.1: Quantification of 8 atomic layer stripping studies. The first 4 were not exposed to a CO_2 purge. The amount of charge for the first 4 experiments translates to 0.5 ML. The second 4 were exposed to a CO_2 purge step and the charge also translates to 0.5 ML.

Exp #	# Cd Layers	CO_2 Purge	Charge (uC)	Average (uC)	ML
1	1	No	405		
2	1	No	425		
3	1	No	415		
4	1	No	439	421	0.5
1	1	Yes	433		
2	1	Yes	443		
3	1	Yes	430		
4	1	Yes	424	432	0.5

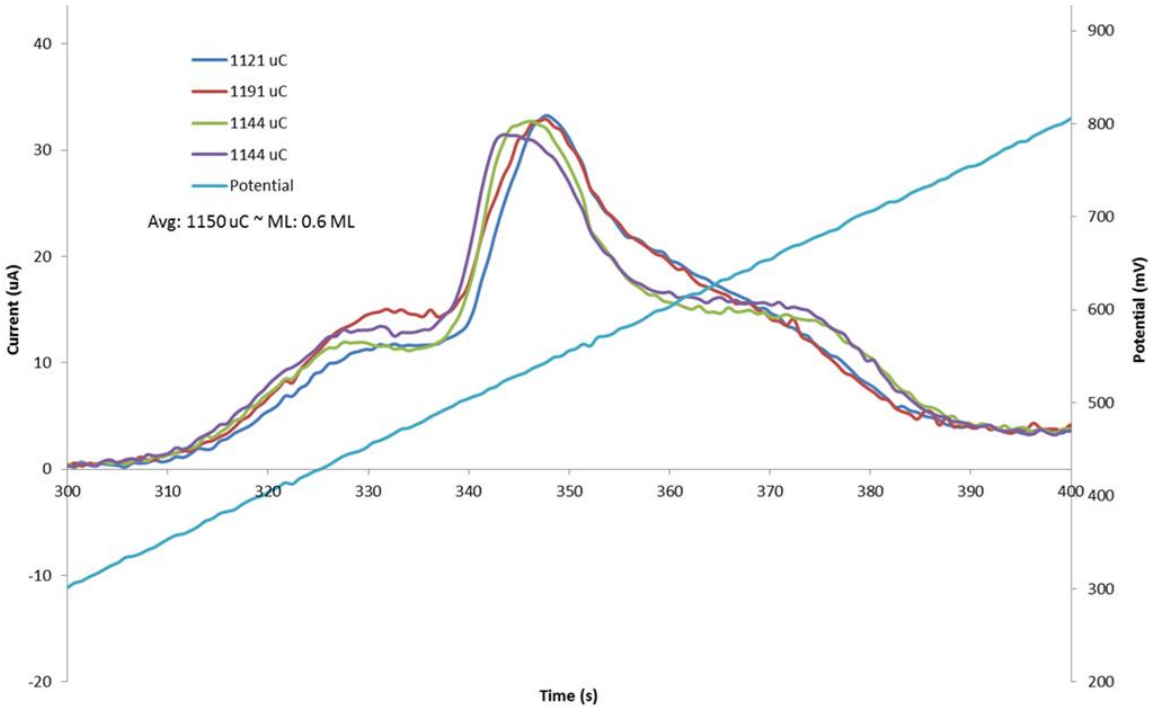

Figure 6.7a: Current vs time Te oxidation in pH 3 $NaClO_4$ (No CO_2 step performed). The amount of Te oxidation charge translates to ~0.6 ML.

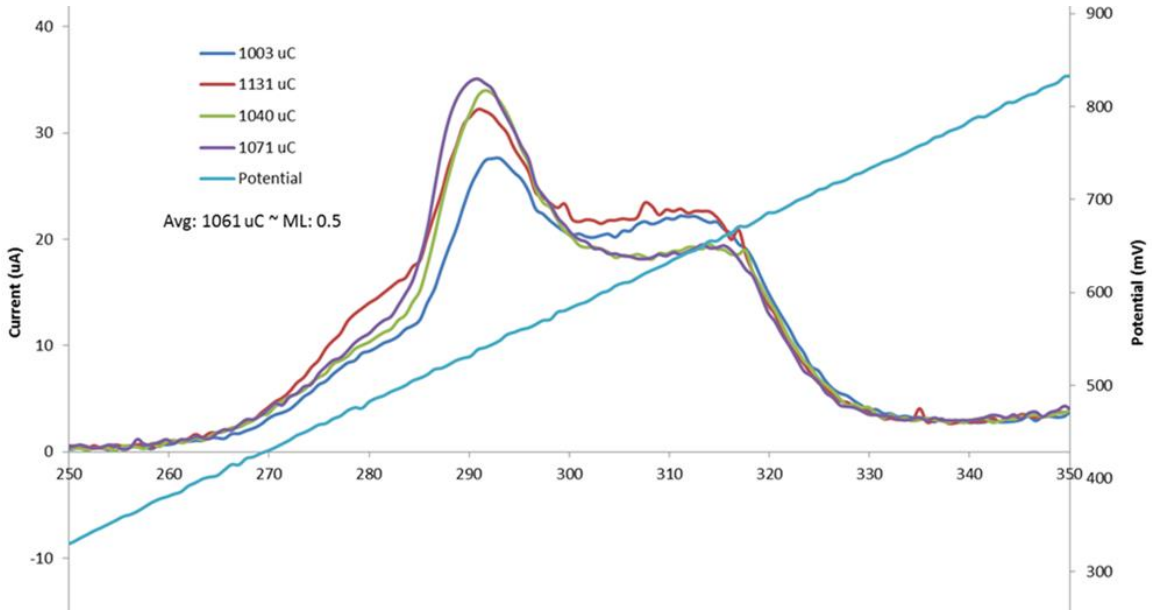

Figure 6.7b: Current vs Time Te Oxidation in pH 3 $NaClO_4$ (CO_2 step performed). The amount of Te oxidation charge translates to ~0.5 ML, a 20% drop in coverage compared to samples not exposed to CO_2.

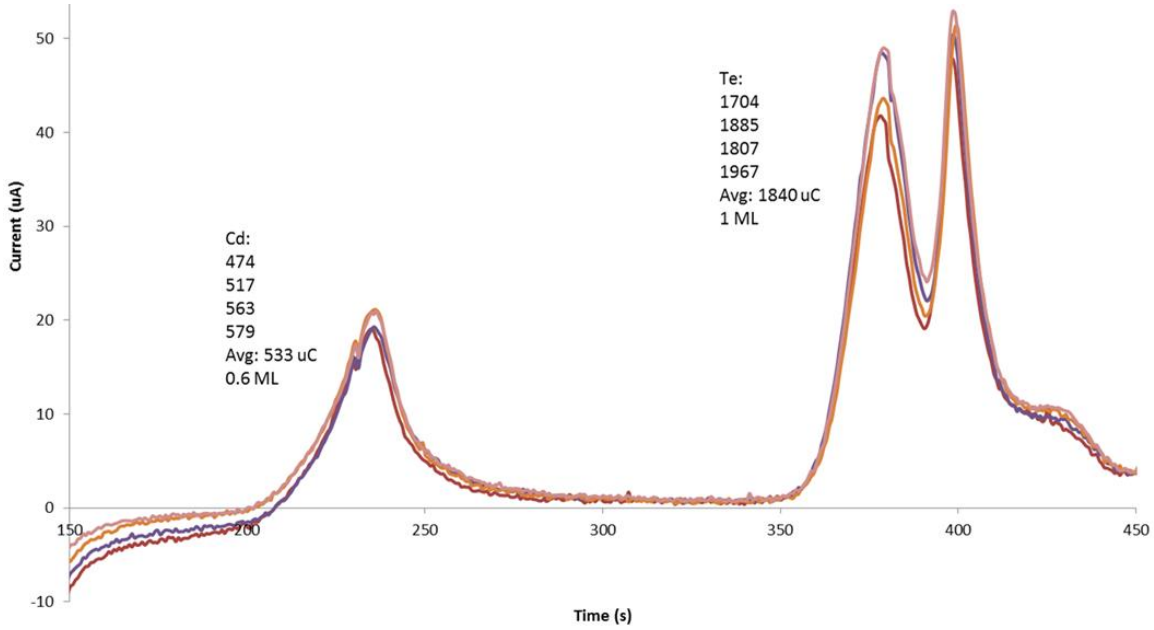

Figure 6.8a: Oxidation of TeCdTe deposition on Au in pH 3 Sodium Perchlorate (No CO_2 treatment). The amount of Cd oxidation is 0.6 ML and the total amount of Te was 1 ML.

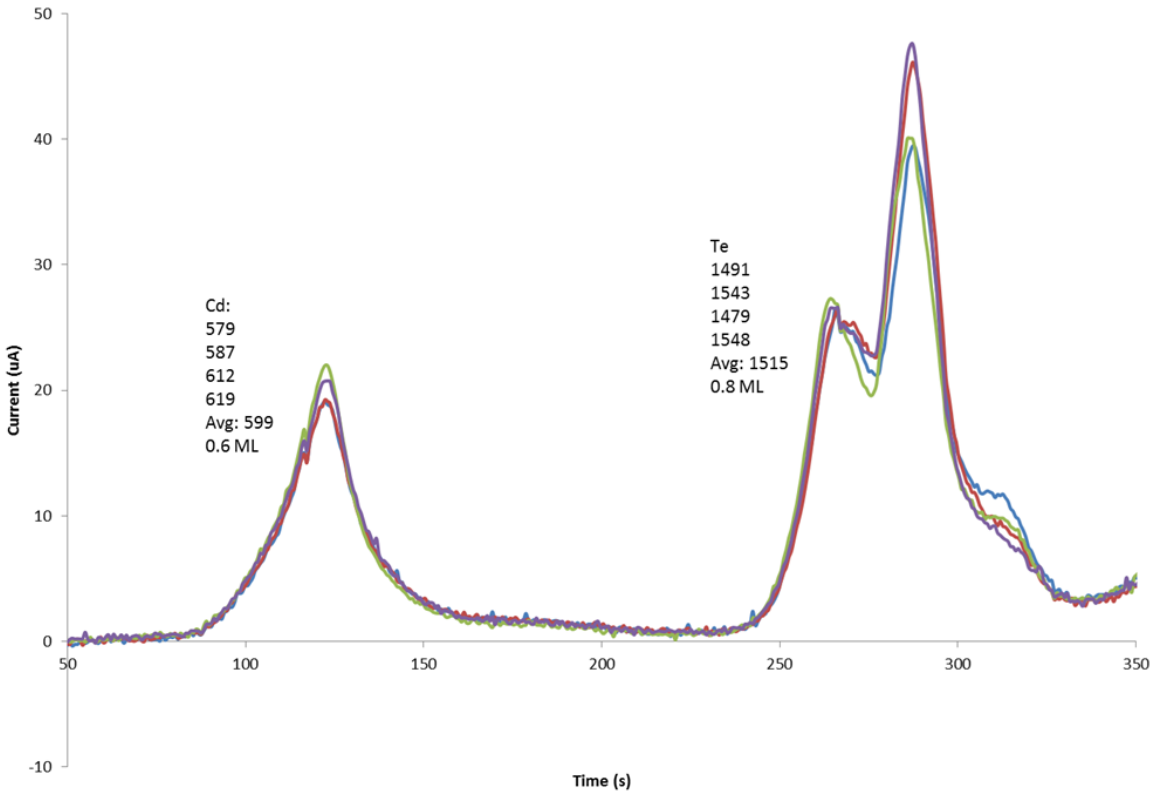

Figure 6.8b: Oxidation of TeCdTe deposition on Au in pH 3 Sodium Perchlorate with CO_2 treatment. The amount of Cd oxidation remains constant at 0.6 ML but the amount of Te decreases to 0.8 ML, a loss of 20% when compared to a deposit not exposed to CO_2.

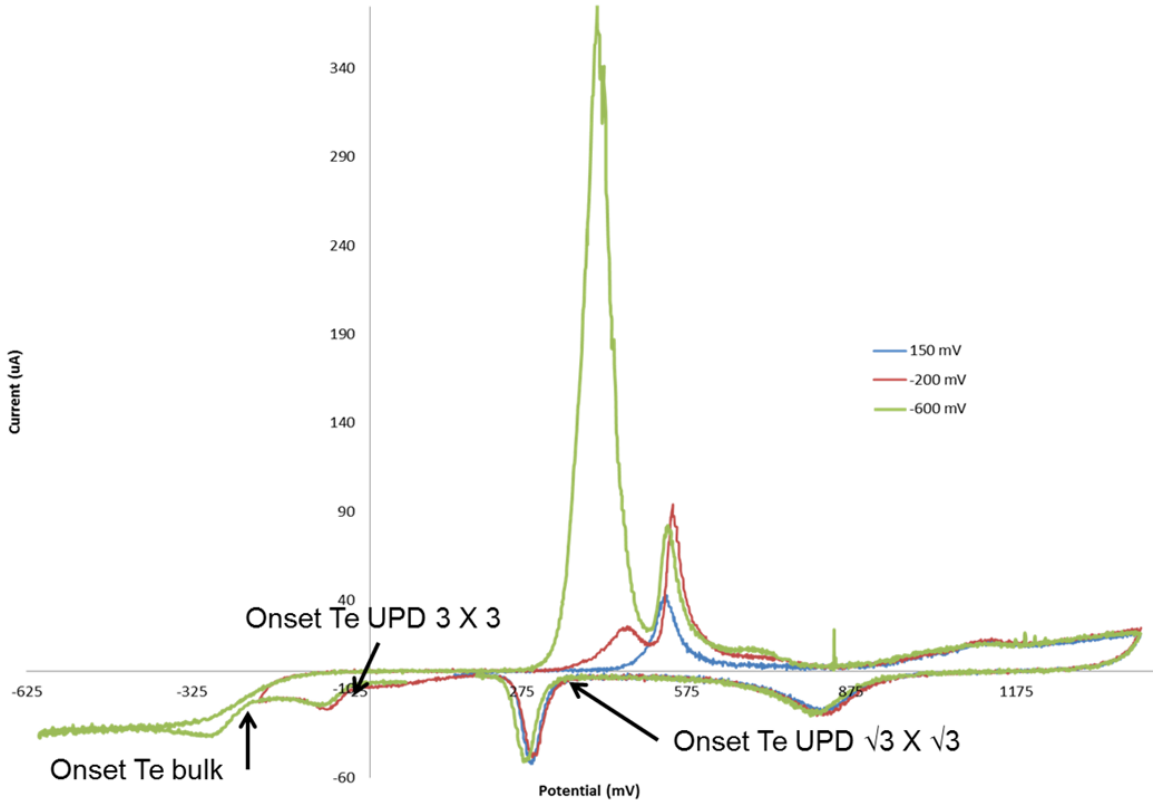

6.9a: CV of a 2.1 cm^2 Au electrode in 0.1 mM Te, pH 3, vs an Ag/AgCl reference electrode, at a scan rate of 10 mV/sec. The flow rate was 4 mL/min.

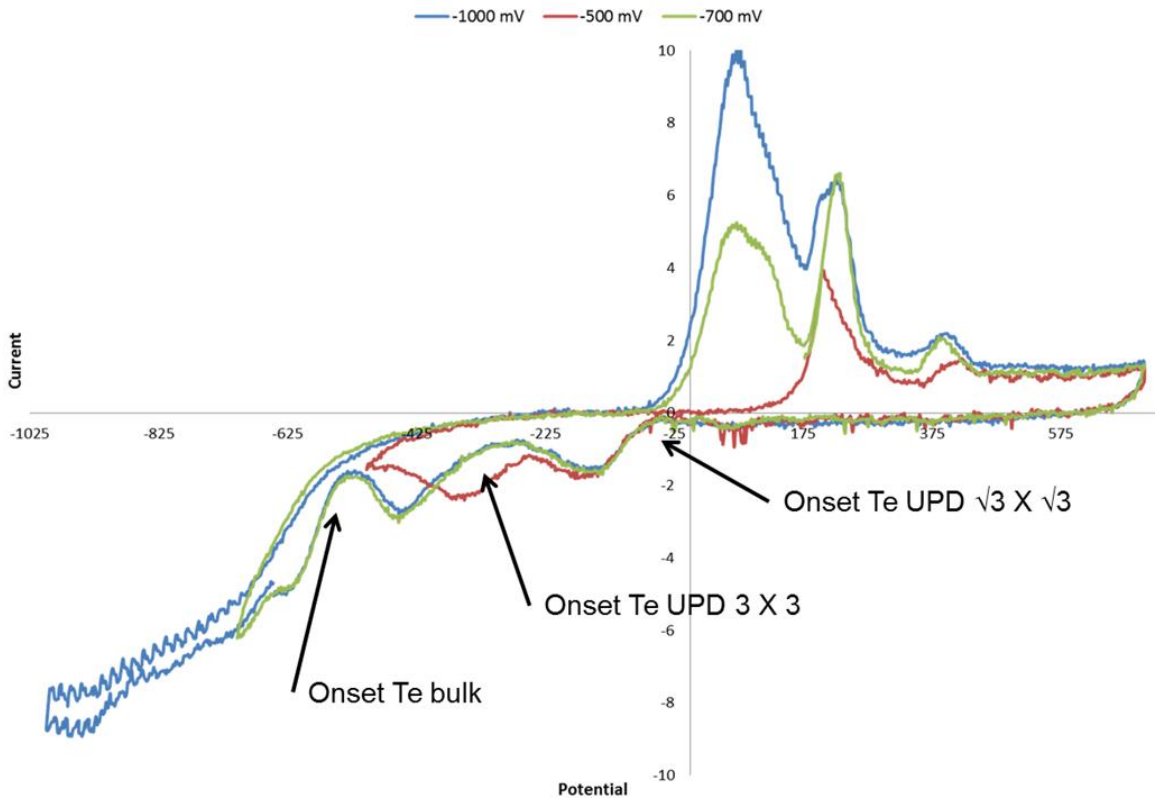

6.9b: CV of a 2.1 cm^2 Au electrode in 0.1 mM Te, pH 9, vs an Ag/AgCl reference electrode, at a scan rate of 10 mV/sec. The flow rate was 4 mL/min.

CHAPTER 7

CONCLUSION AND FUTURE STUDIES

The formation, characterization, and optimization of absorber layer materials made with PP-ALD and E-ALD was the focus of this dissertation. Chapter 2 investigated crystalline deposits of cuprous selenide (Cu_2Se) over a range of conditions formed using a potential pulse version of atomic layer deposition (PP-ALD). Cyclic voltammetry (CV) was used to estimate Anodic and Cathodic cycle potentials for the formation of Cu_2Se, which were then systematically examined to optimize the cycle. The dependence of the deposit thickness and stoichiometry as a function of the Cathodic and Anodic pulse potentials were investigated as well as the dependence on the time used for the Anodic pulse. Film thicknesses, from spectroscopic ellipsometry, were shown to be proportional to the number of cycles performed. Deposit homogeneity, investigated visually as well as by using EPMA, concluded the optimum deposition conditions from these studies were 0.13 s pulse to -50 mV followed by a 0.5 s pulse to +50 mV repeated to achieve the desired thickness. The linear growth with the number of cycles (0.02 nm/cycle) was consistent with a layer-by-layer growth process and the pulsing achieved the control expected from a surface limited process. SEM images also suggested the deposit's growth as a function of the number of cycles was consistent with a layer-by-layer mechanism. XRD showed the deposits to be polycrystalline orthorhombic films, with possibly a trace of cubic, as deposited.

The deposition of 60 nm thick In_2Se_3 films, formed using PP-ALD, was described in Chapter 3. Cyclic voltammetry (CV) was used to determine approximate cycle potentials, and anodic and cathodic potentials were systematically examined to optimize the potential pulse program for In_2Se_3. Film thickness was a function of both the Anodic and Cathodic potentials. The optimum growth rate was consistent with previous PP-ALD studies where similar concentrations and pulse times were employed, 0.02 nm/cycle. The use of the potential pulse cycle for film growth resulted in surface limited control over the deposit stoichiometry each cycle, and thus a layer-by-layer growth process. In this report, the anodic potential was used to remove excess In by oxidative stripping at a potential where the energetics of compound formation controlled the stoichiometry. The deposit stoichiometry, determined by EPMA, remained constant over a range of conditions, with a Se:In ratio of 1.5. No XRD pattern was obtained from the as deposited films, though annealing to 300°C for 30 min produced a pattern consistent with hexagonal polycrystalline In_2Se_3.

In Chapter 4 Indium (III) selenide, In_2Se_3, thin films were deposited at room temperature from a pH 3 and pH 1 aqueous solution containing both In^{+3} and Se^{+4} ions using PP-ALD in order to determine optimum solution pH. Because of solution stability and more predictable thin film growth, an In solution made with a pH of 1 was more desirable than solution made with a pH of 3. PP-ALD In_2Se_3 deposits made with pH 1 solution were 60 nm thick and those made using pH 3 were 10 to 20 nm unless a significant overpotential is used. Deposit thickness increased as the deposition potential was investigated at more and more negative potentials since more In can be deposited. In the pH 1 solution, the thickness was not significantly affected as the oxidation potential

was moved more positive since the In oxidized should only be less stable bulk. In the pH 3 solution though, the amount of In oxidized was linear until all In was removed from the surface above 200 mV. The ratio of Se:In remained consistent at ~1.5 unless the deposition potential was not negative enough to reduce In or the oxidation potential was too positive and oxidized all the In from the deposit. No crystallographic patterns could be obtained from the thin films.

Chapter 5 focused on whether Se^{+6} was a viable replacement to Se^{+4} precursor for future PP-ALD studies and if the presence of Cu UPD affected Se^{+6} deposition kinetics. Cyclic voltammetry (CV) exposed changes in the electrochemical profile for Au in Se^{+6} ions when compared to the profile of Au in Se^{+4} ions. Many features, such as highly packed Se layers, were not present in a Se^{+6} solution. Since a significant negative deposition potential was needed to overcome thermodynamic differences, Se^{+6} deposition began near the potential Se reduced to the soluble selenide species. A CV of an Au substrate treated with underpotentially deposited Cu showed the amount of Se deposited from Se^{+6} solution was slightly higher, 0.3 ML, compared to the Se amount deposited on an untreated Au surface from the same solution, 0.1 ML. While the presence of UPD Cu seems to have an effect on the amount of Se^{+6} removed from solution, the amount is not beneficial to a method such as PP-ALD since growth times would need to be increased to obtain practical film thicknesses.

Finally, Chapter 6 discussed the use of CO_2 exposure as a method of reducing defect inducing gasses such as O_2 and H_2. An investigation of gasket material is also presented which demonstrated butyl rubber was superior at excluding O_2 from the cell. O_2 and H_2 were eliminated from the system by purging the cell with CO_2 periodically

however, deposition is inhibited by exposure to the basic rinse during the purge step. Preliminary stripping studies revealed Cd is not affected by CO_2 purging, but a 20% loss is observed when Te is exposed to a CO_2 purge.

Future work will combine the PP-ALD cycles for Cu_2Se and In_2Se_3 to create the ternary absorber layer material $CuInSe_2$ (CIS). It is critical to understand how one materials will behave in the presence of the other and performing studies similar to the ones in chapters 2 and 3 will shed light on how CIS deposition can be optimized. PP-ALD cycles should also be optimized for new substrate materials since Au is too expensive for large scale production. ITO/FTO and Mo are popular alternative contact materials. There have been very few E-ALD studies conducted on oxide substrates so treatment chemistries to remove the oxide layers is essential. New materials such as Sn, Zn, Cd, Te, and S should also be investigated as possible precursors for PP-ALD grown thin films. CZTS/Se is one example of a highly desired multi-junction, PV absorber layer material because of its tunable bandgap and elemental abundancy. A device could be fabricated and tested at various stages of the growth process. E-ALD CdS chemistry and other n-type window layer materials could be combine with the CIS/CZTS materials, tested, and improved. The applicability of PP-ALD for 3rd generation solar cells should also be investigated. Due to nanostructures on the substrate materials, less absorber layer material is required and E-ALD growth methods excel at growing thin-films in the nm range. The conformal growth demonstrated by PP-ALD would be an excellent resource to homogenously coat nanostructures. Finally, investigating possible Cd shielding of Te during CO_2 exposure might help reduce material loss and improve deposit quality.

Further investigation of Te deposition in basic medium might improve our understanding of Te loss during CO_2 purges.